

## Measurement of very-low frequency noise

**Citation for published version (APA):**

Lopez de la Fuente, J. (1970). *Measurement of very-low frequency noise*. [Phd Thesis 1 (Research TU/e / Graduation TU/e), Electrical Engineering]. Technische Hogeschool Eindhoven. <https://doi.org/10.6100/IR94820>

**DOI:**

[10.6100/IR94820](https://doi.org/10.6100/IR94820)

**Document status and date:**

Published: 01/01/1970

**Document Version:**

Publisher's PDF, also known as Version of Record (includes final page, issue and volume numbers)

**Please check the document version of this publication:**

- A submitted manuscript is the version of the article upon submission and before peer-review. There can be important differences between the submitted version and the official published version of record. People interested in the research are advised to contact the author for the final version of the publication, or visit the DOI to the publisher's website.
- The final author version and the galley proof are versions of the publication after peer review.
- The final published version features the final layout of the paper including the volume, issue and page numbers.

[Link to publication](#)

**General rights**

Copyright and moral rights for the publications made accessible in the public portal are retained by the authors and/or other copyright owners and it is a condition of accessing publications that users recognise and abide by the legal requirements associated with these rights.

- Users may download and print one copy of any publication from the public portal for the purpose of private study or research.
- You may not further distribute the material or use it for any profit-making activity or commercial gain
- You may freely distribute the URL identifying the publication in the public portal.

If the publication is distributed under the terms of Article 25fa of the Dutch Copyright Act, indicated by the "Taverne" license above, please follow below link for the End User Agreement:

[www.tue.nl/taverne](http://www.tue.nl/taverne)

**Take down policy**

If you believe that this document breaches copyright please contact us at:

[openaccess@tue.nl](mailto:openaccess@tue.nl)

providing details and we will investigate your claim.

MEASUREMENT OF  
VERY-LOW FREQUENCY NOISE

JULIO LÓPEZ DE LA FUENTE

MEASUREMENT OF VERY-LOW FREQUENCY NOISE

# MEASUREMENT OF VERY-LOW FREQUENCY NOISE

PROEFSCHRIFT

TER VERKRIJGING VAN DE GRAAD VAN DOCTOR IN DE  
TECHNISCHE WETENSCHAPPEN AAN DE TECHNISCHE  
HOOGESCHOOL TE EINDHOVEN, OP GEZAG VAN DE  
RECTOR MAGNIFICUS PROF. DR. IR. A.A.TH.M. VAN TRIER,  
HOGLERAAR IN DE AFDELING DER ELEKTROTECHNIEK,  
VOOR EEN COMMISSIE UIT DE SENAAT TE VERDEDIGEN  
OP DINSDAG 30 JUNI 1970 DES NAMIDDAGS TE 4 UUR.

DOOR

JULIO LÓPEZ DE LA FUENTE

GEBOREN TE NEGURI-GUECHO

DIT PROEFSCHRIFT IS GOEDGEKEURD DOOR DE PROMOTORS  
PROF. DR. H. GROENDIJK  
EN  
PROF. DR. J.J. ZAALBERG VAN ZELST

## CONTENTS

*Preface* 7

### *I Very-low frequency noise*

Introduction 9

1 Stationarity and ergodicity of random phenomena 10

2 Electrical noise. Its power density spectrum 13

3 Low-frequency current noise 15

(A) Flicker noise 15

(B) Burst noise 19

### *II The measurement of noise power spectra*

1 The measurement of a random process 23

2 The measuring system 27

3 Low Q window 28

4 Prewhitening 30

5 Required measuring time  $T$  and statistical error  $\epsilon$  of a measurement 32

6 The integrating-averaging power instrument 34

7 Sources of error 35

### *III The measuring channel* 39

1 Block 1 : Noise sources 40

2 Block 2 : Pre-amplifier 42

(A) Low drift 43

(B) Low-noise design 50

(C) Low-distortion considerations 52

(D) Pre-amplifier circuit 54

3	Block 3 : Wide-band prewhitening filter	57
4	Block 4 : Ultra-low frequency active filter	60
5	Block 5 : Main amplifier	66
6	Block 6 : Selective low-pass filter	68
7	Block 7 : Analogue multiplier	70
8	Block 8 : Hybrid integrator-averager	70

#### *IV Measurements and analysis of low-frequency noise*

(A)	Flicker Noise in Resistors	72
1	Experimental state of art	72
2	Considerations on measurements	73
3	Quasi-stationary noise in resistors	76
(B)	Burst Noise in Transistors	79
4	Analysis	79
4.1	Unsymmetrical random telegraph signal	80
4.2	Spectrum of burst noise with flicker noise superimposed	86
5	Measurements of burst noise in transistors	88
	Summary	95
	References	98
	Acknowledgements	107
	Curriculum vitae	108

## PREFACE

The history of electronic noise is nearly as old as the electronic devices themselves. Although in 1918 Schottky developed a quantitative study of shot noise, it was not felt necessary to develop very low noise amplifiers. At that time radio communications had little need for supersensitive receivers since the limiting noise which originated from atmospheric and statics was outside the receiver.

Similarly, until the arrival of the present age of instrumentation and control in the very low frequency range, as required in geophysics, servomechanisms, modern control systems and, most recently, in medicine, there has been no motivation for the study of very low noise amplifiers and electronic components in the very low frequency range.

All kinds of noises are almost equally annoying to the user of electronic devices, if in one way or another the noise interferes with the detection of the desired signal. Nevertheless, not all noises have the same fundamental importance. For instance, induced hum and microphonic noise can be reduced below the level of detection by means of shielding and of a careful lay-out of the design.

But other types of noise as Johnson or Nyquist noise, shot noise,  $1/f$  noise and burst noise appear to be more intimately bound to the very nature of the electronic devices, and therefore they set their own noise levels. Unlike their physical sources, which may differ from type to type, these noises are random and generally stationary functions of time. But with respect to  $1/f$  noise the stationarity of the process may not exist for all electronic devices.

Actually, work still remains to be done in the design of circuits that will yield the minimum noise figure within the band of frequen- 7



cies in question and in the desired range of operating parameters. However, even more significant, much more remains to be investigated experimentally concerning the fundamental behaviour of the noise processes themselves. Naturally, such an investigation requires the use of very low noise circuits. Hence, the advance of knowledge of noise moves along the double rail track of low noise circuits and components. Consequently, noise problems will still remain with us for a long time to come.

Within the extensive area covered by the noise problems of to-day, a new look is taken at the  $1/f$  noise and the burst noise of carbon film resistors and planar bipolar transistors at very low frequencies.

## VERY-LOW FREQUENCY NOISE

### Introduction

The very word "noise" is something disturbing, because of the lack of intelligibility it carries within itself rather than its sound effect. Noise is everywhere in nature although frequently one cannot hear it, since its scientific meaning goes far beyond its primitive sense of an unpleasant acoustical wave. Thus the word "noise" is taken to mean generally a cause of disturbance in no matter what field of interest.

The ancient discovery of light bodies being attracted by a bar of amber softly rubbed with a cloth is attributed to the philosopher Thales of Milete<sup>1-1</sup> in 600 B.C. This property was named "electricity", since the amber had the Greek name of "ἤλεκτρον". Many centuries later, in 1891, George J. Stoney<sup>1-2</sup> was to use the term "electron" for designating the elementary negative particle, which since then has become an instrument of energy and information inseparable from mankind.

But already in 1828 R. Brown<sup>1-3</sup> observed that particles of pollen or dust suspended in a liquid showed random motion. Almost a century later it was predicted that a similar phenomenon with electrons would occur in an electrical conductor, yielding a spontaneous generation of a random E.M.F. across the terminals of the conductor.

Although man has learned to control the electron for its multiple purposes, his control is limited. The limitation comes about from the electron being affected by the surroundings in which it is handled. The medium leads the electron to behave variously and manifoldly, the behaviours appearing to us as disturbances or as electronic noise.

The first striking property of noise is to give a unique observation each time the phenomenon is contemplated. Thus, the movement of the electrons in a conductor gives rise, among other effects, to a random terminal voltage which determines the ultimate sensitivity of information transmitted through the conductor. Therefore, man has always fought against noise as a cause of disturbance with a better knowledge of its origin and energy content, the aim being to decrease its effects.

In the following pages we will be concerned mainly with certain types of electronic noise measured by an appropriate detecting system. The specific physical origin or possible sources of noise will be treated in so far as their consideration leads to the design of a low-noise measuring system for random phenomena and helps to obtain new insights into the nature of noise in the very low frequency range. We will measure the noise energy spectrum and determine certain behaviour properties of some electronic components.

### 1. Stationarity and ergodicity of random phenomena

In order to study the noise properties of devices and the noise behaviour of circuits we need essentially a certain amount of mathematical background on probability, statistical and Fourier analysis.

Our measurements involving noise sources will give a large amount of data from a physical phenomenon, which when observed can be classified under the concept of random and not deterministic phenomena.

When the relation between cause and effect of a physical behaviour is expressible by an explicit mathematical relationship, the phenomenon is called deterministic and its behaviour may be periodical or transient. On the contrary, a phenomenological behaviour is called random when no explicit mathematical expression can be found for the cause-effect relationship, because two observations of the phenomenon may not give the same value. Hence, any given observation represents only one of the many possible results which might occur.

The collection of all possible observations of the random phenomenon is known as a stochastic or random process, while a group of observations constitute an ensemble of the process.

It is here, in manipulating the random data of the ensemble that statistics has become the reasoning instrument since an individual factor has little influence on the phenomenological behaviour which is subjected to the overwhelming presence of a multitude. This fact is the basis of the law of the large number of observations.

In electricity it is synonymous to speak about random processes  $x(t)$  or fluctuating electrons, namely electrical noise. Hence the terms "fluctuation" and "randomness" refer to related physical quantities.

One important property of statistical techniques is that every parameter is considered with an average value and with the fluctuations from this average. The fluctuation around an average value:

$$\mu = \lim_{N \rightarrow \infty} \frac{1}{N} \sum_{k=1}^N x(t_k) \quad (1.1)$$

is best described by the probability density distribution  $P(x)$ , which prescribes that for any instant of time the chance that  $x(t)$  is inside the interval  $(x, x + dx)$  equals  $P(x)dx$ . Thus, the probabilistic knowledge of the instantaneous value of the phenomenon is represented by some probability distribution type such as the binomial, Poisson or Gaussian.

As the interval  $\tau$  between two individual observations of the random process increases, the averaged product correlates the general dependence of the data values into a function called the autocorrelation function:

$$R(\tau) = \lim_{N \rightarrow \infty} \frac{1}{N} \sum_{k=1}^N x(t_k) x(t_k + \tau) \quad (1.2)$$

For deterministic data,  $R(\tau)$  persists for all displacement values of  $\tau$ . But for a random process the autocorrelation function tends to zero as  $\tau$  tends to infinity, and is a bounded function in the time domain. The Fourier transform of the autocorrelation function yields the spectral power density function of the random process and contains significant relations with the characteristic behaviour of the measuring system (see chapter 2).

Nevertheless, the observation of the power spectrum in itself gives little information concerning the identity of the source of fluctuations, since many different disturbing sources may have the same power density distribution.

When the statistical properties remain the same for ever, the process is called stationary. Now, in practice the random process is observed during a finite interval  $T$  during which we obtain a certain average  $\mu_T$  and an autocorrelation function  $R_T(\tau)$ . When  $\mu_T$  and  $R_T(\tau)$  tend to have a constant value as the observation time  $T$  over which they are computed is increased, the process is said to be stationary in practice. When the statistical properties do not remain the same for ever, the process is called non-stationary. But, when the statistical properties of a process are changing sufficiently slowly in order not to show appreciable change during the period  $T$  of any one observation of the phenomenon, the process is named quasi-stationary.

The problem of determining the conditions under which averages of a stochastic process as observed on one sample can be ultimately identified with corresponding averages on an ensemble of samples, leads to the consideration of an ergodic process. In general, a stochastic process is said to be ergodic, if the time-averaged mean value of a sample (equation (1.1)) and the time-averaged autocorrelation function of that sample (equation (1.2)), as well as other statistical properties, are equal to their corresponding ensemble averaged value  $\mu_x(t)$ ,  $R_x(t, t + \tau)$ , ..... where:

$$\mu_x(t) = \lim_{N \rightarrow \infty} \frac{1}{N} \sum_{k=1}^N x_k(t) \quad (1.3)$$

and

$$R_x(t, t + \tau) = \lim_{N \rightarrow \infty} \frac{1}{N} \sum_{k=1}^N x_k(t) x_k(t + \tau) \quad (1.4)$$

Thus, only stationary random processes can be ergodic. In practice, most of the physical phenomena that produce stationary random data correspond to ergodic processes<sup>1-4</sup>. Nevertheless, we shall come across some non-ergodic processes.

## 2. Electrical noise. Its power density spectrum

Let us consider now the fluctuation of electrons in an arbitrary body or the "electrical noise" as it is more commonly called.

Johnson and Nyquist showed that the fluctuation of electrons has to be considered as an important factor when designing sensitive electrical networks. So important, in fact, that the level of fluctuation determines the limit of sensitivity. Apparently we have reached a dead end. But there is a way out, which consists in exploring backwards the possible paths that end in such a fluctuating situation. These paths lead to the atomistic character of a particular electrical conduction mechanism. Sometimes, when we are not able to reach the end of the path of exploration we shall study the energy contents of the fluctuations while regarding their possible noise sources.

Surely enough, many of these paths have crossings and even sometimes run parallel, indicating the interference and simultaneous presence of different causes. Hence, an even larger complexity is introduced then in identifying the physical source. We have to admit that the explanation of noise appears to be paradoxal to-day, since so many different theories are proposed for any one type of noise. But it is hoped that eventually it will be possible to follow a unique or at least the shortest path towards the source within this labyrinth of theories.

Nyquist<sup>1-5</sup> showed that a resistor of R ohms at a temperature of T °K which is in thermal equilibrium with its surroundings, develops at its terminals and in an effective bandwidth  $\Delta f$  an open circuit noise voltage  $e_n$  whose rms value is given by:

$$e_n = \sqrt{4kTR\Delta f} \quad (1.5)$$

where k is Boltzmann's constant.

Thermal noise is caused by the thermal agitation of electrons in conductors and semi-conductors. Its power density may be determined from thermodynamics and statistical mechanics. Now, thermodynamic entropy is a measure of disorder or of the uncertainty about the microscopic 13

state of a thermodynamic system. Then, from the point of view of energy generated and heat dissipated a physical system where the entropy is maintained at a constant level, is said to be randomly stationary<sup>1-6</sup>. Such is the case for the thermal noise of an element being measured at a constant temperature.

But Nyquist's formula applies only to thermal equilibrium conditions, and electrical devices do not operate in such conditions, since a current usually flows through them. This current is the basis of a noise current source.

In a vacuum diode the noise owing to its d.c. anode current is known as shot noise, which is the result of fluctuations in the instantaneous number of electrons in transit caused by the random electron emission of the cathode. The mean square value of shot-noise current  $\overline{i_n^2}$  in a saturated diode where  $I_d$  is the direct current of the diode,  $-q$  is the electronic charge, and  $\Delta f$  is the effective noise bandwidth under consideration, is given by<sup>1-7</sup>:

$$\overline{i_n^2} = 2 q I_d \Delta f \quad (1.6)$$

In (1.6) the frequency of measurement must be low enough to avoid transit-time effects and high enough to avoid low-frequency effects covered in the following sections.

Thermal noise and shot noise, as given by equations (1.5) and (1.6), are independent of the measuring frequency and so have a flat power density spectrum  $S(f)$  known as "white spectrum". Nevertheless, active and passive devices carrying a current show a noise power density level higher than the theoretical values given by (1.5) and (1.6), and their total power density distribution is of the type given by Fig. 1.1.

Three distinct regions are shown in Fig. 1.1. (i) On the right is the high frequency region, where  $S(f)$  increases proportionally to  $f^\alpha$ , with  $\alpha \approx 2$ , from a frequency value  $f_2$  which is usually in the MHz range. (ii) The medium frequency region corresponds to the white noise, where  $S(f)$  is constant down to some frequency value  $f_1$ . The actual value of  $f_1$  depends on the type of device in question, the

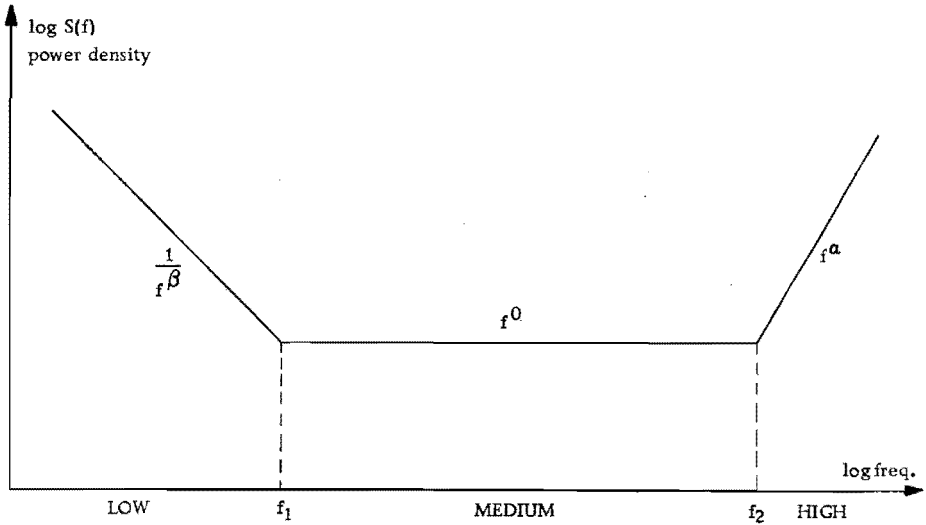


Fig. 1.1 Noise power density spectrum

individual sample, and its operating mode. Thus, for a low-noise vacuum tube  $f_1$  is around 1 kHz, while for a transistor it can be 50 Hz, both devices operating at 1 mA d.c. current. (iii) The third region refers to the low and very low frequencies, following a law proportional to  $f^{-\beta}$ ; with  $0 \leq \beta \leq 2$ .

It is in this last region that lies our main interest.

### 3. Low-frequency current noise

#### (A) Flicker noise

The term "current noise" is meant to include all noise types other than thermal noise (1.5) and shot noise (1.6) which appear in a device carrying a current. Although the physical cause of the additional noise level is not clear, many experiments have shown that the noise spectrum at low frequencies has the following type of law:

$$S(f) = K \frac{I^a}{f^\beta} \quad (1.7)$$

where  $I$  is the d.c. current,  $a \approx 2$  and  $0 < \beta \leq 2$ . The coefficient  $K$  is an empirical factor involving the geometry<sup>1-8</sup> and material of the 15



device and depending weakly on the temperature in a way not precisely known<sup>1-9</sup>.

When this phenomenon was first discovered in vacuum tubes<sup>1-10</sup>, showing a value of  $\beta$  close to unity, it was called "flicker noise". To other devices with similar spectra other names are given such as "1/f noise", "excess noise", "semi-conductor noise", "low frequency noise", "contact noise" and "pink noise".

Flicker noise seems to appear everywhere. Apart from vacuum tubes it may be found in resistors<sup>1-11</sup>, thin carbon films<sup>1-12</sup>, carbon microphones<sup>1-13</sup>, thermistors<sup>1-14</sup>, bipolar transistors<sup>1-15</sup> and semi-conductor diodes, photoconductors<sup>1-16</sup>, quartz crystal oscillators<sup>1-17</sup>, and in field-effect transistors<sup>1-18</sup>. We see that most of the materials in which 1/f noise arises can on one ground or another be classified as semi-conductors. Our main interest will cover resistors and transistors. Although the general case is for  $\beta \approx 1$  in equation (1.7), there are some interesting cases in which  $\beta$  is greater than unity.

From the consideration of the noise power in a frequency band from  $f_1$  to  $f_2$  it can be seen that

$$\int_{f_1}^{f_2} S(f) df = \frac{K}{1-\beta} f^{1-\beta} \Big|_{f_1}^{f_2} \quad (1.8)$$

yielding infinite mean power when  $\beta$  is  $\leq 1$  and  $f_2$  extends to infinity or when  $\beta$  is  $\geq 1$  and  $f_1$  extends to zero frequency. Therefore, such a law as given by equation (1.7) cannot hold for all frequencies, and it is then necessary that  $\beta$  becomes smaller than one at some very low frequency and is larger than one at high frequencies. But up to the present no low frequency has been found in experiments below which the value of  $\beta$  in (1.7) decreases. (Note).

---

(Note). A possible way out of this difficulty is presented by Malakof<sup>1-19</sup>, who seems to have been the first to point out the possibility of flicker noise being non-stationary with stationary increments, i.e. flicker noise is quasi-stationary.

In order to encompass these considerations as well as the experimental evidence, the low frequency region of Fig. 1.1 is developed into the representation of Fig. 1.2. Thus, the importance of the parameter  $\beta$  is emphasised.

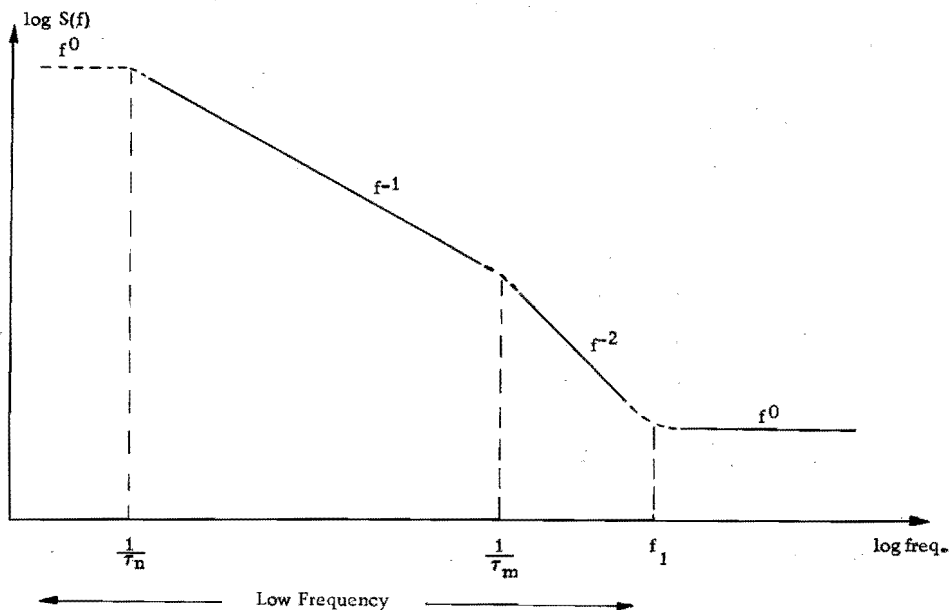


Fig. 1.2 Low-frequency noise power density spectrum

Indeed, after the first work of Bernamont<sup>1-11</sup> several investigators followed his line of study. Meyer and Thiede investigated thin carbon films confirming the value of  $a=2$  in equation (1.7) but obtaining a variation in  $\beta$ ,  $1 \leq \beta \leq 2$ .

It is known that good vacuum diode tubes with a tungsten filament have a flat spectrum down to about 30 Hz and then start to increase as  $f^{-2}$  or even sometimes as  $f^{-3}$  as the frequency decreases<sup>1-20, 1-21</sup>.

An experimental  $f^{-2}$  may be understood as pertinent to a spectrum law:

$$S(f) = K \frac{\tau}{1 + (\omega\tau)^2} \quad (1.9)$$

where  $\tau$  is the mean lifetime of a single event which affects the conductivity of the sample,  $\omega\tau$  is to be considered sufficiently

large,  $K$  is a constant, and  $\omega$  is the angular frequency. If the transit time of an electron from cathode to anode in a vacuum diode or similarly the generation-recombination time of an electron in a semi-conductor diode, is considered as the lifetime of the single event, equation (1.9) represents the noise spectrum of shot noise. But, in case a continuous distribution of  $\tau$  is considered with a probability distribution of  $\tau$  proportional to  $1/\tau$  between limits  $\tau_m$  and  $\tau_n$ , an  $f^{-1}$  law results as a sum of all possible spectra of type (1.9) in a certain frequency range.

It may occur that of the spectrum components of type (1.9) some are much larger in magnitude than the other ones. Then, the whole spectrum of Fig. 1.2 can be represented by a sum of a uniform component, an  $f^{-1}$  component and one or several components  $\tau/(1 + (\omega\tau)^2)$ , yielding the spectrum relation<sup>1-22</sup>:

$$S(f) = A + \frac{B}{\omega} + \frac{C\tau}{1 + (\omega\tau)^2} \quad (1.10)$$

In fact, the spectrum relation (1.10) has been verified experimentally in semi-conductors as germanium filaments, p-n junctions and transistors, as well as in vacuum tubes and mos transistors very recently. A summary of this evidence follows now according to the times of their discovery.

Noise was studied in an n-type germanium filament<sup>1-23</sup> in the spectral range 1 kHz to 10 MHz. The spectrum followed a curve close to (1.10) with a lifetime  $\tau$  of 1  $\mu$ sec. Other authors<sup>1-24</sup> have found, in the lower frequency range of 10 Hz to 100 kHz, that germanium filaments may show a clear change in  $S(f)$  from  $f^{-2}$  to  $f^{-1}$  as the frequency decreases. The spectrum appeared to follow equation (1.10) and some samples showed "bumps" around 300 Hz, where a shot-noise component was assumed to exceed the  $f^{-1}$  component. Similar results have been reported<sup>1-25</sup> for a narrow germanium p-n junction which was forward biased. The spectrum in the range of 100 Hz to 20 kHz may be represented by (1.10), so that a peak or bump is also present when the  $f^{-1}$  component is subtracted.

18 More recently, noise power of different planar transistor types with-

in the range of 1 Hz to 10 kHz showed a spectrum law  $f^{-\beta}$  with  $0.96 < \beta < 1.23$ <sup>1-26</sup>. Certain transistor types at 100 Hz and lower frequency values exhibited an additional noise component of the form (1.9). This last component could not be attributed to shot effect since lifetimes of msec and longer were required for explaining the spectrum.

Recently, the anomaly in the flicker noise spectrum, with  $f^{-\frac{3}{2}}$  between 10 Hz and 10 kHz, was also observed in vacuum tubes with oxide cathodes<sup>1-21</sup>. The anomaly appeared in the range of 100 Hz to 1 kHz and was caused by an additional component in the noise spectrum which varied according to  $(1 + (\omega\tau)^2)^{-1}$ . In mos transistors<sup>1-27</sup> a spectrum bump of extra current noise at 5 kHz was found in addition to the  $f^{-1}$  component for the total current noise spectrum, following equation (1.10) in the frequency range of 20 Hz to 40 kHz.

### (B) Burst Noise

While flicker noise is ubiquitous, burst noise seems to be sporadic in nature. The latter is somehow associated with the former.

In addition to flicker noise, irregularly distributed large pulses of low frequency, sometimes called "bursts", often appear in materials carrying a current. These bursts produce an audible effect in radio receivers described as crackles. In the noise power density spectrum the anomalies these bursts produce may often be represented by a specific relaxation time  $\tau$  giving a relation similar to equation (1.9).

Burst noise has been found in resistors and in semi-conductor devices. The description of the phenomenon is a complex task, as may be seen in the following exposition, owing to the diversity of devices and their operating conditions under which burst noise was observed.

Campbell and Chipman<sup>1-28</sup> as well as many others<sup>1-14, 1-29, 1-30</sup> observed bursts of irregular shape as abnormal fluctuations in the records of current noise from carbon resistors. The bursts did not necessarily occur at a high mean level of current, since narrow current paths exist in carbon resistors where on several spots high current densities may occur.

A more defined form of burst noise with a step waveform, similar to an unsymmetrical random telegraph signal, suggesting temporal transition between two states of conduction appears frequently in semiconductor devices.

In fact, Pay<sup>1-31</sup> found that a point-contact germanium diode at 1 mA reverse current gave an almost regular rectangular noise wave of 500 Hz. He related the phenomenon to the Zener effect, a breakdown by an avalanche mechanism.

Planar and mesa structure silicon diodes were studied at the much lower reverse current of 50  $\mu\text{A}$ <sup>1-32</sup>. Flat-topped current pulses of 30  $\mu\text{A}$  and 17  $\mu\text{A}$  at approximately 20 kHz were observed before reaching the avalanche situation. The bursts were thought to be associated with microplasmas and had the peculiar feature that as the reversed current was increased (1 - 300  $\mu\text{A}$ ), the interval between pulses decreased, until finally the microplasma saturated and no "off" pulses were observed.

In some devices, as in low voltage reverse biased germanium junctions<sup>1-33</sup>, the current-noise wave consists primarily of a square wave with steps of  $10^{-8}$  A in amplitude, which are much smaller than the typical microplasma pulses described above. The pulse amplitude and the switching rate changed slowly with the reverse voltage, but in a different manner than for the microplasmas. The measured time duration of the positive and negative pulses suggested a Poisson probability distribution, while the variation of the pulse height with temperature indicated that possibly random thermal fluctuations caused on-off switching of a conduction path. The physical cause of such a burst-noise phenomenon was believed to be not an avalanche breakdown but the surface effects.

Bistable current fluctuations have been found also in the reverse-biased emitter-to-base junction of p-n-p germanium diffusion transistors, within the range of low reverse voltages far below the breakdown situation<sup>1-34</sup>. Increasing the reversed bias had no influence on the pulse rate, which followed a Poisson distribution; but it caused a linear increase in the pulse height (which was of the order of 20 nA) until a saturation level of the pulses was reached

around 10 V. The pulse rate increased with temperature and the power density spectrum followed a clear  $f^{-2}$  law over two decades (20 kHz to 200 Hz) changing to an  $f^{-1}$  spectrum below 200 Hz.

More extensive work has been done on the burst noise of transistors in the forward mode of operation<sup>1-35, 1-37</sup>. Among the 40 planar transistors tested, 23 had burst noise, while only one in 25 transistors of diffusion or mesa structure showed bursts. The bursts appeared as a random telegraph signal with a magnitude depending on the temperature, the base resistor, and the biasing current (20 - 200  $\mu$ A). The pulse lengths had nearly a Poisson probability distribution and extended from some hundreds of microseconds to some minutes. We have also observed this type of burst noise in transistors and have found pulses as long as thirteen minutes. Some transistors present three or even four levels of pulse height which are considered to be independent series. According to the authors<sup>1-37</sup>, within the frequency range of  $10^{-2}$  Hz to 10 kHz and for the current levels mentioned above, a spectrum  $f^{-1}$  was verified. Unfortunately no indication was given concerning the deviation from a substantially  $1/f$  dependence.

In order to separate surface effects from bulk effects, gate-controlled diodes and transistors have been studied<sup>1-38</sup>. Burst noise, both gate-voltage dependent and independent, was observed. An advantage of this structure is that it becomes possible to use the gate electrode, which is placed on the base-emitter junction, to turn on and off the burst-noise source. In the frequency range of 20 Hz to 40 kHz, the diodes showed noise spectra  $f^{-2}$  down to 1 kHz and a change to  $f^{-1}$  at 40 Hz, while the transistors had an  $f^{-\beta}$  spectrum with  $\beta \sim \frac{3}{2}$  down to 100 Hz, and then  $\beta$  became smaller than unity.

Under the name of "popcorn noise" has appeared in literature a low-frequency (10 Hz to 40 kHz) step fluctuation noise. It is most often encountered in the integrated operational amplifiers and is probably due to the integrated planar transistors which jitter erratically between two or more values of  $h_{fe}$ <sup>1-39, 1-40</sup>. The step am-

plitude at the input of the device may reach a level of 50  $\mu\text{V}$  or an equivalent input noise current of 200 pA.

Burst noise certainly does not occur or at least is not detected in each device made by a given process nor even from the same wafer. Nevertheless, from experimental evidence<sup>1-35, 1-41</sup> there is a good indication that the general planar technology introduces a substantial basis for the appearance of burst noise in semi-conductor devices.

Although the information of sections 3 and 4 is overwhelming, we may note the following. Some unified considerations can be made if the exponent value  $\beta$  of equation (1.7) and the shape of the noise power spectrum curve are taken as the basis of comparison in the noise behaviour of the different components and of the operating conditions.

Therefore, we intend to investigate the behaviour of the parameter  $\beta$  as well as the intensity of the flicker-noise spectrum in resistors and transistors.

With respect to the burst noise, since it has a well-defined waveform in transistors, a mathematical analysis of its spectrum will be made and compared with actual noise power measurements. Assuming a relationship between the flicker and burst noise components at very low frequencies, we will arrive at a picture close to the actual noise power spectrum curve.

But let us first establish in the following chapter the theoretical basis required for the construction of a measuring channel of power spectra.

## THE MEASUREMENT OF NOISE POWER SPECTRA

### 1. The measurement of a random process

It is our intention to measure the power spectra of some stochastic or random processes and we shall see that it can be done by a hybrid system that combines analogue and digital techniques. The reasons for measuring power spectra as a parameter that gives information about noise may be understood from the following considerations.

When considering noise currents or voltages,  $f(t)$ , very little information about the behaviour of  $f(t)$  is obtained from the knowledge of an instantaneous value, because instantaneous values may differ much in magnitude and may also be lacking in reproducibility. Neither it is possible to predict the past or the future behaviour of  $f(t)$  from only the instantaneous values observed during an interval  $T$ . However, averaged functions of  $f(t)$  over a long time  $T$  can lead to a more extensive knowledge of the signal's behaviour.

For a stationary random process,  $f(t)$ , the average value over the past, present, and future is its d.c. component value  $\overline{f(t)}$ . Now, the average value of the fluctuations of  $f(t)$  around  $\overline{f(t)}$  is zero but their variance, i.e. the averaged squares of the differences between  $\overline{f(t)}$  and its instantaneous values  $f(t)$ , is a positive quantity:

$$\overline{(f(t) - \overline{f(t)})^2} = \overline{\phi(t)^2} = \lim_{T \rightarrow \infty} \frac{1}{2T} \int_{-T}^T \phi(t)^2 dt \quad (2.1)$$

If  $\phi(t)$  is the voltage across a resistor of  $1\Omega$  or the current flowing through the load of  $1\Omega$ , the numerical value of  $\phi(t)^2$  is equal to that of the power dissipated by the voltage or the current in



the resistor load. Therefore,  $\phi(t)^2$  is a relevant feature of the random generating process  $f(t)$  and it is customary to speak about  $\phi(t)^2$  as being a power quantity, even if its dimension is not that of a power.

In practice,  $\phi(t)$  it is a noise signal of small magnitude and an amplifier is needed to increase its level before we can manipulate it. We would also like to have a unique input-output correspondence of the noise signals that will allow true interpretation of the input data. The simplest choice is to use a linear amplifier.

Let us apply a sinusoidal voltage  $A_i \cdot \exp j\omega t$  to the input of the linear amplifier and obtain an output voltage  $A_o \cdot \exp j(\omega t + \theta)$ ; here  $A_o$  and  $A_i$  are real numbers. Then the transfer function of the linear system is defined as:

$$H(\omega) = A_o \exp j(\omega t + \theta) / A_i \exp j\omega t = A_o / A_i \cdot e^{j\theta} \quad (2.2)$$

where  $A_o/A_i$  is known as the gain factor of the system at the frequency  $\omega$  of consideration, and  $\theta$  is called the phase angle. It can be proved<sup>2-1</sup> that:

$$H(\omega) = \int_{-\infty}^{\infty} h(\tau) e^{-j\omega\tau} d\tau \quad (2.3)$$

where  $h(\tau)$  is the response of the system initially at rest to a unit impulse at  $\tau=0$ . Now, the output  $\phi_o(t)$  resulting from an input signal  $\phi_i(t)$  to a linear system can be written as a convolution or superposition integral:

$$\phi_o(t) = \int_{-\infty}^{\infty} \phi_i(t) h(t-\tau) d\tau = \int_{-\infty}^{\infty} h(\tau) \phi_i(t-\tau) d\tau \quad (2.4)$$

where  $h(\tau)$  appears as the weighting function of a linear system which, by exploring the past of the input function, with its unit-impulse response, supplies the output function.

However, for a random process we are interested statistically only in average values not of the time functions themselves but in

the time averaged quadratic values. Let us first consider the autocorrelation function  $\bar{\Phi}(\tau)$ , which is defined as:

$$\bar{\Phi}(\tau) = \overline{\phi(t) \phi(t+\tau)} = \lim_{T \rightarrow \infty} \frac{1}{2T} \int_{-T}^T \phi(t) \phi(t+\tau) dt \quad (2.5)$$

From (2.5) the power as given by equation (2.1) can be obtained by letting  $\tau \rightarrow 0$ , i.e.  $\bar{\Phi}(0)$ . Now, the integral  $\int_0^{\infty} |\bar{\Phi}(\tau)| d\tau$  exists. Therefore, the Fourier transform of  $\bar{\Phi}(\tau)$  can be taken.

When we consider at the input of a linear system with transfer function  $H(\omega)$  the autocorrelation function  $\bar{\Phi}_i(t)$  of the stationary random process, we may write for the autocorrelation function  $\bar{\Phi}_o(t)$  at the output <sup>2-2</sup> :

$$\bar{\Phi}_o(\tau) = \iint_{-\infty}^{\infty} h(t) h(\eta) \bar{\Phi}_i(t + \tau - \eta) dt d\eta \quad (2.6)$$

Expression (2.6) enables us to obtain, entirely from operations in the time domain, the output autocorrelation function from an input autocorrelation function and the weighting function of the system. If we apply a Fourier transform to (2.6), having made the change of variables  $\mu = \tau + t - \eta$ , we may write:

$$\frac{1}{2\pi} \int_{-\infty}^{\infty} \bar{\Phi}_o(\tau) e^{-j\omega\tau} d\tau = \int_{-\infty}^{\infty} h(\eta) e^{-j\omega\eta} d\eta \int_{-\infty}^{\infty} h(t) e^{j\omega t} dt \times \frac{1}{2\pi} \int_{-\infty}^{\infty} \bar{\Phi}_i(\mu) e^{-j\omega\mu} d\mu$$

which by the Wiener-Khinchine theorem yields:

$$S_o(\omega) = H(\omega) H^*(\omega) S_i(\omega) = |H(\omega)|^2 S_i(\omega) \quad (2.7)$$

where  $S_o(\omega)$  and  $S_i(\omega)$  represent the power density spectrum of the output and input of the system, respectively.  $S(\omega)d\omega$  is the amount of average power present within an infinitesimal bandwidth  $d\omega$  centered at a specific frequency  $\omega$ .

Now, since  $\bar{\Phi}(\tau)$  and  $S(\omega)$  are a pair of reciprocal relations in a Fourier transform, we have for  $\tau \rightarrow 0$  :  $\bar{\Phi}(0) = \int_{-\infty}^{\infty} S(\omega) d\omega$ , which is the **25**

total power. Then, integrating both sides of equation (2.7) and having replaced  $\overline{\Phi}_0(\omega)$  by its equivalent through equations (2.5) and (2.1), we obtain for the output power:

$$\overline{\phi_0(t)^2} = \overline{\Phi}_0(\omega) = \int_{-\infty}^{\infty} S_0(\omega) d\omega = \int_{-\infty}^{\infty} |H(\omega)|^2 S_i(\omega) d\omega \quad (2.8)$$

where  $\phi_0(t)$  corresponds with the instantaneous output fluctuations of the linear system. The right-hand side of equation (2.8) represents a spectrum in which  $|H(\omega)|^2$  appears as a weighting factor of the input power density spectrum. Therefore, if the linear system is considered to be a narrow filter with bandwidth  $\Delta\omega$  and centered at  $\omega_0$  it is possible to scan the total power of the random process into its power frequency components. In fact, (2.8) yields:

$$\overline{\phi_0(t)^2} = \int_{\omega_0 - \frac{\Delta\omega}{2}}^{\omega_0 + \frac{\Delta\omega}{2}} |H(\omega)|^2 S_i(\omega) d\omega \quad (2.9)$$

and assuming that for a stationary random process  $S_i(\omega)$  corresponds to a smooth spectrum, we may write (2.9) as:

$$\overline{\phi_0(t)^2} = S_i(\omega_0) \int_{\omega_0 - \frac{\Delta\omega}{2}}^{\omega_0 + \frac{\Delta\omega}{2}} |H(\omega)|^2 d\omega \quad (2.10)$$

so that  $S_i(\omega_0)$  may be obtained from a measurement of  $\overline{\phi_0(t)^2}$  using that particular frequency filter, provided that the integral on the right-hand side is known. This integral represents the area of the power spectral window corresponding with the filter.

Thus, equation (2.10) provides a simple relation that allows us to calculate the spot power density of the input random stationary process  $f(t)$  from averaged quadratic fluctuations at the output of the linear system and the integral of the squared gain factor of the system, having avoided every complication by phase. As  $\omega_0$  is varied, the whole power density spectrum is obtained.

In practice, owing to the finite observation time  $T$  of the random process, estimates are made on average values by observing the random process during a sufficiently long time  $T$ .

## 2. The measuring system

The application of a filter in equation (2.10) demands two requirements:

I : in the frequency domain the bandwidth  $\Delta\omega$  must be sufficiently small with respect to the smooth region of the power spectrum being considered.

II : in the time domain, the unit-impulse response  $h(\tau)$  of the filter requires a certain time  $\tau_m$  in order to vanish. This time must be smaller than the observation time  $T$  for obtaining a complete response of the system to the input.

Therefore, the system's behaviour of such a selective filter centered at  $\omega_0$  has the following expression:

In the frequency domain:

$$H(\omega) = \begin{cases} \neq 0 & \text{within } \omega_0 \pm \Delta\omega/2 \\ = 0 & \text{elsewhere} \end{cases}$$

In the time domain:

$$h(\tau) = \begin{cases} \neq 0 & \text{for } 0 < |\tau| < \tau_m < T \\ = 0 & \text{for } |\tau| > \tau_m \end{cases}$$

Now, the evaluation of  $\overline{\phi_0(t)^2}$  in (2.10) is obtained by integrating over an infinite time. But in practice, for a stationary random process an approximate value  $\overline{\phi_{OT}(t)^2}$  is obtained with a certain statistical accuracy  $\epsilon$  (see section 5) by integrating over a sufficiently long time  $T$ .

Therefore, at a particular spot frequency value  $\omega_0$ , having measured during time  $T$ , we obtain for equation (2.10):

$$S_{iT}(\omega_0) = \overline{\phi_{OT}(t)^2} / k\Delta\omega \quad (2.11)$$

where  $k\Delta\omega$  is the area of the power spectral window of the filter.

Fig. 2.1 shows a block diagram of the measuring system for power

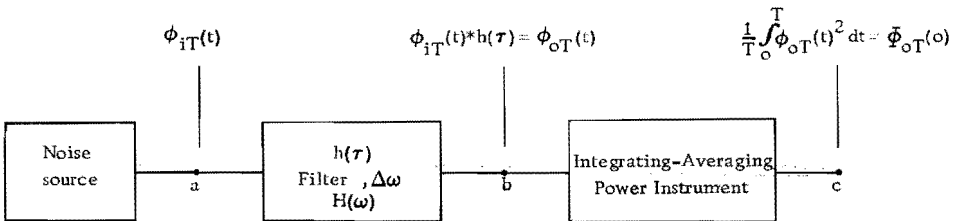


Fig. 2.1 Block diagram of the measuring system.

spectra of a noise source by using a selective frequency filter and an integrating-averaging power instrument. In fact, let  $\phi_{iT}(t)$  represent the fluctuations of the noise source around its average value during an interval of time  $T$ . Then, in the time domain at point b in Fig. 2.1 the convolution of  $\phi_{iT}(t)$  and  $h(\tau)$  yields  $\phi_{oT}(t)$  through equation (2.4), while at point c the output represents  $1/T \cdot \int_0^T \overline{\phi_{oT}(t)^2} dt$  which corresponds to an autocorrelation value  $\overline{\Phi_{oT}}(0)$  through equation (2.5), an approximation to the exact value  $\overline{\Phi_{oT \rightarrow \infty}}(0)$ ; and dividing by  $k\Delta\omega$ , we obtain  $S_{iT}(\omega)$ .

It is seen from the above considerations that the lay-out of Fig. 2.1 is sufficient for resolving equation (2.11).

### 3. Low Q window

In practice, a filter with a flat response and a sharp cut-off is only realisable by a complex circuit. A narrow-band filter has a large  $\tau_m$  value while a filter with a small  $\tau_m$  introduces an undesired effect upon the spectral window owing to the appearance of large sidelobes. Blackman and Tukey<sup>2-3</sup> have shown that a filter with a theoretical square lag-window  $h(\tau)$  gives in the output power a first sidelobe in the spectral window as high as 20% of the main-lobe and it is negative (Fig. 2.2). Measuring noise through such a filter, at its output we would also obtain contributions to the noise by frequencies far apart from the central frequency  $\omega_0$ .

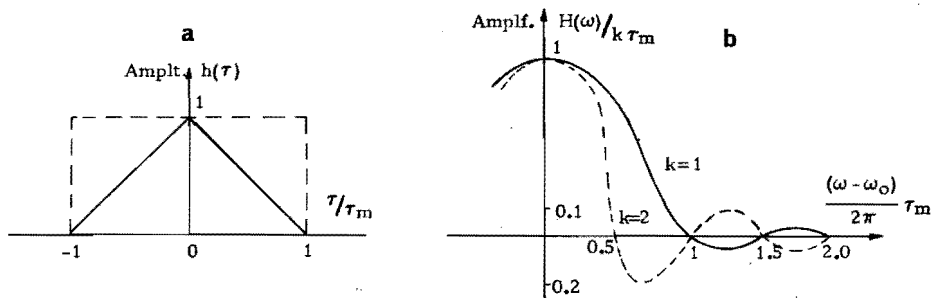


Fig. 2.2 a) Lag window.

b) Spectral window.

As the shape of the lag window is changed into a triangular shape, the amplitudes of the sidelobes in the spectral window are reduced very rapidly, being at most 1% or 2% of the height of the mainlobe. Thus, the main power contribution is now by far restricted to a much smaller region around  $\omega_0$ .

Special windows have been designed, such as the "hamming" and "hanning" windows, with the aim of producing very small sidelobes. But Blackman<sup>2-4</sup> points out that any special window cannot eliminate the need for prewhitening and the rejection of filtrations, while good prewhitening and rejection filtration can eliminate the use of special windows. Therefore, a logical and practical compromise may be reached by the design of a wide bell-shaped filter, namely, a low Q filter.

Low Q filters tend to be bell-shaped. But their rejection filtration is not so good since their frequency characteristic curve  $H(\omega)$  has non-zero amplitude tails that extend over some decades of the frequency spectrum. Therefore, very large signals outside the pass-band are not well rejected, and so leak through the tails of the filter and give an extra power contribution at the output of the system.

Even when the above large signals are not present in the measurement in question, and a white noise spectrum is to be measured, one further consideration has to be made. The output power at  $\omega_0$  in Fig. 2.1 is then proportional to the total area under the bell-shaped curve  $|H(\omega)|^2$  of the filter. At low spot frequency values of  $\omega_0$ , the actual bandwidth is necessarily small and a situation may be reached in which the area under the two side-tails of the bell curve is considerable with respect to the central area. Then, an appreciable error results in the output power measurement localised at  $\omega_0$ . Consequently, a high-pass and a low-pass filter section must be added to the low-Q bell-shaped filter, if an improvement is to be expected from the measuring system. Thus, the block of  $H(\omega)$  corresponds in practice to Fig. 2.3.

Since the spectrum range under consideration is the very-low frequency band  $10^{-2}$  Hz to 20 Hz, it seems convenient that the low-

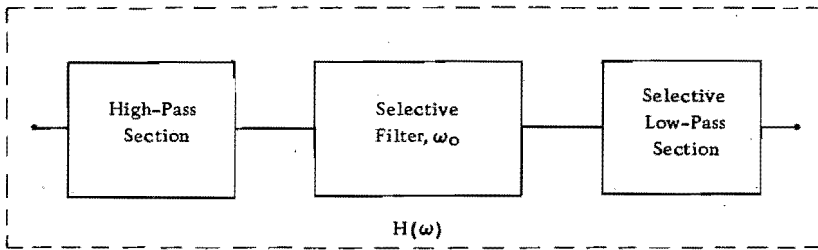


Fig. 2.3 Block diagram of the filter,  $H(\omega)$ .

pass section be selective in order to obtain a sharp cut-off response on the high-frequency side tail. The high-pass section is realisable by a prewhitening filter placed in front of the selective filter, as may be seen in the following section.

In the power density spectrum representation a logarithmic scale is foreseen to be convenient, and equally spaced value of  $\log \omega_0$  are desired. This leads us to choose the  $\omega_0$  values per decade as follows:

k. 1,  $k.\sqrt[3]{10}$ ,  $k.\left[\sqrt[3]{10}\right]^2$  or  $\omega_0$ : 1, 2.15, 4.64 per decade.

By this choice we obtain 11 points in the power spectrum of interest so that a well-approximated curve can be drawn.

#### 4. Prewhitening

Prewhitening consists in filtering the data before their analysis is started, in order to remove the possible excessive influence of spectral peaks and thus obtain a smooth power spectrum at the output. Consequently, any interference between different components is minimised and a picture closer to the real spectrum appears after recolouring.

The objective of prewhitening is to minimise the total mean square error of an estimated value <sup>2-5</sup> and to decrease considerably the peak of the spectrum near the d.c. component. At the same time, saturation by this part of the spectrum is avoided in the amplifiers needed for the measuring system, and a flat or a white noise spectrum is analysed at the output. Therefore, prewhitening should be done as early as possible in the system so that the selective

filter operates under equivalent power relations independently of the spot frequency value  $\omega_0$  under consideration.

The main difficulty lies in the necessity of knowing "a priori" the shape of the input power spectrum to be analysed and that this shape may require highly flexible filters which are often difficult to design.

Fortunately, in our present work we aim at measuring power density spectra of the type:

$$S_i(\omega) = K\omega^{-(1+b)}, \quad 0 < (1+b) \leq 2 \quad (2.12)$$

that have a smooth slope such as usually corresponds to very low frequency noise spectra. From the above considerations a good choice of the whitening function seems to be:

$$|H(\omega)|^2 = k_1\omega \quad (2.13)$$

in the frequency band of interest.

Introducing equations (2.12) and (2.13) into (2.7) we obtain:

$$S_o(\omega) = k_2 \omega^{-b} \quad (2.14)$$

where  $k_2$  is a constant and  $0 < |b| \leq 1$ . Equation (2.14) represents a smooth power spectrum linearly related to the input power spectrum. Hence, the recolouring of the output data becomes a simple matter.

Now, by designing a filter with a voltage amplitude characteristic curve as  $|H(\omega)| = k_3 \sqrt{\omega}$  in a wide band, we obtain a high-pass section behaviour in this band. Hence, the prewhitening and the high-pass section filter may be obtained by one and the same section in Fig.2.3. This high-pass section automatically filters out the very lowest frequencies, which may be regarded as slow drifts of the d.c. component and the input signal  $\phi_i(t)$  is processed as having zero mean value.



Therefore, the procedure proposed with this type of prewhitening yields output values which are practically d.c. unbiased, increasing the accuracy of the power density spectrum analysis especially at low signal levels and at very low frequency values.

### 5. Required measuring time T and statistical error $\epsilon$ of a measurement

Assuming the sample record of  $\phi_o(t)$  is averaged over a time interval T and corresponds to a stationary random process with zero mean value and with a smooth spectrum, for the time average of  $\phi_o(t)^2$ , in its frequency representation inside a bandwidth  $\omega_o \pm B_e/2$ , we have <sup>2-6</sup> :

$$\epsilon^2 = \frac{(S_o(\omega_o) - \overline{S_o(\omega_o)})^2}{S_o(\omega_o)^2} \approx (B_e T)^{-1} + \frac{1}{576} \left( \frac{B_e}{\ell(\omega)} \right)^4 \quad (2.15)$$

where,  $\epsilon$  = statistical error or normalised mean error of the estimate of  $S_o(\omega_o)$

$S_o(\omega_o)$  = estimated value of the output power density at  $\omega_o$

$\overline{S_o(\omega_o)}$  = final estimate or average value of  $S_o(\omega)$

$\ell(\omega)$  = is called the spectral bandwidth of the random

process  $\phi_o(t)$  and is given by:  $\ell(\omega) = |S_o(\omega)/S_o''(\omega)|^{\frac{1}{2}}$

T = true averaging time in seconds

$B_e$  = the bandwidth in Hz of the narrow-band resolution filter  $H(\omega)$ .

In the case where  $\epsilon$  is relatively small,  $\epsilon \leq 0.2$ , the sampling distribution of the mean value of  $S_o(\omega_o)$  may be approximated by a normal distribution with mean value  $S_o(\omega_o)$  and a standard deviation (s.d.)  $\epsilon \cdot S_o(\omega_o)$ . Then, in practice, for all repeated measurements the true value lies within the interval  $S_o(\omega_o)/(1 \pm 2\epsilon)$ , with a 95 per cent. confidence level.

When the power spectrum is properly resolved the second term of equation (2.15), known as the bias error, will usually be negligible and (2.15) reduces to:

$$32 \quad \epsilon = \text{s.d. } S_o(\omega_o) / S_o(\omega_o) \approx (B_e T)^{-\frac{1}{2}} \quad (2.16)$$

The resonant response of a linear system gives a properly resolved measurement if the physical bandwidth  $B_e$  of the analyser is  $B_e < \frac{1}{4} B_{sr}$ , where  $B_{sr}$  is the half-power point bandwidth of the narrowest peak in the power spectrum being measured.  $B_e < \frac{1}{4} B_{sr}$  is taken as a practical criterion. This criterion should limit bias errors to less than 3%, when power spectra of physically random data are measured and  $B_e T \gg 1$  is assumed<sup>2-7</sup>.

An essential question still remains to be answered. What is the true bandwidth  $B$  to be introduced into equation (2.16)? For  $B$  we should take the noise bandwidth, i.e. the bandwidth of an assumed rectangular filter that passes through a white noise signal with the same mean square values as the physical filter. Then, when the input is white noise and we have a single-tuned filter with half-power bandwidth  $B_e$ ,  $B = \pi/2 \cdot B_e$ . Thus in practice we have the relation:

$$\epsilon \approx \left( \frac{\pi}{2} B_e T \right)^{-\frac{1}{2}} \quad (2.17)$$

Table I has been obtained using equation (2.17) for a bank of filters with equal  $Q$  factor of 5 and for the spot frequency values chosen in section 3 within the spectrum range 20 to  $10^{-2}$  Hz.

Frequen-

cy: Hz	$\epsilon = 7.5\%$				$\epsilon = 5.0\%$				$\epsilon = 2.0\%$			
	Days	hrs	min	sec	Days	hrs	min	sec	Days	hrs	min	sec
19.8				28.58	1			43				7 3.28
10.0				56.58	2			7.32				13 15.77
4.64		2		2	4			34.4				28 35
2.15		4		23		9		52.2	1	1		41.27
1.0		9		26		21		13.2	2	12		37.74
0.464		20		19.5		45		44	4	45		50.29
0.215		43		52	1	38		42	10	16		52.75
0.100		1	34	18.8	3	32		12.4	22	6		17.46
0.0464		3	23	15	7	37		20.5	1	23	38	23.17
0.0215		7	18	40		16	27	0.5	4	6	48	47.77
0.010		15	43	8	1	11	22	4	9	5	2	54.7
	Days	hrs	min	sec	Days	hrs	min	sec	Days	hrs	min	sec

If  $\epsilon = 7.5\%$  a total time of 1 day and 5 hours is needed to measure the spectrum of interest, while if  $\epsilon = 2\%$  the time needed rises to 17 days and 5 hours. Consequently, some compromise must be made between the desired statistical error and the frequency value under observation. High spot frequencies may be resolved with a 2% statistical error, while low frequencies with at most 5% error lead to a total measuring time of 3 days for the same spectrum range. A random measuring order will smooth out possible fluctuations of the estimates and the repetition of certain measurements will indicate if significant changes have taken place in the random process during the total measuring time of the spectrum.

### 6. The integrating-averaging power instrument

In the time domain the integrating-averaging power instrument of Fig. 2.1 may be regarded as being an autocorrelator (Fig. 2.4). In equation (2.11) the integration of the squared value of  $\phi_o(t)$  is needed. In practice,  $\phi_o(t)^2$  is given by  $\phi_o(t) \cdot \phi_o(t+\tau)$  as  $\tau$  tends to zero. By using an analogue multiplier, this product is easily obtained, since some phase shift or time delay exists in practice between the two inputs, although it should be as small as possible. The output of the multiplier is a voltage quantity of squared-volt units having very low frequency components, which when measured by any analogue reading instrument, will yield a fluctuating value and not a mean value as desired.

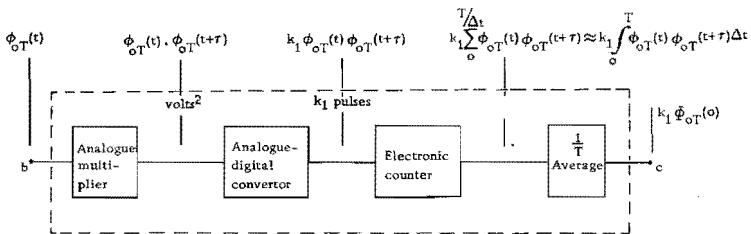


Fig. 2.4 Block diagram of the integrating-averaging power instrument.

Furthermore, as seen in section 5 the required measuring time  $T$  is at least 15 hours for the lowest frequency value. If an analogue integration, e.g. by a Miller integrator, is performed during the above time  $T$ , serious difficulties may be encountered with respect to drifts of the zero level and input currents as well as to the necessity of a large voltage condenser.

These difficulties can be avoided by using an analogue-to-digital convertor with a high sampling rate  $\Delta t$ , where  $\phi_o(t)^2$  is continuously converted or sampled into a proportional number of pulses. These can be added by an electronic counter yielding in practice a continuous integration over the time  $T$ . Averaging the integration over the observed time  $T$ , gives the autocorrelation function  $\Phi_{oT}(\tau)$  for a delay time  $\tau$ . For  $\tau \rightarrow 0$  we obtain the average power of  $\phi_{oT}(t)$ .

The capacity of the counting operation is increased very considerably by the simple addition of a 6-digit mechanical counter which indicates the number of times the electronic counter saturates. With the instrument used, a 100-day integration can be reached at a counting rate of 100 K pulses a second before the mechanical counter also saturates.

Care must be taken that the sampling frequency  $1/\Delta t$  is at least twice as high as the highest frequency present to avoid the introduction of aliasing. Half the sampling frequency is known as the folding or Nyquist frequency  $f_N = 1/2\Delta t$ . The term "aliasing" refers to the fact that high frequencies and low frequencies may share the same sampling points in time and thus an uncertainty is introduced with respect to the frequency value of the measurement being done. Hence, a safe way to reduce the possibility of aliasing is to filter out the high frequency components of  $\phi_o(t)$  before it is sampled and to use a high sampling rate.

## 7. Sources of error

Under the term "sources" we wish to include the main causes that disturb the general trend of measurements, whether the source be a measuring procedure, a circuit type or a side effect in the realisation of an electrical approach.

In this section some practical compensations and corrections are pointed out. The main sources of error are listed below, although some have already been considered in the previous sections:

a Very low frequencies.

b Leakage of power through the spectral sidelobes and the tails of  $H(\omega)$ .

c Aliasing.

d The frequency selectivity procedure.

#### a Very low frequencies

The true d.c. level of  $f(t)$  can be easily set to zero by subtracting the mean value of the signal or, in practice, by introducing a large blocking capacitor in the circuit. But then, very low drifts of the mean value may still appear as ultra low frequencies, producing a large peak in the spectrum near to the zero frequency<sup>2-8</sup>.

The best error compensation seems to lie in the application of a filter that prewhitens down to zero frequency. Indeed, use was made of such a prewhitening filter having a  $k\sqrt{\omega}$  voltage amplitude characteristic curve and a d.c. blocking capacitor as its input.

Furthermore, throughout the measuring system, the use of differential amplifier stages with strong d.c. feedback will substantially contribute to low drifts. A large blocking capacitor may be placed at the input of the analogue-digital convertor to reduce the contribution of the d.c. offset level at the output of the analogue multiplier.

#### b Leakage of power through the spectral sidelobes and tails of $H(\omega)$

This problem appeared in section 3. The practical solution is given by the combination of a low Q filter and a low-pass filter section. The cut-off frequency of the low-pass section is synchronised with the selective frequency value of the filter. The low-pass section decreases the contribution by leakage through the high frequency tail of the filter. The prewhitening filter attenuates the filter's

### c Aliasing

The problem of aliasing was considered in section 6. As a consequence of the sampling introduced by the analogue-digital convertor, high frequency components appear as low frequencies.

The analogue-digital convertor used has a sampling rate of 10  $\mu\text{sec}$ . The corresponding Nyquist frequency is 50 kHz which is twice the internal clock frequency of the analogue multiplier. Hence, the sampling rate is sufficiently high to avoid aliasing.

The high frequency noise components do not alias because they are attenuated by a by-pass capacitor to ground placed after the selective filter and by the low-pass section of Fig. 2.3.

### d The frequency selectivity procedure

The frequency selectivity with a bell-shaped characteristic curve may be obtained by placing a Twin-T circuit in the feedback loop of an operational amplifier. The circuit diagram is shown in Fig. 2.5, where A is a differential-stage amplifier. Owing to the se-

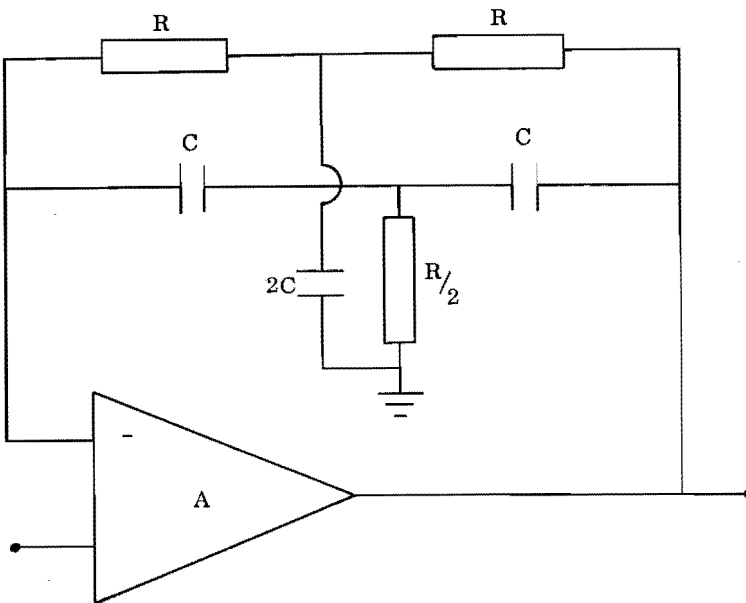


Fig. 2.5 Selective amplifier with a Twin-T fed back circuit.

lectivity at very low frequencies, down to  $10^{-2}$  Hz, it is convenient to have a d.c. path in the feedback loop. The selectivity is obtained by varying simultaneously the values of the three capacitors or of the three resistors.

Now, shot-noise power is proportional to the d.c. current and flicker-noise power to the square of the d.c. current. Thus, within the spectrum band of interest ( $10^{-2}$  Hz to 20 Hz), if the three resistors of the Twin-T circuit are the variable elements, they will be changed by a factor of  $2.10^3$  and consequently also the d.c. current. Therefore, this selectivity procedure will yield a considerable change in the flicker and shot noise power of the Twin-T circuit.

On the contrary, with variable capacitors, the d.c. current in the Twin-T circuit will be constant and the same noise producing elements will remain in the circuit for all frequency values of measurement.

Bull<sup>2-9</sup> came across a similar situation in a selective amplifier, but he said he did not know whether the excessive noise in his case arose in the valves known to have low-noise levels or in the circuit resistors or again, perhaps from the method of reducing the bandwidth. It seems probable that the cause was the selectivity procedure realised by changing the resistor values.

From the above considerations the correct selectivity procedure to be applied to low-noise operation at very low frequencies appears to be realised by varying simultaneously the three capacitors and not the resistors.

## THE MEASURING CHANNEL

Summarising the block diagrams of Figs. 2.1, 2.3 and 2.4 of chapter II with the practical considerations already mentioned, we arrive at a convenient lay-out for a low-frequency noise power measuring channel.

Now, assuming that the pre-amplifier and the amplifiers have a flat band response down to d.c. and a broader bandwidth than the spectrum band in question, the measuring system proposed in chapter II is not affected either in the time domain or in the frequency domain. Therefore, we will design and construct the following measuring channel as shown in Fig. 3.1.

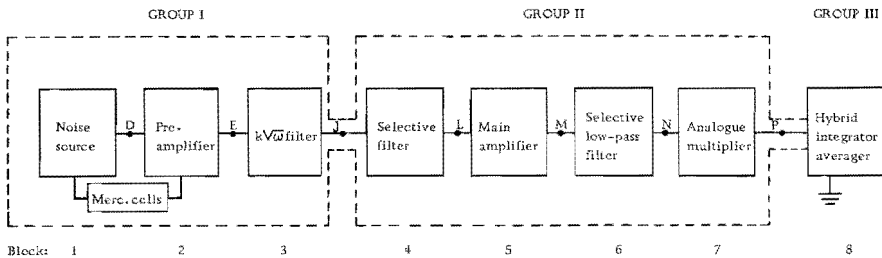


Fig. 3.1 The measuring channel

Three block-groups can be distinguished in Fig. 3.1. The first group, which encloses blocks 1, 2 and 3, delivers at point J a sufficiently strong voltage noise signal  $\phi(t)$  with a white noise power spectrum for a  $1/f$  input noise spectrum within the frequency range of interest, viz.  $10^{-2}$  Hz to 20 Hz. The second group elaborates the selective frequency window centered at  $\omega_0$  and delivers at point P a proportional squared value of the voltage noise. Group III does the integration and averaging of  $k\phi^2(t)$  over the prescribed observation time T.



The blocks of group I are thermally, electrostatically and magnetically shielded to avoid as much as possible any external interference, especially from the frequency of the power mains. The first group is energised by mercury cells and has its shield materially joined to that of group II by means of a sleeve shield, inside which a coaxial cable transmits the signal from group I.

Group II is also thermally and magnetically shielded. It is powered from a floating output power supply; the same applies to all its blocks. Their common ground is earthed at the grounding point of the integrating block, the unique earth point for the whole measuring channel. The output signal at point P is transmitted with a coaxial cable within a sleeve shield, grounded at its end.

Inside groups I and II silica gel is enclosed to maintain a dry surrounding. In the following pages we will consider each block diagram of the lay-out of Fig. 3.1.

#### 1. Block I: Noise sources

Two types of noise sources have been measured, namely carbon-film resistors and bipolar transistors of the npn and pnp types. The noise sources are operated at very low current levels, viz. 1 to 2  $\mu\text{A}$ . It was suspected that such an operating mode would allow the appearance of relevant features obscured at higher current levels by, for instance, dissipation effects.

The different noise-source networks are shown in Fig. 3.2. A noise voltage is evolved by the noise source between points F and G, and is fed by a large dry tantalum capacitor,  $C_1$ , into the pre-amplifier; the first stage of which is also shown in Fig. 3.2a. The pre-amplifier has a differential input stage with equal source resistors ( $50\text{ k}\Omega$ ) connected as in a bridge type network and d.c. balanced at the two bases. After the adjustment of the potentiometer  $50\text{ k}\Omega$  (or  $2\text{ k}\Omega$ ) in Fig. 3.2-a (or b and c), point F has the same d.c. level as point D. The same is done in the pre-amplifier for points F' and D'. Therefore, by means of this adjustment the leakage currents of capacitors  $C_1$  and  $C_2$  are very small, of the order of less than  $10^{-10}\text{ A}$ , and the coupling of the noise source to the



The energy of the circuit is supplied from mercury cells which are known for their very stable output voltage at low drain currents, for their relatively high current capacity (3400 mA.h for the type used), and for their very low voltage noise of approximately  $4 \mu\text{V}_{\text{pp}}/\text{cell}$ , max.

As noise-resistor source we used cracked-carbon film resistors. They are known to be made of small-size crystal graphite and larger amorphous coal grains, and possibly with oxygen atoms as bridges between the graphite and the coal. The resistors had a standard value of  $10 \text{ M}\Omega \pm 10\%$ ,  $1/16 \text{ W}$ , and when measured in the bandwidth 0.06 Hz to 60 Hz, noise peak voltages from  $40 \mu\text{V}$  to  $400 \mu\text{V}$  were observed for the different units under consideration.

For the case of a transistor noise source a  $100 \text{ M}\Omega$  resistor was introduced for biasing the transistor. The resistor was made of an inorganic film deposited on a ceramic rod and was hermetically glass-sealed against moisture and other contaminants. Its temperature coefficient was  $0.5\%/^{\circ}\text{C}$  and its low output noise is negligible on the load resistor  $R_L$ .

Noisy transistors were chosen as sources owing to their observed burst noise with an approximate repetition rate of 0.1 sec or longer, and thus the burst noise is observable in the frequency range of interest. The burst voltages at point F were from  $100 \mu\text{V}$  to  $400 \mu\text{V}$  for the different transistors, when operated at a collector current of  $1.5 \mu\text{A}$ .

## 2. Block 2: Pre-amplifier

Sometimes, in order to obtain a very low drift amplifier, quite a number of compensating elements are introduced in the circuit. The final result may be an increased output noise level. Therefore, our aim is to design a pre-amplifier as simple as possible with the smallest number of active and passive elements. At the same time a transistor operating mode is to be found that can combine the advantages of low-drift and low-noise operation.

Pederson<sup>3-1</sup>. The hushing operation of a transistor consists in biasing the transistor with practically zero voltage drop from collector to base. The authors pointed out that an appreciable improvement is obtained in the current noise behaviour and on the 1/f noise spectrum of a transistor operated in the hushed-mode. This improvement will always be obtained even if the transistor shows low noise figures for its normal mode operation. Therefore, hushing a transistor will yield a reduced noise behaviour in much the same way as negative feedback is the tool for obtaining ultimate amplifier linearity, independent of the non-linear characteristics of the active element.

A closer look at the hushed-mode brings forward some properties of this low noise operation which are also features used for low drift in low-level signal amplification and for low distortion operation. These features are summarised as follows:

- (a) low collector current operation<sup>3-2</sup>
- (b) low collector junction temperature<sup>3-3, 3-4, 3-5</sup>
- (c) improvement of the common-mode rejection for a differential stage<sup>3-6</sup>
- (d) practically constant current gain
- (e) reduction of the non-linearities in transistors<sup>3-7</sup>
- (f) possibility of using a complementary transistor-compound stage<sup>3-8</sup>

Let us now first consider a transistor stage under the following points of view: (A) Low drift, (B) Low noise, (C) Low distortion. These points of view will include the above features in a non-systematic manner. Then, secondly, we will realise an actual pre-amplifier according to these points of view.

#### (A) Low drift

Transistor temperature problems are not necessarily difficult. But the design of a high-performance amplifier requires great attention to many details and some amount of skill if the transistor parameters are to be sufficiently stable over a long period of time.

In an amplifier the main source of drift is to be found in the first stage and to a much smaller extent in the second stage, caused by

In silicon transistors at low collector-to-base voltages  $\Delta I_{CBO}$  is very small, viz. of the order of  $10^{-12}$  A/ $^{\circ}$ C, which makes the fourth term of (3.6) negligible. The third term is reduced considerably by the hushed-mode operation, as will be seen in (3)  $I_{CBO}$ . For equal source resistance  $R_{s1} = R_{s2} = R_s$ , the second term  $(\Delta V_{BE1} - \Delta V_{BE2})/R_s$  becomes negligible as follows from the considerations about equation (3.3). Therefore, the main contribution is the first term and we arrive at:

$$\Delta I_{B1} - \Delta I_{B2} \approx I_{B1} \frac{\Delta \beta_1}{\beta_1} - I_{B2} \frac{\Delta \beta_2}{\beta_2} \quad (3.7)$$

According to (3.7) the input drift is small because  $\Delta \beta/\beta$  is typically less than 1%/ $^{\circ}$ C. We can make it still lower by decreasing the operating current  $I_C$  and by using a high  $\beta$ . Therefore, a second conclusion is that the input transistors should be a matched pair in  $\beta$  values at equal  $V_{BE}$  voltages; high  $\beta$  values at very low  $I_C$  are desired.

Fortunately, large  $\beta$  values are possible in planar transistors even at practically zero  $V_{CB}$  and at very low operating currents. We have found experimentally that at an  $I_C$  of 10  $\mu$ A and at  $V_{BE}$  constant, in some transistor types the value of  $\beta$  at  $V_{CB}$  equal to 100 mV is decreased only by 10% with respect to its value for  $V_{CB}$  equal to 2 V. The cause of the small decrease in  $\beta$  seems to be the high collector-to-base contact potential, which is 0.7 V for silicon. In germanium transistors this contact potential is only 0.30 V and the  $\beta$  values are decreased by a factor 2 to 3 for operating conditions similar to the above. Thus, silicon transistors should be used for the hushed-mode operation.

### (3) $I_{CBO}$

The leakage current  $I_{CBO}$  consists of four components. Two of them, a and b, are mainly due to temperature action and the other two, c and d, to the voltage.

a. In the base region, for any temperature pairs of electrons and holes are generated.

b. Under the influence of thermal action, too, extra electrons and holes are generated on the collector surface by surface energy states.

c. A third component arises in the collector depletion region, the volume of which depends on the material resistivity, the junction area and the voltage  $V_{CB}$  across it.

d. Surface impurities, moisture and other insulating materials as  $SiO_2$  contribute to the fourth component, which depends also on the surface potential.

Now, operating the transistor at low current and voltage bias means lowering the operating temperature of the transistor and, therefore, decreasing components a and b. At the same time the hushing operation will decrease component c and reduce the excess current due to an inversion layer<sup>3-16, 3-17</sup> in the base region produced by the surface potential.

Since in silicon transistors  $I_{CBO}$  doubles for every  $15^\circ C$  increase in temperature<sup>3-18</sup>, it is important that  $I_{CBO}$  is small in order to neglect the third and fourth terms in equation (3.6). We may conclude that the hushed-mode operation is appropriate for low drifts.

#### (4) Improved collector-source current

In d.c. coupled amplifiers intrinsically stable current sources are important, since fewer compensating elements are needed and thus the total noise level is reduced indirectly.

Baxandall and Swallow<sup>3-19</sup> have designed a new current source circuit. Fig. 3.3 is a slightly modified version to be used as a one-half circuit of a differential stage. Essentially, it is a pnp-npn compound transistor which may be considered as a pnp unit between the points E, B, C. It has a very high input impedance and a high d.c. current amplification factor. The input transistor is hushed-mode operated.

(i) Temperature compensation. The main features of its temperature analysis are as follows.

(i-1) The voltage change  $\Delta V_{BE}$  from points B to E due to the effects 47

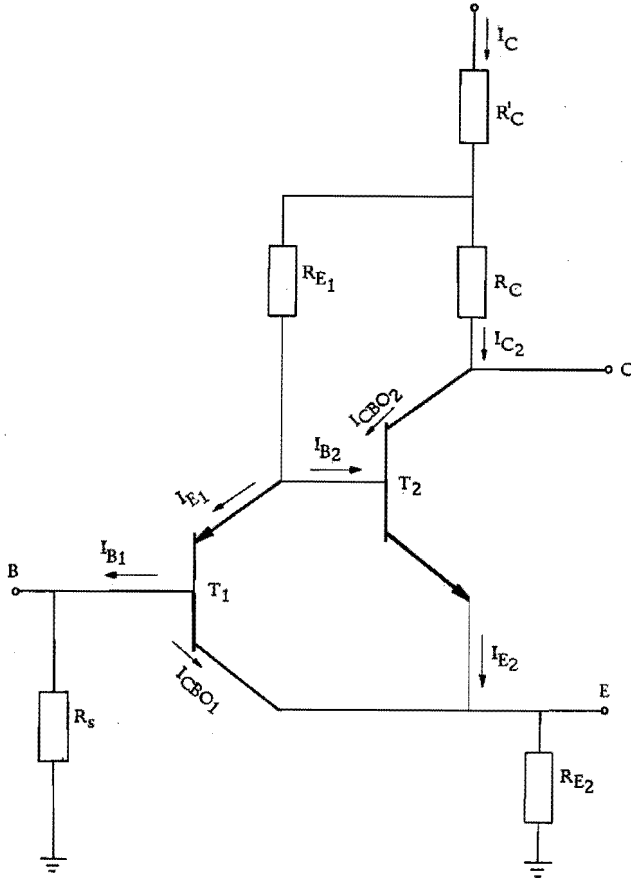


Fig. 3.3 The compound transistor stage

of ambient temperature changes on the emitter-base voltages of the two transistors will largely balance against each other. This  $\Delta V_{BE}$  across the current determining resistor  $R_{E2}$  produces an output current variation,  $\Delta I_{C2}$ , at point C. Assuming  $\Delta V_{BE}$  to have a negative temperature coefficient of  $0.25 \text{ mV}/^\circ\text{C}$ , then for 2.5 V across  $R_{E2}$ ,  $\Delta I_{C2}/I_{C2} = (-0.25 \text{ mV}/2.5 \text{ V})/^\circ\text{C} = -0.01\%/^\circ\text{C}$ .

But  $\Delta V_{BE1}$  produces a change in  $I_{E1}$  across  $R_{E1}$  and hence another change in  $I_{C2}$ ,  $\Delta I'_{C2}$ . Assuming 1V across  $R_{E1}$  and across  $R'_C$ , with  $I_{E1}$  being 10% of  $I_{E2}$  and  $\Delta V_{BE1}$  equal to  $-2.8 \text{ mV}/^\circ\text{C}$ , the output current change is  $\Delta I_{C2}/I_{C2} = -(2.8 \text{ mV}/(1\text{V} + 1\text{V} \cdot 10))/^\circ\text{C} = -0.025\%/^\circ\text{C}$ . Thus at the output point C a total change of  $I_{C2}$  smaller than  $0.04\%/^\circ\text{C}$  may be expected.

(i-2) Since the total  $I_{CBO_2}$  is transmitted to the emitter of  $T_2$  via  $T_1$ ,  $\Delta I_{C_2}$  caused by  $\Delta I_{CBO_2}$  is almost compensated by the negative feedback action of  $R_{E_2}$ . The transistor  $T_1$  is hushed-mode operated and therefore the  $I_{CBO_1}$  is negligible.

(i-3) The variation of the current gain,  $\Delta\beta_2$ , causes  $I_{B_2}$  to change, but this change is also transmitted to the emitter of  $T_2$  and almost compensated.

(i-4) The compound transistor CBE has no compensation for  $\Delta\beta_1$  caused by temperature variations. Since  $I_{E_1}$  is taken as 10% of  $I_{E_2}$ , we should expect  $\Delta\beta_1 \ll \Delta\beta_2$ .

(i-5) The temperature variations of  $I_{B_1}$  due to  $\Delta I_{BCO_1}$  will be very small since  $T_1$  is hushed-mode operated. Thus the input thermal drift of the silicon compound transistor is small even for large  $R_s$  base resistances.

## (ii) Current amplification

The d.c. current amplification factor of the compound transistor,  $\beta_{cp}$ , defined as  $I_{C_2}/I_{B_1}$  is:

$$\beta_{cp} = \beta_2 I_{B_2} / I_{B_1} = I_{E_2} / I_{E_1} \times (\beta_1 + 1) \cdot \beta_2 / (\beta_2 + 1) \quad (3.8)$$

Assuming  $\beta_2 \geq 100$  in  $T_2$ :

$$\beta_{cp} = (\beta_1 + 1) \cdot I_{E_2} / I_{E_1} \quad (3.9)$$

Therefore, if we assume  $I_{E_1}$  to be 10% of  $I_{E_2}$  and  $\beta_1$  equal to 100,  $\beta_{cp} = 10^3$ .

(iii) Input impedance. For a C.E. stage and taking the small signal current amplification factor to be equal to  $\beta$ , the input impedance is given by  $(\beta + 1)(r_e + (1 - \alpha)r_b)$ , where  $r_e$  and  $r_b$  are the total resistance on the emitter and base. Considering Fig. 3.3 to be one half of a differential stage, point E is virtually grounded and the input impedance becomes:

$$Z_{in} = (\beta_1 + 1) \left[ r_{b_1} (1 - \alpha_1) + r_{e_1} + R_{E_1} // (\beta_2 + 1)(r_{b_2} (1 - \alpha_2) + r_{e_2}) \right] \quad (3.10) \quad 49$$



where // means "in parallel". Neglecting the contributions due to the factor  $(1-\alpha)$  and replacing the dynamic emitter resistance by its equivalent  $26/I_E \Omega$  ( $I_E$  in milliamperes), we arrive at:

$$Z_{in} = (\beta_1 + 1) \left[ \frac{26}{I_{E1}} + R_{E1} // (\beta_2 + 1) \frac{26}{I_{E2}} \right] \quad (3.11)$$

### (B)-Low-noise design

It is known that the noise of a transistor with conventional operating parameter values increases when the collector current is decreased below a certain optimum value. But it was found<sup>3-1</sup> that even when the noise of a transistor in a conventional circuit is low, it can always be reduced by the hushing principle. Thus, there is an optimum operating current with a hushed-mode collector-to-base voltage.

Now, just from the point of view of low noise figure, an optimum operating current  $I_E$  may be obtained. Noise factor is defined as the ratio of the total mean square noise voltage at the output of a transistor to the mean square noise voltage at the output resulting from the thermal noise in the source resistance  $R_s$ . The noise factor of a transistor in a C.E. configuration is given by<sup>3-20</sup>:

$$F_E = 1 + r_b/R_s + r_e/2R_s + 1/\beta \cdot 1/2R_s r_e \left( 1 + f/f_c \cdot \sqrt{\beta/\alpha} \right) (R_s + r_b + r_e)^2 \quad (3.12)$$

where  $r_b$  is the incremental base resistance,  $r_e$  the incremental emitter resistance,  $f_c$  the cut-off frequency.

The second term of equation (3.12) is the noise in  $r_b$ , the third term represents the noise due to  $r_e$  and the fourth term is the noise in the collector. Replacing  $r_e$  by its equivalent function of  $I_E$  as above, and assuming  $\beta$  practically independent of  $I_E$ , for  $f \ll f_c$ , equation (3.12) becomes:

$$F_E = 1 + r_b/R_s + 26/2I_E R_s + I_E \left[ R_s + r_b + 26/I_E \right]^2 / 52\beta R_s \quad (3.13)$$

50 Differentiating with respect to  $I_E$  and equating to zero, we obtain

the optimum operating current  $I_{E_{opt}}$  expressed in milliamperes for the minimum noise figure, which is given by:

$$I_{E_{opt}} = 26\sqrt{\beta + 1}/(r_b + R_s) \quad (3.14)$$

Re-introducing  $r_e$  into (3.14) we arrive at the optimum  $R_s$  for minimum noise figure:

$$R_{s_{opt}} = r_e\sqrt{\beta + 1} - r_b \quad (3.15)$$

We note that the minimum noise figure is obtained for a source resistance value lower than when impedance matching conditions are met at the input; here,  $Z_{in}$  is for a CE configuration and is given by  $r_b + r_e(\beta + 1)$ . Hence, this mismatching situation means a loss of power transfer from the source to the transistor, although it yields a better signal-to-noise ratio. For a mismatching situation with  $R_s/Z_{in}$  equal to  $10^{-1}$  it is possible to obtain a noise figure of 1 dB with a relative power loss of approximately 5 dB only<sup>3-21, 3-22</sup>.

Owing to the active element, the input stage always gives some power amplification. Therefore, when operating for low noise conditions, the value of  $R_s$  should be actually chosen more from the point of view of low thermal drift and noise figure than from impedance matching considerations.

The last term in equation (3.12) represents the noise in the collector, but the influence of the surface collector leakage current  $I_{CL}$  as well as the collector reverse saturation current  $I_{CS}$  has been neglected. Now, Hurley<sup>3-23</sup> has considered in detail the noise sources within a transistor. The mean square collector semi-conductor noise voltage,  $(e_c^2)$ , is assumed to be:

$$\overline{(e_c^2)} = K_c \left( V_{CB}/R_{CL} \right)^2 r_c^2 \Delta f/f \quad (3.16)$$

where  $K_c$  is a constant proportional to the volume of the material,  $R_{CL}$  is  $V_{CB}/I_{CL}$ . In practice  $I_{CL}$  is the main component of  $I_{CBO}$  and

much larger than  $I_{CS}$ . From (3.16) we see that the hushed-mode operation will almost eliminate this noise source and then equation (3.12) will represent a noise-figure behaviour closer to reality, with the main source of noise appearing in the emitter.

Therefore, from equations (3.12), (3.15), and (3.16) we conclude that the transistor should be operated in a hushed-mode, at a very low optimum current level and with an approximate impedance mismatching ratio between  $10^{-1}$  to  $10^{-2}$  in order to obtain a very low noise figure of 1 dB.

### (C) Low-distortion considerations

Let us now give some consideration to the linearity of a transistor operating at low currents and bias voltage. Some authors have analysed the cross-modulation and the intermodulation noise in transistors<sup>3-21, 3-24, 3-25</sup>. Here we will consider the input and output diodes of a CE configuration with respect to their linear behaviour.

Let the output current of the signal  $i_c$  be expressed as a function of the operating voltage,  $v_c$ , i.e.  $i_c = f(v_c)$ . Then, expanding  $i_c$  into a Taylor's series around an operating point  $v_{c1}$ , the signal current is expressed as a function of its linearity and non-linearities:

$$i_c = i_c \Big|_{v_{c1}} + \frac{1}{1!} (v_c - v_{c1}) \frac{di_c}{dv_c} \Big|_{v_{c1}} + \frac{1}{2!} (v_c - v_{c1})^2 \frac{d^2 i_c}{dv_c^2} \Big|_{v_{c1}} + \frac{1}{3!} (v_c - v_{c1})^3 \frac{d^3 i_c}{dv_c^3} \Big|_{v_{c1}} + \dots \quad (3.17)$$

It is known that the intermodulation distortion is caused by a non-linearity or curvature of second and higher even orders, while a curvature of third or higher odd orders produces cross-modulation<sup>3-21, 3-24, 3-25</sup>. For our present analysis and measurements we are interested in reducing the intermodulation distortion.

second order<sup>3-26</sup>. Therefore, operating the output diode of the transistor at the inflexion point of the static characteristic curve will yield a vanishing second derivative at  $v_{c1}$  in the Taylor's series expansion of  $i_c$ , and consequently the intermodulation distortion is cancelled. The static characteristic curve of the collector-base diode is shown in Fig. 3.4-a. As the operating base current  $I_B$  decreases, the curves become more parallel to the voltage axis and the inflexion points P are shifted to lower  $V_{CE}$  values and consequently to lower  $V_{CB}$  values. It is seen that for very low operating currents, if the inflexion point is chosen as the operating point, the transistor becomes operated in a hushed-mode and will produce low distortion.

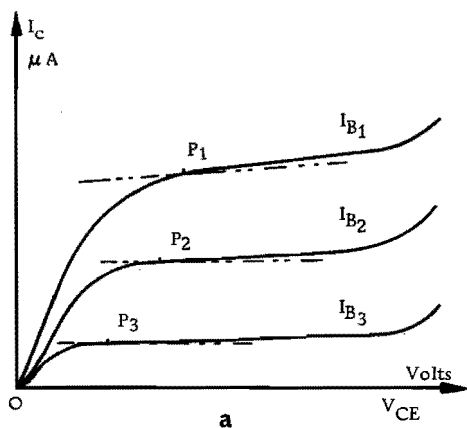


Fig. 3.4 Static characteristic curves of a C.E. configuration; silicon junctions. a) output curve, b) input diode, semilog scale, c) input diode, linear scale.

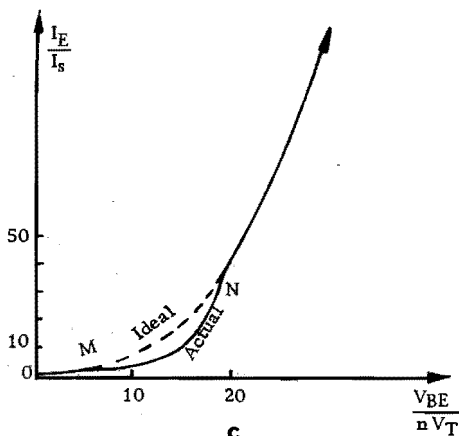
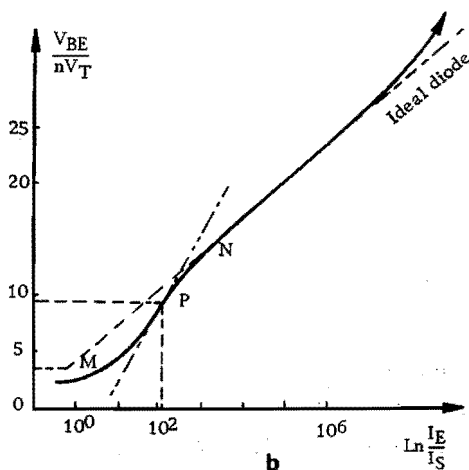


Fig. 3.4-b is taken from Moll<sup>3-27</sup> and represents the static characteristic curve of the ideal input emitter-base diode given by the relation  $I_E = I_s \cdot (\exp qV_{BE}/nkT - 1)$ , dotted line. Here,  $kT/q$  is the thermal potential  $V_T$ , which is approximate 26mV at room temperature.  $I_s$  is the saturation current of the reverse-biased diode and  $n$  is a parameter,  $1 \leq n \leq 2$ . Having neglected the term  $-I_s$  in the above expression, it is represented on a semilog scale in Fig. 3.4-b. But in practice the diode follows the "actual" curve. At low current values we note an increase of the slope<sup>3-28</sup>.

When Fig. 3.4-b is represented on a linear scale we obtain Fig. 3.4-c and we note that the MN section of the actual diode curve has an increased slope with respect to the ideal curve. Therefore, the curve becomes more linear than for the ideal diode expression with the possibility of having also an inflexion point at a very low emitter current value. Hence, at very low  $I_E$  values the linearity of the input diode is improved and, in a transistor, corresponds to the situation of being hushed-mode operated.

Therefore, from the considerations made throughout parts (A), (B), and (C) we conclude that the hushed-mode operation in transistors leads to low drift, low noise and low distortion operation.

#### (D) Pre-amplifier circuit

The circuit of the pre-amplifier, Fig. 3.5, consists of three differential stages. The first two stages are designed upon the current source of Fig. 3.3 with  $R_{E2}$  replaced by a better current source, namely a transistor,  $T_5, T_{10}$ . Each of the differential stages is made up of an emitter follower and an amplifier section. The signal is fed back from the output of the second stage via  $T_{12}$  to the second input of the first stage,  $T_3$ . The third stage constitutes a simple differential amplifier,  $T_{11} - T_{13}$ .

High input impedance is obtained by using the temperature compensated compound transistor. The use of current sources as of Fig. 3.3 in a differential arrangement leads to a second order temperature compensated stage, as implied by the circuit configuration. The contribution to the output drift of possible temperature variations still

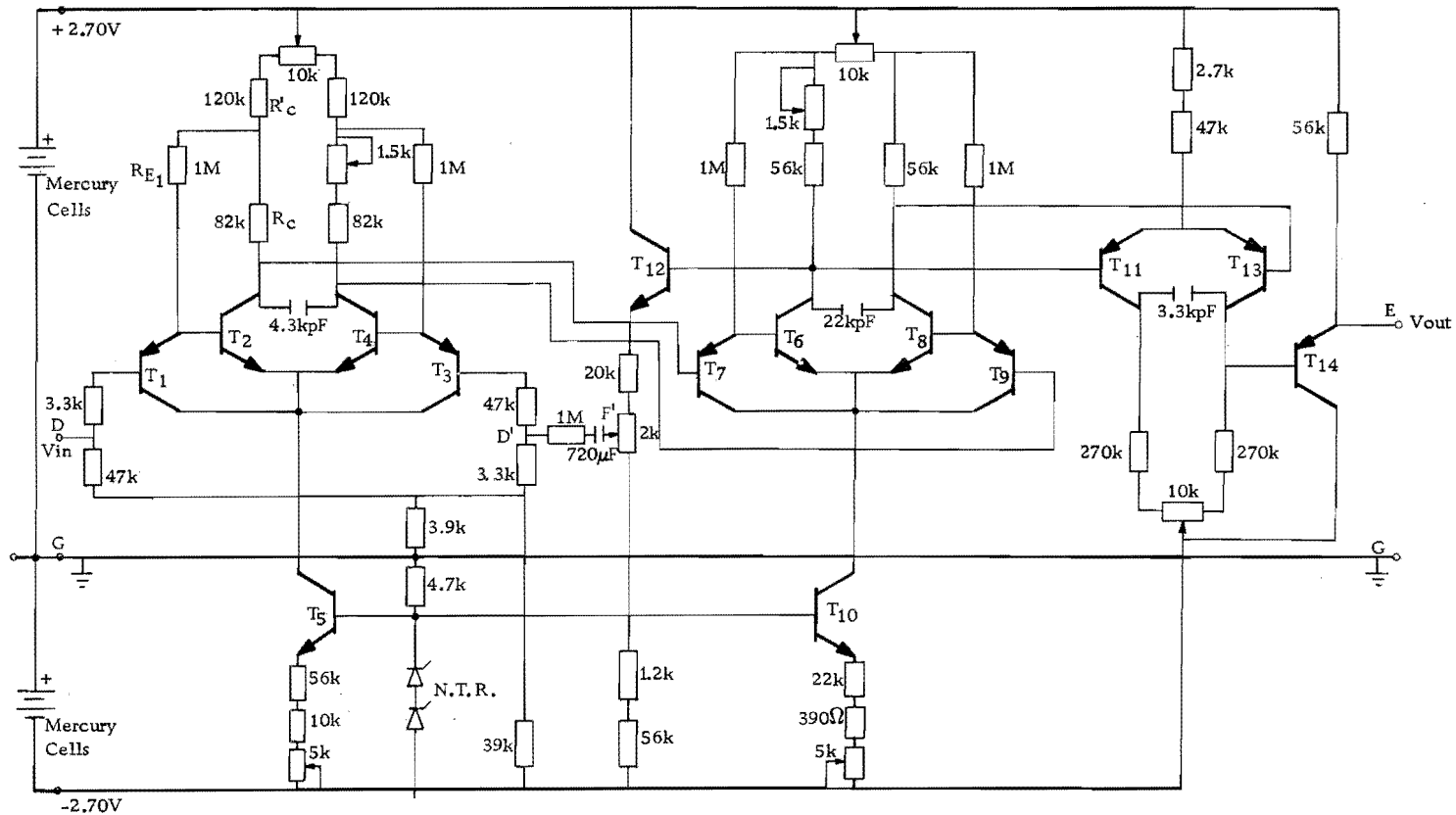


Fig. 3.5 Low noise and low drift pre-amplifier circuit

present are decreased by two effects. First, the transistor pairs  $T_2-T_4$  and  $T_1-T_3$  have matched  $\beta$  values within 2% for the same  $V_{BE}$  bias conditions. Secondly, the transistors of each pair are located on the same crystal chip and the pairs are placed one next to the other. Thus, the temperature and parameter variations of one half,  $T_1-T_2$ , of the differential stage are equal to those of the other half,  $T_3-T_4$ . The current source  $T_5$  of the stage is also on the same crystal chip as  $T_2-T_4$ , (BFX-16), and temperature-compensated on the base by two negative temperature resistors (N.T.R.) of a barrier type. All these considerations can also be applied to the second stage.

The constant bias voltage of the input differential stage is obtained by the potential divider of 39 k $\Omega$  and 3.9 k $\Omega$ . The input circuit resistors are matched within  $10^{-4}$  in order to have practically identical base resistances, with a resistance temperature coefficient of 25 ppm/ $^{\circ}$ C. The other resistors in Fig. 3.5 are also of thin metal film and have also very low noise.

By operating points D' and F', as well as D and F (see section 1), at the same d.c. level, the leakage currents of the tantalum capacitors placed at points F' and F do not affect the input base currents of approximately 10 nA.

All the transistors are operated at very low currents, namely,  $T_1$  at 1  $\mu$ A,  $T_2$  at 10  $\mu$ A. In the second stage,  $T_7$  has an emitter operating current of 1.7  $\mu$ A and  $T_6$  of 22  $\mu$ A. The same may be said of the other half section of these stage respectively. In the third stage,  $T_{11}$  and  $T_{13}$  have a d.c. current of 7  $\mu$ A and the d.c. output level is practically at zero volts.

By adjusting the 10 k $\Omega$  potentiometer in the first stage, it is possible to obtain identical  $V_{BE}$  for  $T_2-T_4$ . Then by adjusting the potentiometer 1.5 k $\Omega$ , both collector voltages are made identical and the second stage has a balanced d.c. input base voltage. This adjusting method is repeated in the second stage yielding the balanced input base voltages of the third.

The first two stages are operated in a hushed-mode, with a  $V_{CB}$  of 50 mV for the emitter follower section and of 300 mV for the amplifier section. Therefore, the properties of low thermal drift, low noise and low distortion may be expected from this pre-amplifier circuit.

A capacitor placed between the collectors of each stage limits the bandwidth, yielding a -3 dB point at 60 Hz in the frequency response of the pre-amplifier.

The over-all voltage gain can be obtained by calculating the voltage gains of each stage and considering the feedback action from the second stage to the first. But owing to the complexity of each differential stage with its own feedback path, even an approximated calculation becomes troublesome and some of the transistor parameter values need to be known at the actual operating currents. Anyhow, the experimentally observed value was approximately  $5 \cdot 10^3$ .

The input impedance, according to (3.11), with a  $\beta_1$  value of 100, is 50 M $\Omega$ . The long term thermal drift was observed to be 0.5  $\mu\text{V}/^\circ\text{C}$  at the input, while the input noise voltage in the 0.06 - 60 Hz frequency band was of the order of  $10^{-7}$  V, peak to peak. This agrees with the later observation on the noise of the total channel, which is mainly due to the noise of the pre-amplifier. The channel turned out to have an input equivalent noise resistance  $R_n$  of 25 k $\Omega$  at room temperature. Its spectrum is white down to 3Hz and then it increases as  $\omega^{-\beta}$ , where  $\beta = 1.68$  (see Fig. 4.1).

The pre-amplifier is energised with  $\pm 2.7$  V from mercury cells. A total amount of 300  $\mu\text{A}$  operating current is needed and the power consumption is 1.5 mW.

### 3. Block 3: Wide-band prewhitening filter

The considerations in chapter 2, section 4, make us interested in a prewhitening filter with a transfer function  $|H(\omega)|$  proportional to  $\sqrt{\omega}$ . Then for any frequency component  $\omega$  of the signal, the output  $v_o$  and input  $v_{in}$  amplitudes of the voltage are related by:

$$v_o = k \sqrt{\omega} v_{in} \quad (3.18) \quad 57$$



Zaalberg van Zelst<sup>3-29</sup> has designed a filter that follows equation (3.18) within a certain frequency range. Such a filter is shown in Fig. 3.6. The appropriate values of resistors and capacitors for the frequency range  $10^{-3}$  to 50 Hz are given below. The component pair  $C_0$ - $R_0$  constitutes a high-pass section filter with a slope of 6 dB/octave. The seven series branches R-C placed in parallel with  $R_0$  reduce the slope to 3 dB/octave. Since there is a capacitor at its input the d.c. component and the ultra-low frequencies of the input signal are blocked.

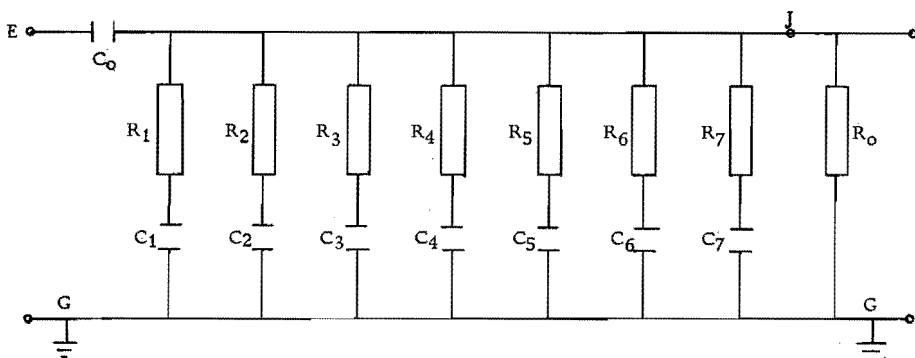


Fig. 3.6. Wide-band prewhitening filter,  $k \sqrt{f}$

The actual values have been realised within  $10^{-4}$  of the prescribed values. The capacitors used are made of polysterene which is the dielectric with characteristics closest to those of mica. The resistors are of the metal film type for values up to 1.5 M $\Omega$ ; three high-quality low-noise carbon resistors APKD are used for larger values. The  $R_0$  resistor is actually the input impedance of the following block 4. The R-C values are given below:

$C_0$ : 63.792 kpF	$R_0$ : 6.5000 M $\Omega$
$C_1$ : 3.3000 $\mu$ F	$R_1$ : 7.1890 M $\Omega$
$C_2$ : 1.5412 $\mu$ F	$R_2$ : 3.8233 M $\Omega$
$C_3$ : 0.79868 $\mu$ F	$R_3$ : 1.9526 M $\Omega$
$C_4$ : 0.41293 $\mu$ F	$R_4$ : 1.0042 M $\Omega$
$C_5$ : 0.21236 $\mu$ F	$R_5$ : 519.09 k $\Omega$
$C_6$ : 108.44 kpF	$R_6$ : 268.97 k $\Omega$
$C_7$ : 57.656 kpF	$R_7$ : 125.64 k $\Omega$

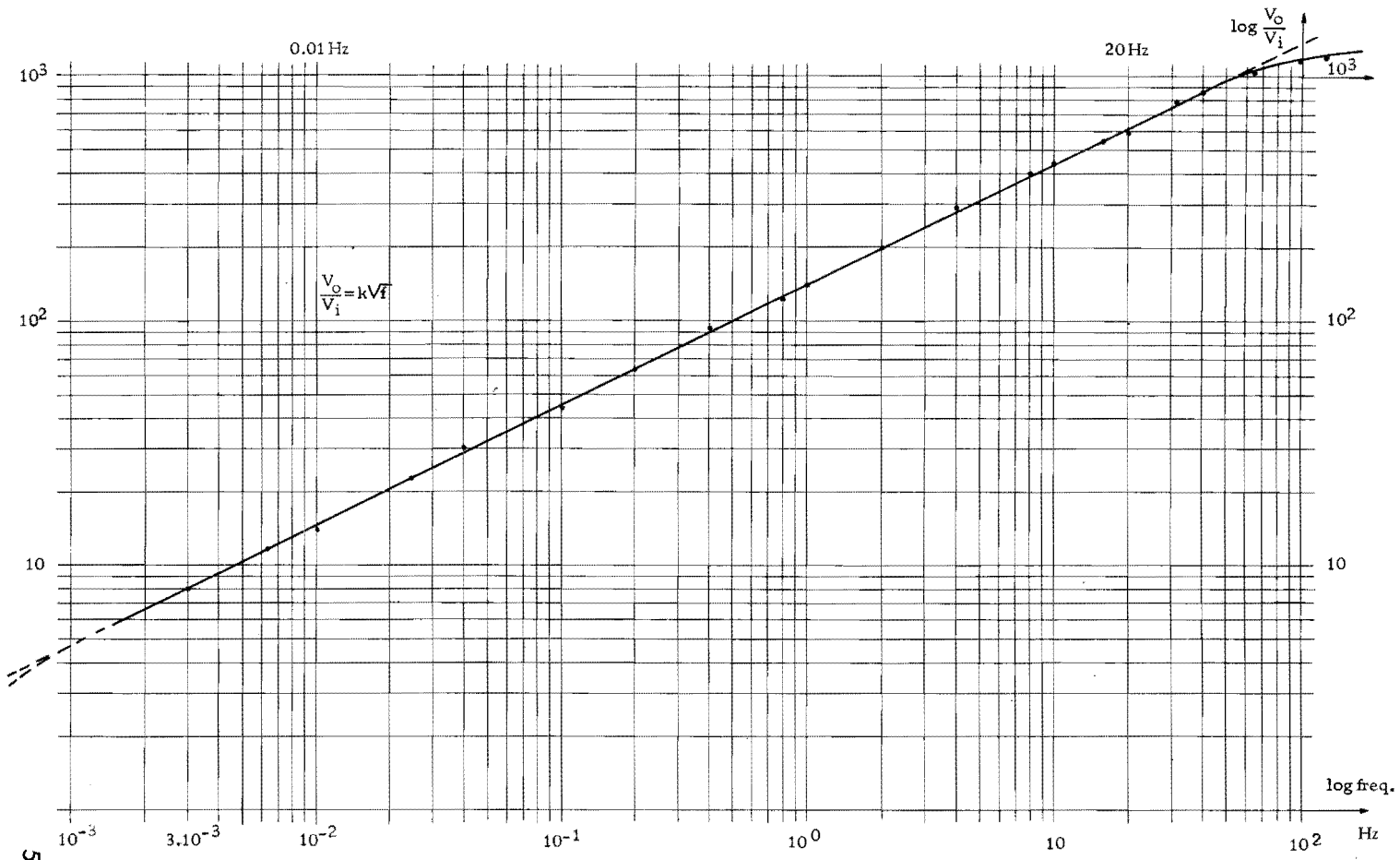


Fig. 3.7 Amplitude transfer characteristic curve of the filter  $k\sqrt{f}$

The measured response of the filter of Fig.3.6 is shown in the graph of Fig.3.7 on a log-log scale. The ratio  $v_o/v_{in}$  follows a  $k\sqrt{\omega}$  law within  $\pm 2.0\%$  in the frequency range  $10^{-2}$  to 20 Hz, yielding a power spectrum  $|H(\omega)|^2$  which follows a  $k^2\omega$  law within less than 4% in the above frequency range.

#### 4. Block 4: Ultra-low frequency active filter

When designing active filters the use of an operational amplifier with a selective network is a straightforward procedure. For frequencies below 10 Hz, L-C selective networks are not convenient since large values of C or L are needed, which are bulky in size and sensitive to external influences, especially the coils. Capacitors, however, are by far less sensitive to pick-ups at low frequencies and there is a much larger variety with respect to values and characteristics in manufacture. Therefore, an R-C selective network is resorted to.

The complex poles of a transfer function  $H(\omega)$  can be realised by means of an active R-C network<sup>3-30</sup>. When the selective network corresponds to a rejection-band and is placed in the feedback path of an amplifier, the compound network becomes a selective active filter. The choice is made for a Twin-T circuit since it can give transmission zeros on the imaginary axis and therefore will permit, at least theoretically, a complex pole pair with any Q value to be realised.

From the theoretical considerations of measurement, chapter 2, section 3, a bell-shaped  $H(\omega)$  filter is required with a low-Q factor. Now, a Twin-T circuit is known to have a characteristic curve similar to a resonant L-C circuit, and hence its form is close to the Gaussian or to a bell-shaped curve when it has a low-Q factor.

Fig. 3.8 shows the symmetrical Twin-T circuit with its source  $R_s$  and load  $R_L$  impedances. The transfer function is given by<sup>3-31</sup>:

$$H(\omega) = \frac{j m}{4 + j m} \quad (3.19)$$

where,  $m = \omega/\omega_0 - \omega_0/\omega$  and the nulling frequency is:

$$60 \quad \omega_0 = 1/RC \quad (3.20)$$

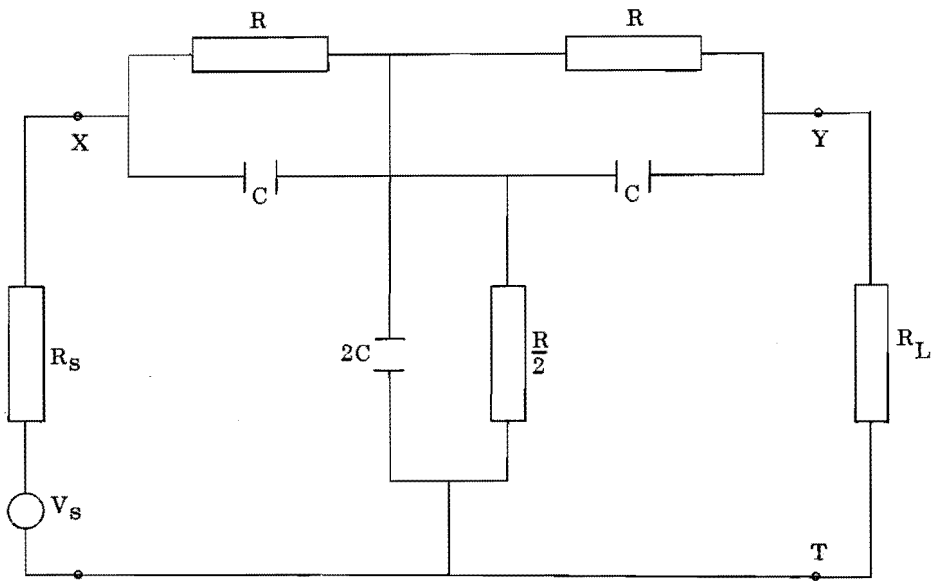


Fig. 3.8 Nulling frequency network using a Twin-T circuit

In order to have an  $H(\omega)$  symmetrical around  $\omega_0$  it is necessary that the relation  $R^2 = 2 R_s R_L$  be satisfied in the actual circuit<sup>3-32</sup>.

When the circuit of the Twin-T is placed in the feedback path of an amplifier with open-loop gain  $A_o$ , and  $m$  is small (as happens at frequency values near to the nulling frequency) it can be shown that the  $Q$  of the selective filter is closely calculated from<sup>3-33</sup>

$$Q = \frac{A_o + 1}{4} \quad (3.21)$$

If an integrated amplifier is used, we may not be able to realise the equation  $R^2 = 2 R_s R_L$  since its output impedance is very small and the needed value of  $R$  must be large in order not to have too large values of capacitance in (3.20) at  $f_0$  of  $10^{-2}$  Hz. Consequently, the input impedance of the operational amplifier must be extremely high. At the same time the signal must be transferred from the  $k\sqrt{\omega}$  filter into the selective filter without affecting the value  $R_o$  of  $6.5 \text{ M}\Omega$  in Fig. 3.6 point J.

These difficulties have been avoided by using the circuit of Fig. 3.9. It consists essentially of a high input impedance, unity gain, 61

amplifier stage  $T_1$ - $T_2$  and of a differential stage  $T_6$ - $T_7$ , with a selective Twin-T circuit in one of the feedback loops. The output is via an emitter follower  $T_9$ .

The input Darlington pair is biased by a potential divider  $R_1$ - $R_2$  of low noise and special carbon APKD resistors. The input impedance at point J is adjusted so as to have the right value to replace the resistor  $R_0$  of Fig. 3.6, which permits a direct coupling of the signal.

The operating input base current of  $T_1 \leq 10$  nA and the compound transistor pair is temperature stabilised doubly. This is done by slightly draining off part of the base current of  $T_2$ <sup>3-34</sup> and secondly, by an overall d.c. feedback through the bleeding resistor  $R_3$ . The latter is connected across points of practically the same d.c. potential level by means of the potentiometer  $R_{13}$ . Temperature variations between  $T_1$  and  $T_2$  are reduced by enclosing both transistors under a common polyesterene cap<sup>3-35</sup>. Polyesterene is a resin which has the property of being a very good temperature conductor and a very high electrical insulator.

Transistors  $T_6$ - $T_7$  are a matched pair within 3% for  $\beta$  values at equal  $V_{BE}$ . Equal base-emitter voltages are obtained by adjusting the potentiometer  $R_5$ . The transistors are mounted together with  $T_8$  on the same crystal chip (BFX-16).

The gain of the differential stage is stabilised by the collector-to-base feedback of  $T_7$  via  $T_9$ . A stable d.c. zero output level is obtained at point L of potentiometer  $R_{12}$  with an output impedance of approximately 330  $\Omega$ . Capacitor  $C_1$  determines the bandwidth from d.c. to 85 Hz for the differential stage while  $C_0$  affects the overall response of the circuit of Fig. 3.9 only for frequencies greater than 60 Hz, reducing the contribution of the high frequency side-tail in the selective filter. All resistors are of the 1%, low noise, 150 ppm/ $^{\circ}$ C, thin metal film type.

R being equal to 4 M $\Omega$  in Fig. 3.8 and  $R_8$  equal to 27 k $\Omega$  in Fig. 3.9, the  $R_L$  needed for a symmetrical characteristic curve of the Twin-T circuit is well approximated by the input impedance of the Darlington pair  $T_4$ - $T_3$ , which has very large  $\beta$  values at low operating cur-

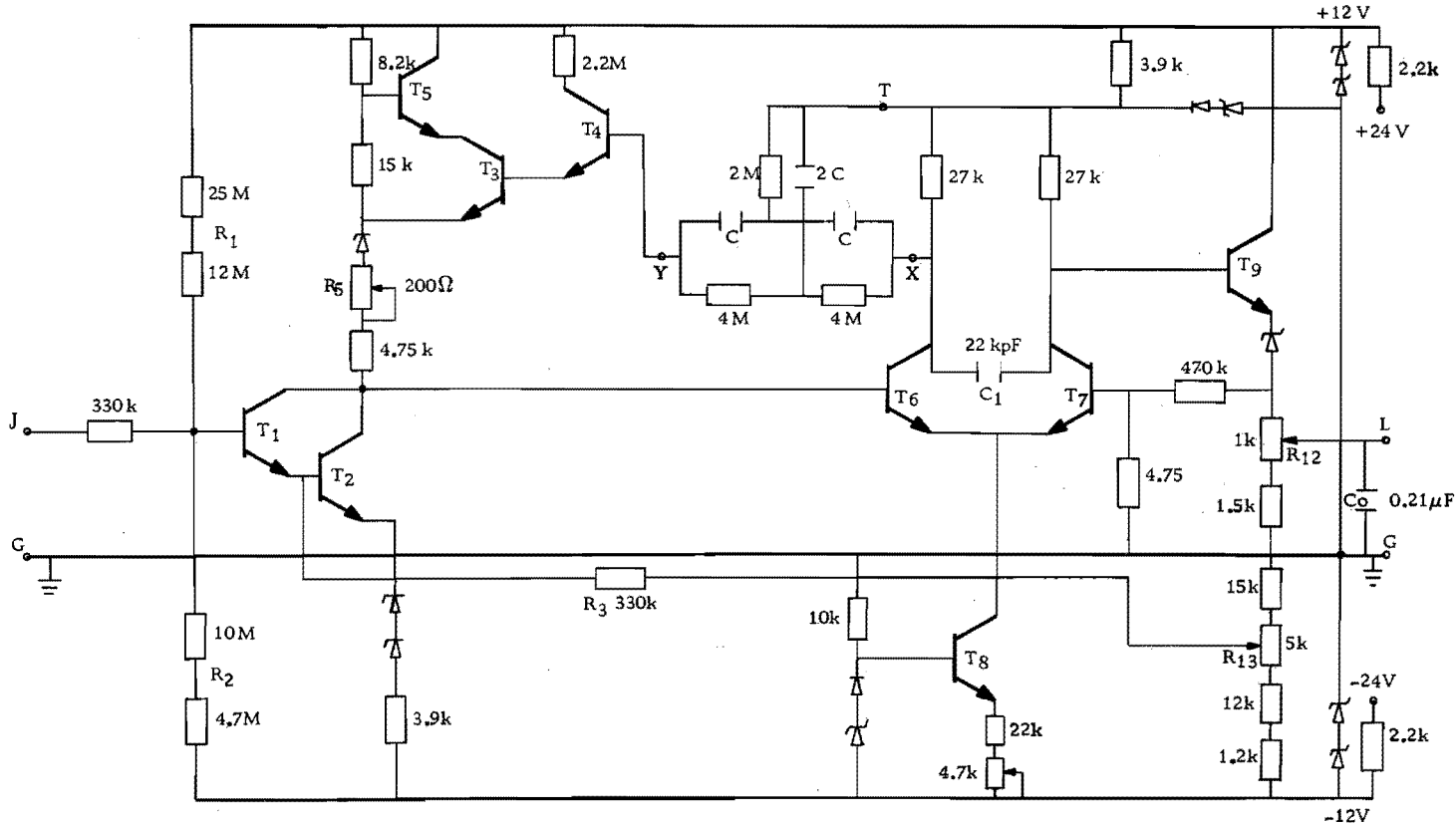


Fig. 3.9 Very-low frequency selective amplifier

rents; the base current of  $T_4$  is 4 nA. Both transistors are operated with low  $V_{CB}$  to have a low noise contribution according to equation (3.16) and are enclosed in a common polysterene cap against temperature changes.

The Twin-T circuit has fixed equal resistor  $R$  values of  $4 \text{ M}\Omega$  within  $10^2$  ppm, the resistors being of the  $1/4 \text{ W}$ , metal film type and having a temperature coefficient of  $25 \text{ ppm}/^\circ\text{C}$ . The capacitors  $C$  are made of polysterene or of mica with values realised within  $10^{-5}$  of the required ones by equation (3.20) for the desired spot frequencies. Their leakage current, of the order of  $10^{-12} \text{ A}$ , is completely negligible. The selective frequency is obtained by exchanging the capacitors (as suggested in chapter 2, section 7) by means of a four-section ceramic switch; all are placed immediately underneath the circuit arrangement of Fig. 3.9. To avoid possible leakage currents owing to humidity a container of silica gel is provided to keep the atmosphere dry.

It was noticed that, owing to the complex wiring of the selective switch, for equal input conditions the amplitude of the selectivity curve decreased slightly as the selective frequency was increased above 2 Hz. The cause seemed to be the parasitic capacitance between several points of the Twin-T circuit, increasing the actual value of  $C$  by  $C_p$ . Indeed, according to this assumption a constant amplitude of the selectivity curve was obtained by decreasing successively  $R/2$  of Fig. 3.8 by an amount  $R'/2$ , within the frequency range 2 to 20 Hz. In Fig 3.10 the resistors  $R_1/2$  and  $R'_1/2$  are in series and their values, as given in the table below, verify the relation  $(R_1 + R'_1)/2 = (R - R')/2$ . The value of  $C_p$  appeared to be 85 pF and this correction method showed to be very efficient in practice.

The constant voltage gain of the network of Fig. 3.9 gives a constant  $Q$  value to the frequency response curve of each filter. Experimentally the value of  $Q$  was set equal to 5 and the frequency response followed well a symmetrical curve centered at  $f_0 = \sqrt{f_1 f_2}$ ,

The bank Twin-T network is shown in Fig. 3.10. The following values of resistors and capacitors were used:

		R	4.000	MΩ			$R_1/2$	1.931	MΩ		
$f_1$	0.010	Hz	C	3.9788	μF	2C	7.9590	μF	$R_1'/2$	83.56	kΩ
$f_2$	0.0215	Hz		1.8468	μF		3.6938	μF		83.40	kΩ
$f_3$	0.0464	Hz		0.85777	μF		1.7140	μF		83.10	kΩ
$f_4$	0.10	Hz		0.39793	μF		0.79585	μF		82.60	kΩ
$f_5$	0.215	Hz		0.18478	μF		0.36923	μF		82.56	kΩ
$f_6$	0.464	Hz		85.732	kpF		171.52	kpF		82.48	kΩ
$f_7$	1.00	Hz		39.775	kpF		79.580	kpF		82.45	kΩ
$f_8$	2.15	Hz		18.500	kpF		36.970	kpF		76.51	kΩ
$f_9$	4.64	Hz		8.5875	kpF		17.160	kpF		55.37	kΩ
$f_{10}$	10.0	Hz		3.9820	kpF		7.9640	kpF		26.93	kΩ
$f_{11}$	19.8	Hz		1.9925	kpF		3.9835	kpF			

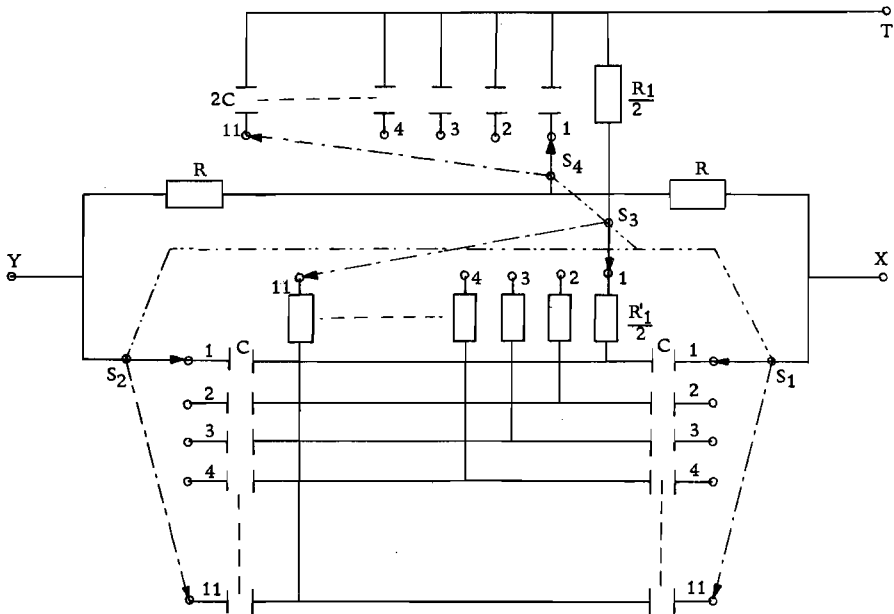


Fig. 3.10 Bank of filters using a Twin-T circuit with the selective switch  $S_1-S_2-S_3-S_4$



## 5. Block 5: Main amplifier

The circuit of Fig. 3.11 shows the selective gain amplifier based on an integrated operational amplifier, RC709D, the gain of which is very large. The operational amplifier is connected as a non-inverting amplifier with an  $R_F$  feedback resistor of 56 k $\Omega$ . The voltage gain of the circuit is given closely by:

$$A_v = 1 + R_F/R_2' \quad (3.22)$$

where  $R_2'$  is the parallel combination of  $R_2$  and the input differential impedance  $R_{in}$  of the amplifier.

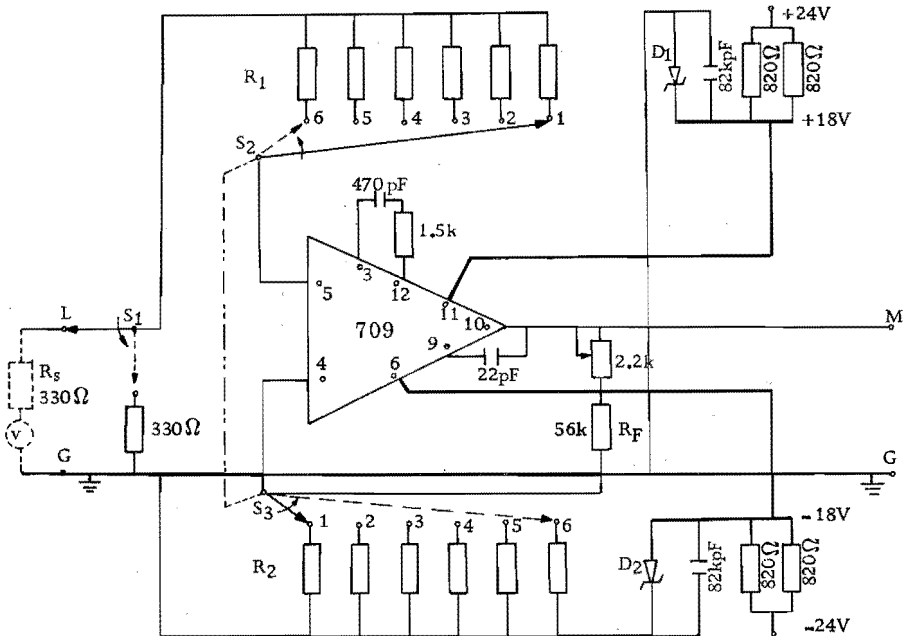


Fig. 3.11 Main amplifier with selective gain adjusted by switch

Now, once the desired voltage gain  $A_v$  is chosen, the required  $R_2$  may be calculated from (3.22). The source impedance of the inverting input  $R_{s2}$  is the parallel combination of  $R_F$  and  $R_2$ . Then a source impedance ( $R_{s1} = R_1 + R_s$ ) at the non-inverting input equal to  $R_{s2}$  is introduced in order to reduce the input differential drifts.

The input signal at terminals L and G is taken from a zero d.c. potential level and a source resistance  $R_s$  of  $330 \Omega$  at the output of block 4. By adjusting the potentiometer of  $2.2 \text{ k}\Omega$  on the feedback path, a zero d.c. output level is obtained at point M.

The actual voltage gains  $A_{v_i}$ ,  $i$  from 1 to 6, are:

$$A_v: 2.0 ; 5.0 ; 7.5 ; 10.5 ; 21.0 ; 31.5.$$

$A_{v_i}$  is selected by means of the switch  $S_2-S_3$ , which simultaneously connects the values of  $R_1$  and of  $R_2$ .

The bank of resistors  $R_1$  and  $R_2$  have small bias currents, are of metal film type, and have a very low noise voltage, viz.  $0.1 \mu\text{V/V}$ . The operational amplifier is frequency compensated to have a flat band response from d.c. to 100 Hz.

The object of switch  $S_1$  is to disconnect the input signal which may have large transients when the selective frequency of the filter is changed, since then the charged capacitors of the Twin-T circuit are replaced by other capacitors.

Taking into account the specified input differential impedance  $R_{in}$  of  $400 \text{ k}\Omega$  and equation (3.22), we find the values of  $R_{1i}$  and  $R_{2i}$  within  $10^{-4}$  to be as follows:

$A_{v1}$	$R_{11}$	27.710 $\text{k}\Omega$	$R_{21}$	56.100 $\text{k}\Omega$
$A_{v2}$	$R_{12}$	11.250 $\text{k}\Omega$	$R_{22}$	14.500 $\text{k}\Omega$
$A_{v3}$	$R_{13}$	7.860 $\text{k}\Omega$	$R_{23}$	9.557 $\text{k}\Omega$
$A_{v4}$	$R_{14}$	5.380 $\text{k}\Omega$	$R_{24}$	6.310 $\text{k}\Omega$
$A_{v5}$	$R_{15}$	2.516 $\text{k}\Omega$	$R_{25}$	2.977 $\text{k}\Omega$
$A_{v6}$	$R_{16}$	1.576 $\text{k}\Omega$	$R_{26}$	1.941 $\text{k}\Omega$

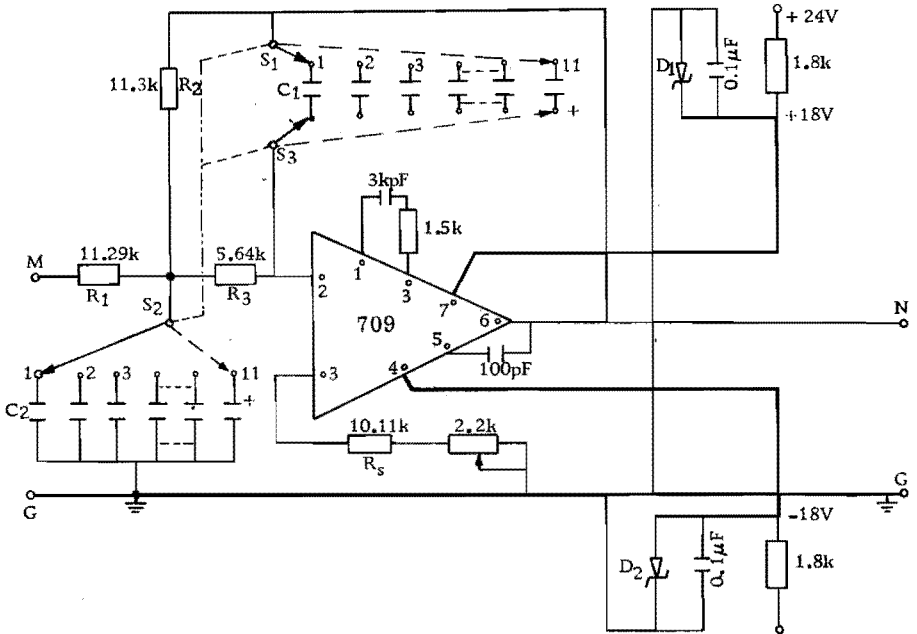
## 6. Block 6: Selective low-pass filter

The bell-shaped characteristic curve of a Twin-T circuit when fed back has tails extending over several decades. Therefore, according to the considerations of chapter 2, section 3, we introduce a low-pass filter with cut-off frequency  $4\omega_0$  in order to decrease the contribution of the high frequency tail in the main filter centered at  $\omega_0$ .

For an operational amplifier with a very large voltage gain  $A_v$  and high input differential impedance, the transfer function  $H(\omega)$  of the circuit of Fig. 3.12 can be shown to be given by<sup>3-36</sup>:

$$H(\omega) = \frac{-A_v \omega_0'^2}{s^2 + a\omega_0' s + \omega_0'^2} = -1/R_1 R_3 \cdot 1 / (s^2 C_1 C_2 + s C_1 (1/R_1 + 1/R_3 + 1/R_2) + 1/R_2 R_3) \quad (3.23)$$

where  $A_v$  is the voltage gain of the circuit,  $s = j\omega$  and  $\omega_0'$  is the cut-off frequency from which the roll-off response is 40 dB/decade.



68 Fig. 3.12 Low-pass active filter with selective switch  $S_1$ - $S_2$ - $S_3$

Now, choosing

$$C_1 = k/\omega'_0 \quad (3.24)$$

equation (3.23) yields:

$$C_2 = 4/a^2 \cdot (A_v + 1)C_1; \quad R_1 = a/2kA_v; \quad R_2 = a/2k = R_1 \cdot A_v; \\ R_3 = a/2k(A_v + 1) \quad (3.25)$$

and the filter shows to have a maximally flat band response for  $a = \sqrt{2}$ .

A source resistor  $R_s = R_3 + R_2/R_1$  is placed at the non-inverting input, for the elimination of the d.c. drifts. The potentiometer of 2.2 k $\Omega$  in series with  $R_s$  allows to obtain a zero d.c. level output. The selected  $\omega'_0$  values are obtained by the use of switch  $S_1$ - $S_2$ - $S_3$  which simultaneously varies the values of  $C_1$  and  $C_2$ .

Now, let us choose the following parameter values;

$$f_0 = 20 \text{ Hz}; \quad f'_0 = 4f_0; \quad C_1 = 0.125 \text{ }\mu\text{F}; \quad A_v = 1; \quad a = \sqrt{2}.$$

Then, from the set of equations (3.27) and (3.28) we obtain:

$$R_1 = R_2 = 11.275 \text{ k}\Omega, \quad R_3 = 5.637 \text{ k}\Omega, \quad C_2 = 0.50 \text{ }\mu\text{F}.$$

The following values of  $C_1$  and  $C_2$  were realised with tantalum and polyesterene capacitors in the bank of low-pass filters of Fig. 3.12:

$f_1$	0.01	Hz	actual	$f'_1$	0.0373	Hz	$C_{1-1}$	1010	$\mu\text{F}$	$C_{2-1}$	251.0	$\mu\text{F}$
$f_2$	0.0215	Hz		$f'_2$	0.0819	Hz	$C_{1-2}$	468.0	$\mu\text{F}$	$C_{2-2}$	116.1	$\mu\text{F}$
$f_3$	0.0464	Hz		$f'_3$	0.176	Hz	$C_{1-3}$	215.0	$\mu\text{F}$	$C_{2-3}$	53.85	$\mu\text{F}$
$f_4$	0.10	Hz		$f'_4$	0.387	Hz	$C_{1-4}$	99.7	$\mu\text{F}$	$C_{2-4}$	24.8	$\mu\text{F}$
$f_5$	0.215	Hz		$f'_5$	0.83	Hz	$C_{1-5}$	46.1	$\mu\text{F}$	$C_{2-5}$	11.58	$\mu\text{F}$
$f_6$	0.464	Hz		$f'_6$	1.79	Hz	$C_{1-6}$	21.55	$\mu\text{F}$	$C_{2-6}$	5.38	$\mu\text{F}$
$f_7$	1.0	Hz		$f'_7$	4.01	Hz	$C_{1-7}$	10.00	$\mu\text{F}$	$C_{2-7}$	2.49	$\mu\text{F}$
$f_8$	2.15	Hz		$f'_8$	8.48	Hz	$C_{1-8}$	4.68	$\mu\text{F}$	$C_{2-8}$	1.167	$\mu\text{F}$
$f_9$	4.64	Hz		$f'_9$	18.5	Hz	$C_{1-9}$	2.17	$\mu\text{F}$	$C_{2-9}$	0.537	$\mu\text{F}$
$f_{10}$	10.0	Hz		$f'_{10}$	40.0	Hz	$C_{1-10}$	1.00	$\mu\text{F}$	$C_{2-10}$	0.248	$\mu\text{F}$
$f_{11}$	19.8	Hz		$f'_{11}$	79.4	Hz	$C_{1-11}$	0.50	$\mu\text{F}$	$C_{2-11}$	0.125	$\mu\text{F}$

## 7. Block 7: Analogue multiplier

A commercial solid-state unit was used, M 101 of Intronics, which operates on a pulse-height pulse-width principle. It has its own internal clock frequency of 25 kHz and can take inputs of  $\pm 10$  volts; the output has a  $10^{-1}$  attenuation constant.

Both input impedances are larger than 75 k $\Omega$  and yield a linearity better than 0.25%. This linearity is defined as the maximum deviation from the best straight line divided by the full scale value. For an output voltage of 20 Vpp, the frequency response is flat within  $\pm 1\%$  from d.c. to 300 Hz and down 3 dB at 1 kHz.

The output drift is  $\pm 0.5$  mV/ $^{\circ}$ C max., while a small amount of output ripple and noise exists, owing to the clock frequency signal; however, the output ripple is only 1 mV max. pp from 5 Hz to 1 kHz. The d.c. offset level is smaller than  $\pm 10$  mV for zero inputs.

## 8. Block 8: Hybrid integrator-averager

The integration is performed by an analogue-digital converter (A-D) and an electronic counter.

As analogue-digital converter was used a type M 651 Beckman voltage-to-frequency converter. The output pulse frequency is precisely proportional to the d.c. input voltage and has an almost instantaneous response to changes in input voltage. Therefore, the output frequency accurately follows the variations of the input voltage.

The A-D converter has full-scale sensitivities of 0.1, 1.0, 10, 100, and 1000 V d.c., yielding a 0 to 100 kHz pulse output for full scale sensitivity, and for both input polarities without switching. Its linearity is better than  $\pm 0.02\%$  of full scale and its input may still be increased by approximately 30% above full scale with an output accuracy of  $\pm 0.15\%$ . The input impedance is 100 k $\Omega$  for 0.1V d.c. input range and 1 M $\Omega$  for all other ranges. A d.c. blocking tantalum capacitor of 340  $\mu$ F was placed at the input of the A-D converter to eliminate the d.c. output offset of the multiplier.

The electronic counter used was a 3734A Hewlett-Packard instrument with five digits display to which a six digit electro-mechanical

counter was connected to count the number of times the electronic counter saturates.

A stop-clock records the measuring time  $T$  prescribed by the theoretical considerations. The electronic mechanical counter result is divided by  $T$  and the bandwidth  $\Delta\omega_0$  at the end of each prescribed frequency  $\omega_0$  measurement. Thus, a quantity is obtained which is proportional to the average noise power density centered at  $\omega_0$ .

## MEASUREMENTS AND ANALYSIS OF LOW-FREQUENCY NOISE

(A) Flicker Noise in Resistors1. Experimental state of art

Bernamont in 1934 was the first observer of noise in excess of thermal noise and which was generated in certain resistors with a steady current through them<sup>4-1</sup>. When the current flows, fluctuations of voltage or current of relatively small amplitude, but with a very uneven distribution, appear at the terminals of the resistor. This phenomenon is normally referred to as current noise or flicker noise.

Experimental results have commonly shown that the spectral density of the current noise is given by the relation:

$$S(\omega) = k I^\alpha \omega^{-\beta} = k' V^\gamma \omega^{-\beta} \quad (4.1)$$

where  $k$  and  $k'$  are constants,  $I$  is the d.c. current,  $V$  is the d.c. applied voltage,  $\omega$  is the angular frequency of measurement. The exponents  $\alpha, \gamma$  and  $\beta$  are parameters. If Ohm's law is valid here,  $\alpha = \gamma$ .

Most investigators<sup>4-1 - 4-10</sup> have found experimentally the value 2 for  $\alpha$  and  $\gamma$  in carbon resistors operated at low-current levels. As to the value of  $\beta$ , there seems to be no agreement. Table 4-1 contains a historical view showing a spread of the  $\beta$  value from 0.6 to 72 1.4 for carbon resistors in the low frequency range  $10^{-4}$  Hz to 1 kHz.

Table 4-1

Investigator:	Year:	Value of			Freq.
		$\alpha$ :	$\gamma$ :	$\beta$ :	Range:
Bernamont <sup>4-1</sup>	1934	2, low current	2	0.88-1.1 low freq. 2, high freq.	96Hz-162kHz
Otto <sup>4-2</sup>	1934		2	1-1.4	5Hz-1kHz
Meyer and Theide <sup>4-3</sup>	1935	2	2	1-2	
Christensen and Pearson <sup>4-4</sup>	1936		1.75-1.9	1	50Hz-10kHz
Abson, Harris and Roberts <sup>4-5</sup>	1946	1.7-1.9		1	0.3Hz-500Hz
Campbell and Chipman <sup>4-6</sup>	1948	2		1.1 low freq. 1.7 high freq.	10kHz-500kHz
Templeton and MacDonald <sup>4-7</sup>	1953	2		1.01	2.510 <sup>-4</sup> Hz- 7.5Hz
Van Vliet, Van Leeuwen, Blok and Ris <sup>4-8</sup>	1954	2		1-1.1	10kHz-1MHz
Kirby <sup>4-9</sup>	1959		1.4-2.2	0.6-1	250Hz-200kHz
Brophy <sup>4-10</sup>	1965	2		1.02	8Hz-10kHz

2. Considerations on measurements

We too have also done measurements on carbon-film resistors and found fluctuations with time in the parameter  $\beta$  in each individual resistor measured and operated at very low current levels. It was thought that such an operating mode would allow the appearance of relevant features which may be obscured at higher current levels.

In addition to the non-constancy of  $\beta$ , some resistors have a very unstable noise with frequent bursts of noise during short periods of time which cannot be considered as normal fluctuations<sup>4-6, 4-8, 4-9</sup>. Campbell and Chipman<sup>4-6</sup>, when measuring carbon resistors, found similar bursts at 150 kHz, but it was not possible for them to determine if the abnormal fluctuations were simultaneously present at



different frequencies. Recently, Williams and Burdett<sup>4-11</sup> found that randomly spaced pulses were often superimposed on the statistically regular current noise in cermet resistor films.

The relative output-noise power density  $\omega \cdot S(\omega)$  was measured for 10 M $\Omega$  carbon resistors with a direct current of 1  $\mu$ A. Fig. 4.1 shows the measurements carried out with a desired statistical error  $\epsilon$  from 2% at a spot frequency of 20 Hz to 7.5% at 0.01 Hz. It took almost three days to measure this spectrum range.

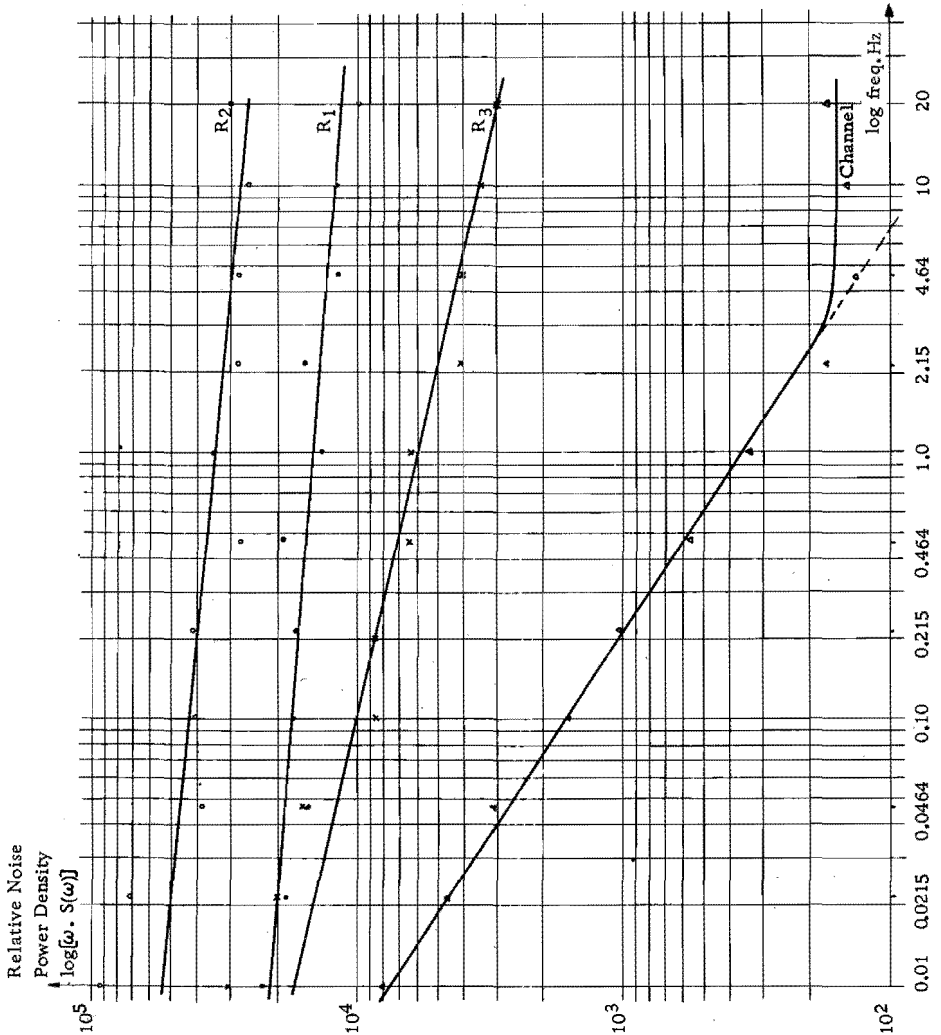


Fig. 4.1 Relative noise power density spectrum of the measuring channel and of the resistors  $R_1$ ,  $R_2$ ,  $R_3$

First, the noise power density of the channel was measured. It is seen to have a white noise spectrum down to 3 Hz and then follows the  $\omega^{-\beta}$  law with  $\beta$  equal to 1.68. At 3 Hz the channel has an equivalent noise resistance  $R_n$  of 25 k $\Omega$  at room temperature and for unity bandwidth.

A straight line fits the eleven spectral points of each of the three measured resistors  $R_1$ ,  $R_2$  and  $R_3$ , when plotted on a log-log scale indicating an input spectrum of the type:

$$S(\omega) = K \omega^{-\beta} \quad 1.09 < \beta < 1.22 \quad (4.2)$$

The resistors  $R_1$ ,  $R_2$ ,  $R_3$  were chosen for being especially noisy samples.

Nevertheless, some points in Fig. 4.1 appear to deviate from the best straight line by much more than the allowable  $\pm 2 \epsilon$ , mainly at the lowest frequencies. It seems we are dealing with fluctuations of fluctuations.

From the theoretical point of view, Mandelbrot<sup>4-12</sup> has shown that functions can be constructed from random repeatable sequences to have a spectral density of the type  $\omega^{-\beta}$ ,  $0 \leq \beta \leq 2$ , which behave more erratically in time than is expected from functions subjected to the Wiener-Khintchine theorem. When averaged over a long time, these functions do not have a Gaussian distribution, and extreme values have a high probability of occurrence, although the marginal distribution of the function may itself be Gaussian.

Indeed, noise measurements on the above cracked-carbon film resistors taken during long periods of time have shown a current noise fluctuating randomly between a high and a low noise level, and having a non-Gaussian distribution. Therefore, it appeared clearly from the above considerations and from the presence of bursts that, if the noise mechanism belonged to a quasi-stationary process, it would be necessary to measure a shorter spectrum range in a shorter time in order to be able to measure the noise during the same operating mode and excitation state of the sample under investigation.

Table 4-II

Measure- ment, N <sup>o</sup>	Time of Measure- ment, hour	Relative Output Noise Power Density: $\omega.S(\omega)$						Slope at output, $\beta-1$	%, $\epsilon$ Statistical Error	%, Max. Deviation from straight- line
		20cs	10.0cs	4.64cs	2.15cs	1.0cs	0.46cs			
1	1 <sup>st</sup> <sub>h</sub>	67	90	104	119	156	147	0.20	9.49	14.8
2	3 <sup>rd</sup> <sub>h</sub>	141	155	157	235	293	337	0.27	9.33	18.7
3	4 <sup>th</sup> <sub>h</sub>	70	63	89	113	164	190	0.31	14.57	22.0
4	5 <sup>th</sup> <sub>h</sub>	68	57	87	105	138	170	0.28	13.58	21.4
5	6 <sup>th</sup> <sub>h</sub>	56	83	100	188 <sup>+</sup>	367 <sup>+</sup>	566 <sup>+</sup>	0.64	16.07	27.0
6	22 <sup>th</sup> <sub>h</sub>	49	64	88	210 <sup>+</sup>	171 <sup>+</sup>	326 <sup>+</sup>	0.54	24.88	40.2
7	24 <sup>th</sup> <sub>h</sub>	146	160	164	283	356	368	0.32	16.28	22.80
8	27 <sup>th</sup> <sub>h</sub>	47	58	87	90	150	163	0.32	10.51	15.46
9	28 <sup>th</sup> <sub>h</sub>	66	81	116	173 <sup>+</sup>	335 <sup>+</sup>	261	0.46	23.01	35.45

Time T needed for | 10%: 16.05s 31.83s 1m8.6s 2m28.05s 5m18.3s 11m26s  
 statist. error  $\epsilon$  | 2%: 7m 3s 13m16s 28m35s 1h1m14s 2h12m38s 4h45m50s

(+): see text.

### 3. Quasi-stationary noise in resistors

The relative output noise power density  $\omega.S(\omega)$  for nine consecutive measurements on the same resistor  $R_2$  of Fig. 4.1, taken within 28 hours with a desired  $\epsilon$  of 10%, is shown in Table 4-II. Taking into account the waiting time required between two measurements at different frequency values, so that the switching transients have died out, a measuring time of 3/4 h was needed for each row of the spectrum range. The values with an asterisk indicate that considerable burst noise was observed during that measurement. A straight line to fit the noise power data, plotted on a log-log scale, was obtained by taking the average value of two groups of ordinates since the abscissae are equidistant, and the line had a slope of the value  $\beta - 1$ .

Taking Table 4-II as a guide, we may conclude the following. There are two groups of measurements. The first contains the measurements 5, 6 and 9. They show a non-stationary behaviour because bursts were observed during measuring, and they have large deviations from the straight line resulting in a non-Gaussian distribution, as is apparent from the last two columns. The second group is formed by the other measurements, which are much closer to what may be expected from a statistical Gaussian distribution and correspond to stationary peri-

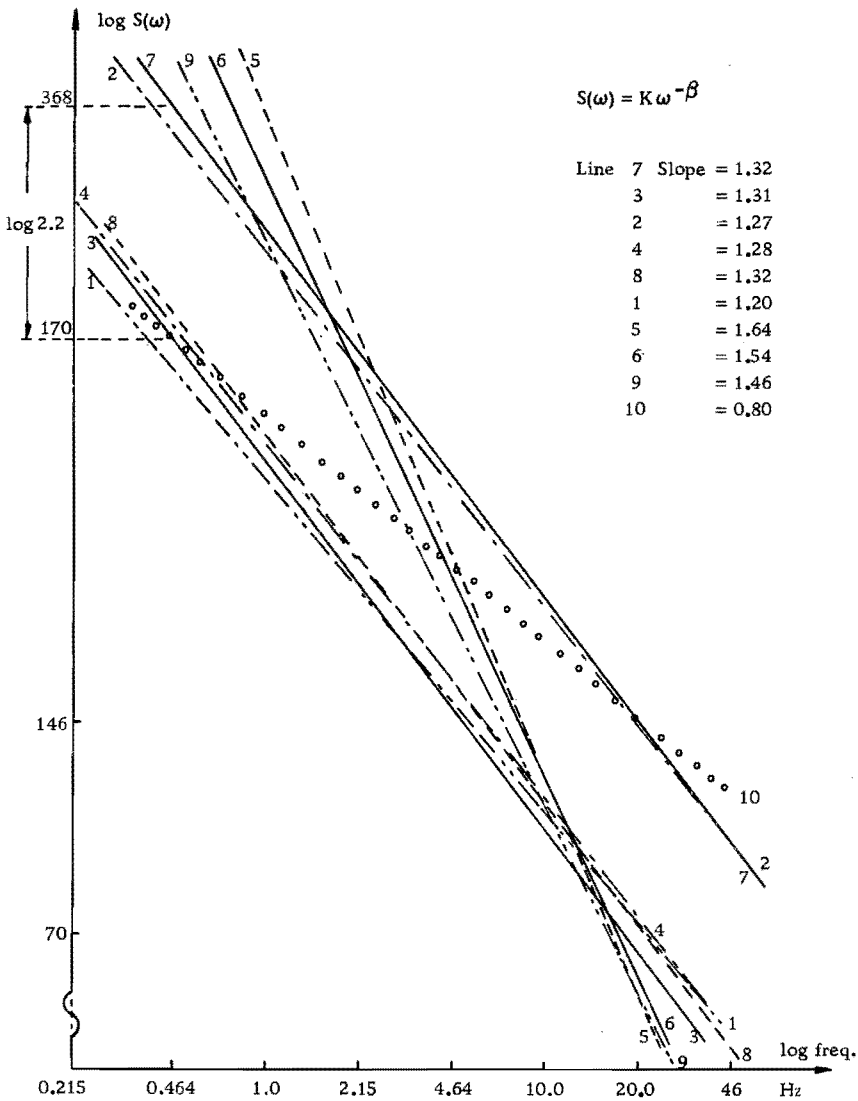


Fig. 4.2 Nine consecutive measurements of current-noise spectrum density as functions of frequency for the carbon resistor  $R_2$ ,  $10\text{ M}\Omega$ , with  $1\text{ }\mu\text{A}$  d.c.

ods of noise with a slope of  $1.28 \pm 0.05$ . Thus its noise spectrum is given by  $S(\omega) = K\omega^{-1.28}$ , where  $K$  may vary by a factor greater than two. The other two sample resistors,  $R_1$  and  $R_3$ , had a  $\beta$  of 1.20 and 1.12 with  $K$  values varying by a factor 2 and 1.4, respectively.

The noise-power data of Table 4-II are plotted in Fig. 4.2 on a log-log scale. Each measurement is represented by its best straight line 77

with its equivalent input slope. It is clear from Fig. 4.2 that there are at least two states of excitation and that the noise power density fluctuates between a high and a low level. Now, if large bursts occurred only during the high-frequency measurements, which is less probable since less measuring time is needed than for low frequencies, a feasible spectrum would have  $\beta \approx 0.8$  (line 10). Hence, the sample in question would have a spread of  $\beta$  from 0.8 to 1.64. This spread agrees with that given in Table 4-I and indicates a difficulty encountered when repeating low-frequency noise measurements. The above considerations were published by the author before<sup>4-13</sup>.

Malakof<sup>4-14</sup> has already considered the possibility of flicker noise being quasi-stationary while following the law of equation (4.1), and concluded that apparently flicker noise can be considered a random non-stationary process with stationary increments. But unfortunately no measurements were carried out under this scope.

More recently, Brophy has studied the probability amplitude distribution of  $1/f$  noise and of Nyquist noise in carbon resistors within the range of 8 Hz to  $10^4$  Hz<sup>4-15</sup>. Brophy found that both types of noise obey a normal distribution law in all the sampling time intervals investigated. But in the case of  $1/f$  noise, the variance of the distribution itself fluctuates in identical sampling intervals. This means that  $1/f$  noise is not stationary in the usual statistical sense such as is true for Nyquist or thermal noise, but rather possesses a weaker form of stationarity.

Brophy himself points out that his experimental technique<sup>4-16</sup> tends to yield greater variance fluctuations in  $1/f$  noise signals than in Nyquist noise signals. This is so because large low-frequency components characteristic of  $1/f$  noise introduce a correlation between successive sampling intervals. Hence, during the same measuring time  $T$  there are fewer independent samples in the case of  $1/f$  noise compared to Nyquist noise, which has a white noise-power spectrum. Statistical fluctuations associated with fewer independent samples tend to cause variations in experimentally determined variances. With our experimental technique (see chapter 2, section 4) of prewhitening

the noise before analysing it we avoid the above correlation introduced by the low-frequency components and, consequently, the statistical fluctuations due to fewer independent samples; nevertheless, we still obtain fluctuations in the output noise-power density spectrum.

Furthermore, assuming that the spectral density of the fluctuations of the variance is constant, as should be for a stationary process, the variance of the variance should decrease with the measuring time  $T$  as  $1/T^{4-17}$ . But this was not observed in the measurements performed by Brophy<sup>4-15</sup>, while we found the following. For the same resistor  $R_2$  as above, the noise power density also fluctuated by a factor 2 during consecutive and identical sampling intervals (now taken for an  $\epsilon$  of 2%) and at the same frequency. Thus, the increase of time  $T$  did not decrease the fluctuating factor 2.

Therefore, we conclude that in some carbon resistors  $1/f$  noise is quasi-stationary, the cause of which may be found in the observed random bursts that change the noise excitation state of the carbon resistor.

## (B) Burst Noise in Transistors

### 4. Analysis

The spontaneous fluctuations of current have obtained special interest among the various random noise phenomena that appear in semiconductor devices. These spontaneous bursts consist of a series of current pulses with constant amplitude and with pulse lengths distrib-

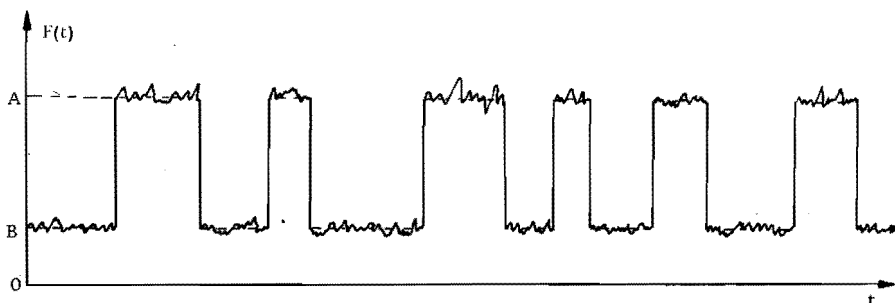


Fig. 4.3 A random telegraph signal

uted statistically. Hence, they are classified as a random telegraph signal, Fig. 4.4, with an extra noise component superimposed.

In the following pages we shall be concerned with obtaining the noise-power density spectrum of the random signal of Fig. 4.3. First, we consider the random telegraph signal alone (Fig. 4.4), and secondly we take into consideration the additional superimposed noise component.

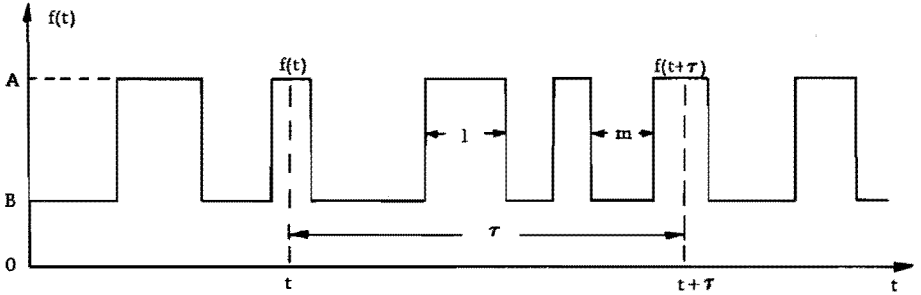


Fig. 4.4 Unsymmetrical random telegraph signal between levels B and A

#### 4.1 Unsymmetrical random telegraph signal

It has been observed experimentally that for most transistors, in which burst noise is found, their random telegraph signal is not a symmetrical one, i.e. when the noise is observed over a long time, the signal is longer at one d.c. level than at the other. We know, also experimentally, that the pulse lengths have a statistical distribution very close to a Poisson one. Let us now obtain the noise-power density spectrum of the noise signal  $f(t)$  of Fig. 4.4.

The function  $f(t)$  represents the pulse-signal noise which varies randomly between two discrete levels A and B, with a probability  $p$  of having value A at any time  $t$ , and a probability  $q = 1 - p$  of having value B; the pulse lengths  $l$  and  $m$  are assumed to have a Poisson distribution.

We will calculate (a) the autocorrelation function and then (b) its Fourier transform, which gives the power spectrum density by the

(a) Autocorrelation function

The autocorrelation function of  $f(t)$  is given by:

$$R_B(\tau) = \overline{f(t) \cdot f(t+\tau)} \quad (4.3)$$

Let  $P_{AB}(\tau)$  represent the probability of  $f(t)$  having at time  $t + \tau$  the value B once it has had at time  $t$  the value A. Then, (4.3) becomes:

$$R_B(\tau) = A p \times A P_{AA}(\tau) + A p \times A P_{AB}(\tau) + B q \times A P_{BA}(\tau) + B q \times B P_{BB}(\tau) \quad (4.4)$$

From Fig. 4.4 we see that, if at time  $t$  the function  $f(t)$  has an amplitude A, in order to have again the value A at time  $t + \tau$ , it is necessary that an even number of transitions between its two levels A and B occur during the interval time  $\tau$ . Therefore, for obtaining  $P_{AA}(\tau)$  we must calculate the sum of all probabilities of an even number of transitions during  $\tau$ , while for  $P_{AB}(\tau)$  we need the sum of all probabilities of an odd number of transitions during  $\tau$ . The same can be said for  $P_{BB}(\tau)$  and  $P_{BA}(\tau)$ , but now starting from level B.

Let us construct our own probability distribution from Fig. 4.4, knowing it is a Poisson type, with the following properties:

- (1) If  $f(t) = A$ , the probability of having a transition in the time interval  $(t, t + \tau)$  is  $\mu \cdot dt$ .
- (2) If  $f(t) = B$ , the probability of having a transition in the same time interval is  $\eta \cdot dt$ .

Starting at level A, the probability of having no transitions in time  $\tau + \delta\tau$ , defined as  $P_o(\tau + \delta\tau)$ , is:

$$P_o(\tau + \delta\tau) = P_o(\tau)P_o(\delta\tau) = P_o(\tau) (1 - \mu\delta\tau) = P_o(\tau) + \frac{dP_o(\tau)}{d\tau} \delta\tau \quad (4.5)$$

considering in the last expression the two first terms of a Taylor's 81



series, and resolving (4.5) we obtain  $dP_o(\tau)/P_o(\tau) = -\mu\delta\tau$ ; the solution of which, knowing that for  $\tau = 0$ ,  $P_o(0) = 1$ , is:

$$P_o(\tau) = e^{-\mu\tau} \quad (4.6)$$

The probability of one transition in the time  $\tau + \delta\tau$ , defined as  $P_1(\tau + \delta\tau)$ , is:

$$P_1(\tau + \delta\tau) = P_o(\tau)P_1(\delta\tau) + P_1(\tau)P_o(\delta\tau) = P_o(\tau)\mu\delta\tau + P_1(\tau) \cdot (1 - \eta\delta\tau) = P_1(\tau) + \frac{dP_1(\tau)}{d\tau} \delta\tau \quad (4.7)$$

which yields the differential equation:

$$\frac{dP_1(\tau)}{d\tau} + \eta P_1(\tau) = \mu P_o(\tau) \quad (4.8)$$

and knowing that for  $\tau = 0$ ,  $P_1(0) = 0$ , the solution of (4.8) is:

$$P_1(\tau) = \frac{\mu}{\eta - \mu} e^{-\mu\tau} - e^{-\eta\tau} \quad (4.9)$$

In general, neglecting the probabilities of having 2, 3, ...n transitions during the time  $\delta\tau$ , the probability of having n transitions in  $\tau + \delta\tau$ , defined as  $P_n(\tau + \delta\tau)$ , is:

for n even  $P_n(\tau + \delta\tau) = P_n(\tau) (1 - \mu\delta\tau) + P_{n-1}(\tau) \eta\delta\tau \quad (4.10)$

and

for n odd  $P_n(\tau + \delta\tau) = P_n(\tau) (1 - \eta\delta\tau) + P_{n-1}(\tau) \mu\delta\tau \quad (4.11)$

Equating (4.10) and (4.11) to the two first terms of a Taylor's series and resolving the equality we arrive at:

n even  $\frac{dP_n(\tau)}{d\tau} + \mu P_n(\tau) = \eta P_{n-1}(\tau) \quad (4.12)$

$$\underline{n \text{ odd}} \quad \frac{dP_n(\tau)}{d\tau} + \eta P_n(\tau) = \mu P_{n-1}(\tau) \quad (4.13)$$

Now, referring  $n$  even and  $n$  odd to a common  $n$  considered as an even number, we may write (4.13) as:

$$\underline{n \text{ odd}} \quad \frac{dP_{n-1}(\tau)}{d\tau} + \eta P_{n-1}(\tau) = \mu P_{n-2}(\tau) \quad (4.14)$$

Differentiating again (4.12) and substituting in it the expressions of  $P_{n-1}(\tau)$  and  $dP_{n-1}(\tau)/d\tau$  from (4.14) and (4.12) we obtain the recurrent differential equation:

$$\underline{n \text{ even}} \quad \frac{d^2}{d\tau^2} P_n(\tau) + (\mu + \eta) \frac{d}{d\tau} P_n(\tau) + \mu\eta P_n(\tau) = \mu\eta P_{n-2}(\tau) \quad (4.15)$$

which may be expressed with the D operator's form as:

$$\left[ D^2 + (\mu + \eta)D + \mu\eta \right] P_n(\tau) = \mu\eta P_{n-2}(\tau) \quad (4.16)$$

Remembering that:

$$P_{AA}(\tau) = \sum_{\substack{n=0 \\ n \text{ even}}}^{\infty} P_n(\tau) \quad (4.17)$$

we sum both members of (4.16) and obtain:

$$\mu\eta \left[ P_0(\tau) + P_2(\tau) + P_4(\tau) + \dots + P_n(\tau) \right] = \left[ D^2 + (\mu + \eta)D + \mu\eta \right] \times \left[ P_2(\tau) + P_4(\tau) + \dots + P_{n+2}(\tau) \right] \quad (4.18)$$

As  $n \rightarrow \infty$ ,  $\sum_{n=2,4,\dots}^n P_n(\tau) = \sum_{n=2,4,\dots}^{n+2} P_n(\tau)$  and (4.18) takes the form:

$$\mu\eta P_0(\tau) = \left[ D^2 + (\mu + \eta)D \right] \sum_{\substack{n=2 \\ n \text{ even}}}^{\infty} P_n(\tau). \quad (4.19)$$

Replacing  $P_0(\tau)$  by its equivalent (4.6) we arrive at a differential equation the solution of which is of the type:

$$\sum_{n=2,4}^{\infty} P_n(\tau) = M + N e^{-(\mu+\eta)\tau} - e^{-\mu\tau} \quad (4.20)$$

and adding to both sides  $P_0(\tau)$ , we have:

$$\sum_{\substack{n=0 \\ n \text{ even}}}^{\infty} P_n(\tau) = M + N e^{-(\mu+\eta)\tau} \quad (4.21)$$

The constants  $M$  and  $N$  are calculated from the knowledge of  $\sum_{n=0,2,\dots}^{\infty} P_n(0)$

$= 1$  and  $\sum_{n=0,2,\dots}^{\infty} P_n(\infty) = p$ , i.e. the sum of probabilities of always having a value  $A$ . The final result is:

$$P_{AA}(\tau) = \sum_{\substack{n=0 \\ n \text{ even}}}^{\infty} P_n(\tau) = p + (1-p)e^{-(\mu+\eta)\tau} \quad (4.22)$$

Equation (4.22) gives the sum of all probabilities of having an even number of transitions in an interval of time  $\tau$ , having started at level  $A$ .

Since at time  $t + \tau$  the signal is either at level  $A$  or  $B$ , we have:

$$P_{AB}(\tau) = 1 - P_{AA}(\tau) \quad (4.23)$$

Then, using the expression of (4.22) we arrive at:

$$P_{AB}(\tau) = \sum_{\substack{n=1 \\ n \text{ odd}}}^{\infty} P_n(\tau) = q - q e^{-(\mu+\eta)\tau} \quad (4.24)$$

Equation (4.24) gives the sum of all probabilities of having an odd number of transitions in an interval of time  $\tau$ , having started at level  $A$ .

By analogous reasoning, having started at level B, we have:

$$P_{BB}(\tau) = \sum_{\substack{n=0 \\ n \text{ even}}}^{\infty} P_n(\tau) = q + (1 - q)e^{-(\mu + \eta)\tau} \quad (4.25)$$

$$P_{BA}(\tau) = \sum_{\substack{n=1 \\ n \text{ odd}}}^{\infty} P_n(\tau) = p - p e^{-(\mu + \eta)\tau} \quad (4.26)$$

Therefore, introducing into (4.4) the sum of the probabilities given by (4.22), (4.24), (4.25) and (4.26), we obtain the autocorrelation function of the burst-pulse signal noise  $f(t)$  of Fig. 4.4, given by:

$$R_B(\tau) = A^2 p(p+q e^{-(\mu+\eta)|\tau|}) + AB pq(1-e^{-(\mu+\eta)|\tau|}) + BA qp \times \\ (1-e^{-(\mu+\eta)|\tau|}) + B^2 q(q+p e^{-(\mu+\eta)|\tau|}) = (Ap + Bq)^2 + \\ (A - B)^2 p q e^{-(\mu+\eta)|\tau|} \quad (4.27)$$

For the particular case of level B being zero, we have:

$$R_B(\tau) = A^2 p (p + q e^{-(\mu+\eta)|\tau|}) \quad (4.28)$$

Equation (4.28) is the autocorrelation function of the unsymmetrical random telegraph signal for one level; and for the case of a symmetrical one,  $p = q = 1/2$  and  $\mu = \eta$ , which reduces (4.28) to:

$$R(\tau) = \left(\frac{A}{2}\right)^2 \cdot (1 + e^{-2\mu|\tau|}) \quad (4.29)$$

and agrees with the result of the autocorrelation function of the Poisson rectangular wave, which appeared for the first time in the work of Kenrick<sup>4-18</sup>.

### (b) Power Spectrum $S(\omega)$

The power density spectrum is given by the following Fourier transform:

$$S(\omega) = \frac{1}{2\pi} \int_{-\infty}^{\infty} R(\tau) e^{-j\omega\tau} d\tau \quad (4.30) \quad 85$$

Then, replacing  $R_B(\tau)$  by (4.27) we obtain:

$$S(\omega) = \frac{1}{2\pi} \int_{-\infty}^{\infty} (Ap+Bq)^2 e^{-j\omega\tau} d\tau + \frac{1}{2\pi} \int_{-\infty}^{\infty} (A-B)^2 pq e^{-(\mu+\eta)|\tau|} e^{-j\omega\tau} d\tau \quad (4.31)$$

The first term of (4.31) is<sup>4-19</sup>:

$$(Ap + Bq)^2 \frac{1}{2\pi} \int_{-\infty}^{\infty} e^{-j\omega\tau} d\tau = (Ap + Bq)^2 \delta(\omega) \quad (4.32)$$

where the expression given by the integral is the delta function  $\delta(\omega)$ , and represents the power of the d.c. current component. For the second term of (4.31) we may drop  $|\tau|$  for  $\tau$  and write:

$$\frac{(A-B)^2 pq}{\pi} \operatorname{Re} \int_0^{\infty} e^{-(\mu+\eta)\tau} e^{-j\omega\tau} d\tau = \frac{(A-B)^2 pq}{\pi} \frac{(\mu+\eta)}{(\mu+\eta)^2 + \omega^2} \quad (4.33)$$

where  $\operatorname{Re}$  means the real part.

Hence, the power density spectrum of Fig. 4.4 is given by:

$$S(\omega) = (Ap + Bq)^2 \delta(\omega) + \frac{(A-B)^2 pq}{\pi} \frac{(\mu+\eta)}{(\mu+\eta)^2 + \omega^2} \quad (4.34)$$

#### 4.2 Spectrum of Burst Noise with Flicker Noise Superimposed

From the observation of burst noise in transistors we have seen that there is a superimposed signal of noise  $\phi(t)$  on the noise current pulses  $f(t)$ . Hence in Fig. 4.3 the total noise signal  $F(t)$  is made up of  $f(t)$  and  $\phi(t)$ .

The flicker noise-power density component is known experimentally to be of the type

$$S_F(\omega) = H I^2 \omega^{-\beta} \quad (4.35)$$

where  $H$  is a constant,  $I$  is the d.c. current and the parameter  $\beta$  is usually near to 1. Since the power density of the flicker noise is proportional to  $I^2$ , the flicker noise current is proportional to

the d.c. current. Hence, the amount of flicker noise at levels A and B is proportional to these levels respectively. Consequently, assuming that the superimposed noise signal  $\phi(t)$  at a d.c. current of 1 A corresponds to the flicker noise, the noise signal  $F(t)$  in Fig. 4.3 is expressed by:

$$F(t) = f(t) + f(t) \cdot \phi(t) = f(t) (1 + \phi(t)) \quad (4.36)$$

The autocorrelation function of  $F(t)$  is given by:

$$R(\tau) = \frac{\overline{f(t) (1 + \phi(t)) \cdot f(t+\tau) (1 + \phi(t+\tau))}}{\overline{(1 + \phi(t) + \phi(t+\tau) + \phi(t)\phi(t+\tau))}} = \frac{\overline{f(t)f(t+\tau)}}{\overline{(1 + \phi(t) + \phi(t+\tau) + \phi(t)\phi(t+\tau))}} \quad (4.37)$$

We assume that the generation process of the burst noise is independent of the generation process of the flicker noise. This assumption is based on the experimental fact that sometimes only one of the two types of noise is present, while at other times both take place; but even then they may appear at different spectrum ranges. These considerations allow us to write (4.37) as:

$$R(\tau) = \overline{f(t) f(t+\tau)} \cdot (1 + \overline{\phi(t)\phi(t+\tau)}) = R_B(\tau) (1 + R_\phi(\tau)) \quad (4.38)$$

where  $R_B(\tau)$  and  $R_\phi(\tau)$  are the autocorrelation functions of the burst noise and of the flicker noise for unity current respectively.

The noise-power density spectrum as given by (4.30) is:

$$S(\omega) = \frac{1}{2\pi} \int_{-\infty}^{\infty} (R_B(\tau) + R_B(\tau)R_\phi(\tau)) e^{-j\omega\tau} d\tau \quad (4.39)$$

The first term of the right-hand side of (4.39) gives the power density spectrum of the burst noise  $S_B(\omega)$  which is known through equation (4.34). Let us calculate the second term:

$$\frac{1}{2\pi} \int_{-\infty}^{\infty} R_B(\tau)R_\phi(\tau) e^{-j\omega\tau} d\tau \quad (4.40) \quad 87$$

Having substituted  $R_B(\tau)$  given by (4.27) we obtain:

$$(Ap + Bq)^2 \frac{1}{2\pi} \int_{-\infty}^{\infty} R_{\phi}(\tau) e^{-j\omega\tau} d\tau + (A-B)^2 p q \frac{1}{2\pi} \int_{-\infty}^{\infty} \left[ R_{\phi}(\tau) e^{-(\mu+\eta)|\tau|} \right] e^{-j\omega\tau} d\tau \quad (4.41)$$

Now, the first term in (4.1) is the power density spectrum of the flicker noise  $S_F(\omega)$ ,  $(Ap + Bq)$  being the d.c. current. Therefore, through (4.35) the first term is:

$$S_F(\omega) = (Ap+Bq)^2 \frac{1}{2\pi} \int_{-\infty}^{\infty} R_{\phi}(\tau) e^{-j\omega\tau} d\tau = (Ap+Bq)^2 H \omega^{-\beta} \quad (4.42)$$

The second term of (4.41) is the power density spectrum of the cross component burst-flicker,  $S_{BF}(\omega)$ , or the cross power spectrum. The integral of the second term is of the same order of magnitude as the integral of the first term; hence, their ratio is of the order of magnitude of  $(A-B)^2 pq / (Ap+Bq)^2$ . Thus the contribution of  $S_{BF}(\omega)$  to the total spectrum is negligible.

Therefore, the noise power density spectrum of Fig. 4.3 is obtained by substituting in (4.39) the values calculated through equations (4.34) and (4.42), having neglected the cross term  $S_{BF}(\omega)$ . The total spectrum  $S(\omega)$  is given by:

$$S(\omega) = (Ap + Bq)^2 \delta(\omega) + \frac{(A-B)^2 pq}{\pi} \frac{(\mu+\eta)}{(\mu+\eta)^2 + \omega^2} + \frac{(Ap+Bq)^2 H}{\omega^{\beta}} \quad (4.43)$$

which agrees well with equation (1.10).

## 5. Measurements of Burst Noise in Transistors

The first time we came across the burst noise in transistors was during the design and construction of the pre-amplifier and of the very low frequency filter (Chapter 3, sections 3 and 5). Since then, our interest in this noise phenomenon has continued to increase especially with respect to bursts of very low frequency.

We have observed in transistors burst noise over 7 decades of frequency,  $10^{-3}$  to  $10^4$  Hz. In general, in any transistor we have ob-

served that the phenomenon extends over approximately 3 decades within the above limits. In comparison with the low frequency noise of carbon resistors there is one significant difference. The measured noise power density value can in general be repeated with  $\pm 2\epsilon$  statistical error for the measuring time T. Only very seldom could the measurement not be repeated with the desired accuracy, a fact that agrees with the slight variation of the variance of noise that has been found in semiconductors and transistors<sup>4-16</sup>. Thus, in practice the random process of burst noise in transistors is a stationary one.

After a tedious observation of the burst noise in transistors the pulse lengths showed a clear Poisson probability distribution. In the frequency range of its appearance the noise power density spectrum follows an  $f^{-2}$  law when the burst noise component is larger than the flicker noise component. Such is assumed to be the situation of the noisy transistors we have chosen for measurement.

It has been particularly difficult to choose the measuring samples. Sometimes, one difficulty arises from the simultaneous presence of more than two levels of noise, even four levels being not rare, resulting in two, three or four series of pulses with different amplitudes among themselves but constant for each series. Another difficulty is that each series may have a different frequency range of pulses yielding a spectrum with more than one "bump". On rare occasions a sample had a random switching "on" and "off" of the pulse series, while in other samples the burst noise could be started or stopped by varying the collector voltage. Finally, it was equally difficult to find samples which, apart from having only one series of noise pulses, had a mean pulse length detectable inside the frequency range of the measuring channel ( $10^{-2}$  to 20 Hz).

Among 30 bipolar transistors with burst noise we have found 3 to which the above difficulties do not apply and are therefore measurable in accord to our needs and means. Two samples are npn transistors and the third one is a pnp type. All three are operated at a collector current of approximately 2  $\mu$ A, giving output burst pulses from 400  $\mu$ V max. to 100  $\mu$ V max. amplitude across a resistor load (Chapter 3, section 2).



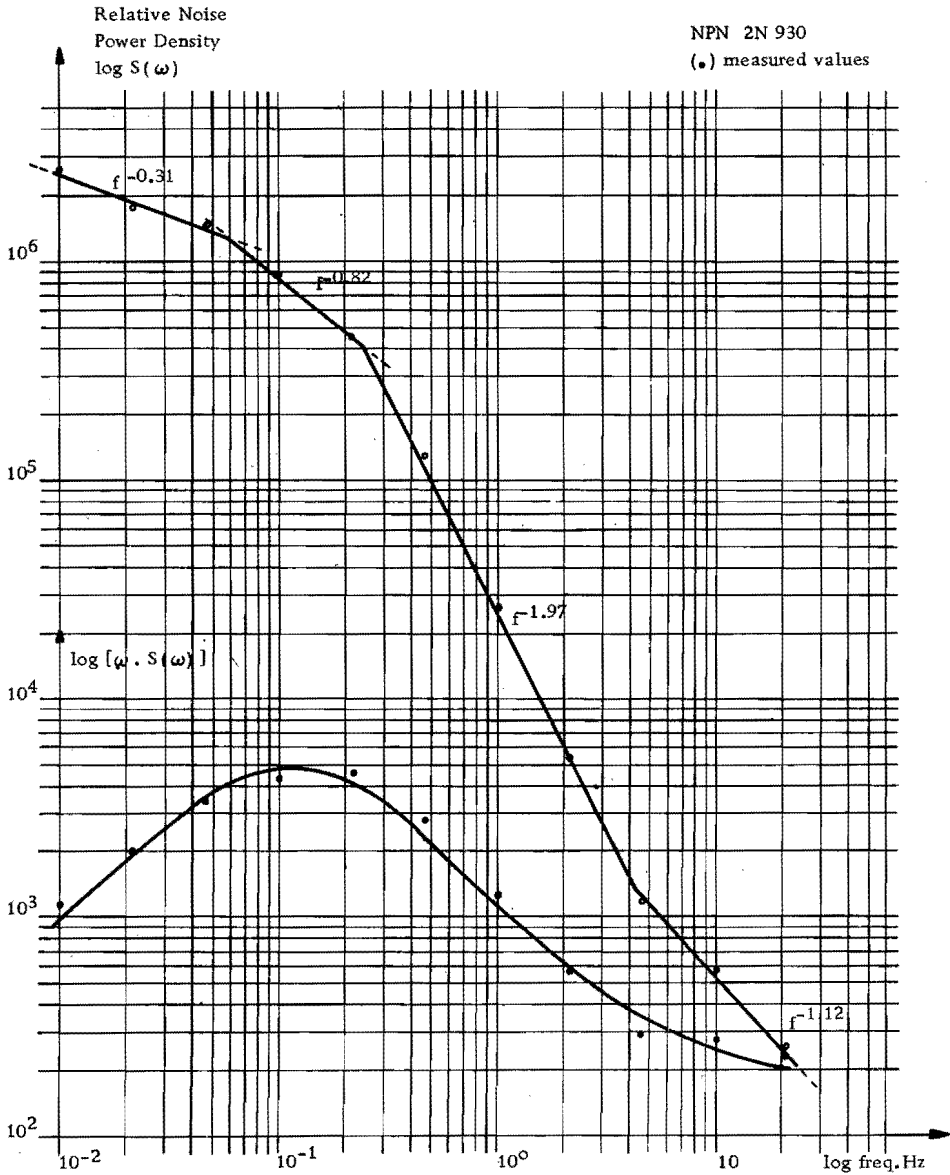


Fig. 4.5 Relative magnitude of the noise power density spectrum  $\omega \cdot S(\omega)$  of a transistor, with very-low frequency burst noise present. Estimated curve of  $S(\omega)$

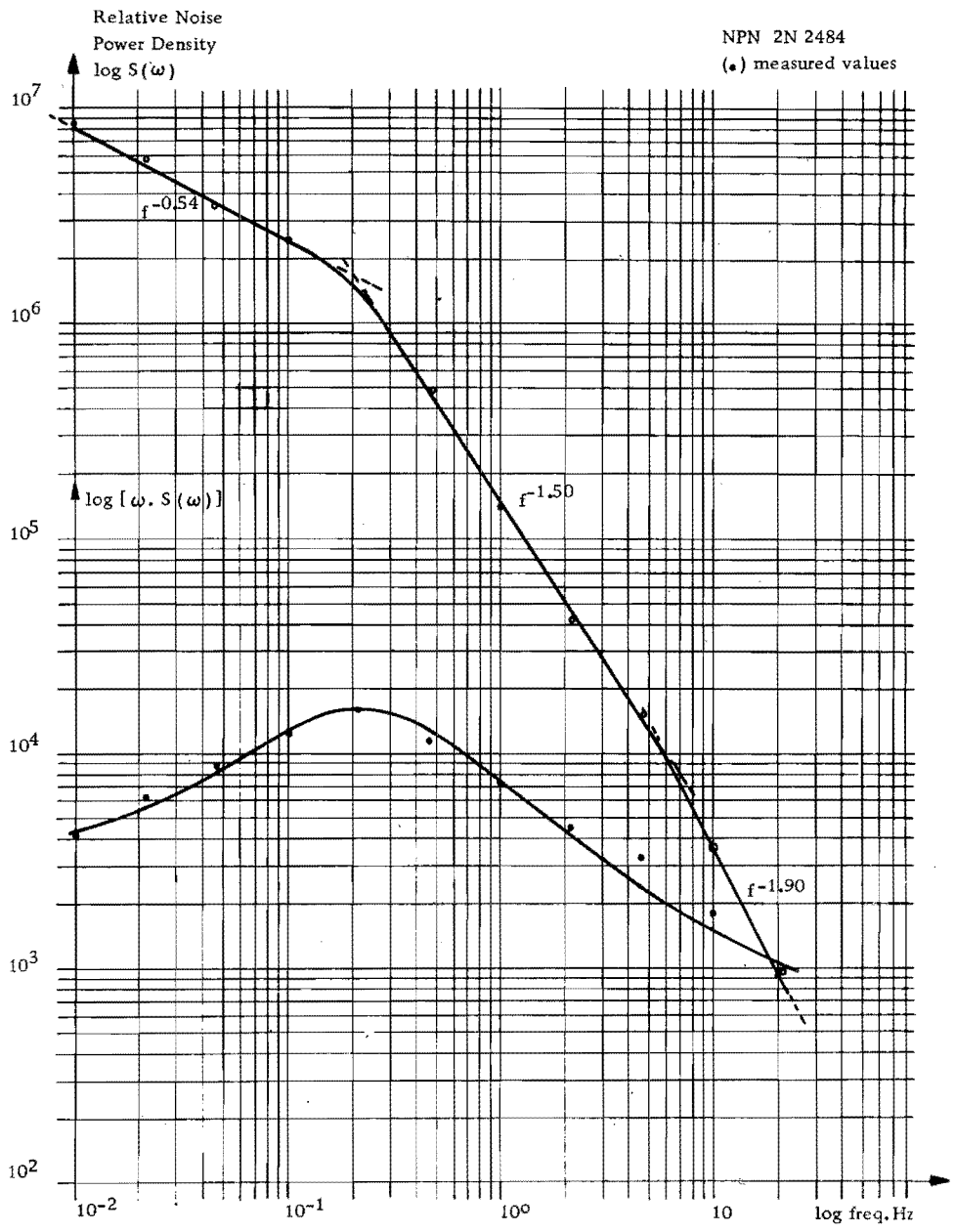


Fig. 4.6 Relative magnitude of the noise power density spectrum  $\omega \cdot S(\omega)$  of a transistor, with very-low frequency burst noise present. Estimated curve of  $S(\omega)$

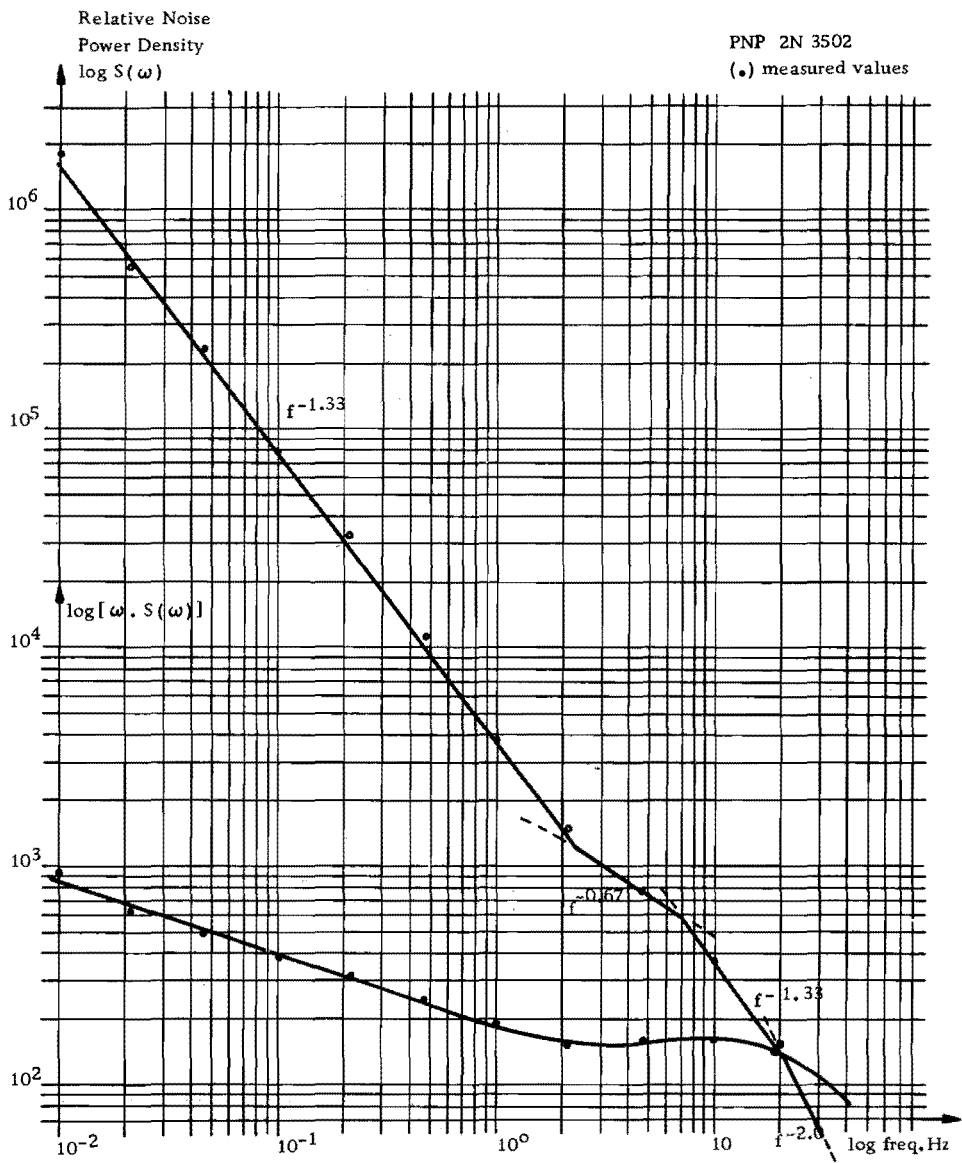


Fig. 4.7 Relative magnitude of the noise power density spectrum  $\omega \cdot S(\omega)$  of a transistor, with very-low frequency burst noise present. Estimated curve of  $S(\omega)$

Owing to the prewhitening filter the measured values correspond to  $\omega \cdot S(\omega)$  for each transistor under investigation.

Figs. 4.5, 4.6, and 4.7 represent the relative magnitude of the  $\omega \cdot S(\omega)$  spectrum for the three transistors. This spectrum was measured with an  $\epsilon$  of 2% for the frequencies of 20 and 10 Hz, an  $\epsilon$  of 5% for the frequencies down to  $2.15 \cdot 10^{-2}$  Hz, and of 7.5% for the  $10^{-2}$  Hz.

Each graph shows a clear bump around the mean burst frequency  $f_b$ , which has been observed on the oscilloscope. The burst noise component appears clearly in Figs. 4.5 and 4.6, while in Fig. 4.7 the flicker noise component is prominent.

Each graph has been recoloured i.e. the ordinates have been divided by  $\omega$  and drawn in the same figure to obtain a relative magnitude curve of the real input spectrum  $S(\omega)$ . The new curve is approximated by straight line sections and made to pass through an arbitrarily chosen point.

The recoloured curve approximates well the curve of Fig. 4.8, where arbitrary flicker and burst noise components are shown. In fact,  $\log S(\omega)$  of Fig. 4.5 can be made to correspond to the NPQR section of Fig. 4.8, while  $\log S(\omega)$  of Figs. 4.6 and 4.7 would correspond to the NPQ and MNPQ sections, respectively, in Fig. 4.8.

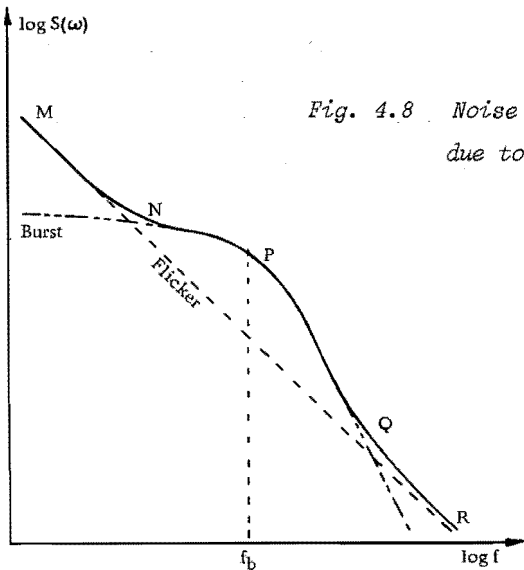


Fig. 4.8 Noise power density spectrum  $S(\omega)$  due to burst noise and flicker noise

Owing to the input d.c. blocking capacitor of the measuring channel the first term in the right-hand side of equation (4.43) is suppressed in the measurement. Taking into consideration the prewhitening action, we obtain, at the output of the channel the noise power density spectrum  $\omega \cdot S(\omega)$ , given by:

$$\omega \cdot S(\omega) = \frac{(A-B)^2 pq}{\pi} \frac{(\mu+\eta) \omega}{(\mu+\eta)^2 + \omega^2} + \frac{(Ap+Bq)^2 H \omega}{\omega^\beta} \quad (4.44)$$

The best fit of the experimental values to equation (4.44) is obtained by means of a computer programme of the last squares method. The computerised parameter values are the following:

	$(A-B)^2 pq/\pi$	$(Ap+Bq)^2 H/(\mu+\eta)^{\beta-1}$	$(\mu+\eta)$	$\beta-1$
$\omega \cdot S(\omega)_{4.5}$ :	9696	100	0.109	-0.075
$\omega \cdot S(\omega)_{4.6}$ :	29438	1762	0.22	+0.18
$\omega \cdot S(\omega)_{4.7}$ :	169	71	14	+0.34

The computerised values of  $\omega \cdot S(\omega)$  for the above parameters are plotted on a curve in their corresponding figures and the experimental values are seen to follow equation (4.44). Hence, we have obtained an estimated value of the exponent  $\beta$  of the flicker noise component and we may conclude that equation (4.43) represents the noise power density spectrum of an electronic device in which flicker and burst noise are simultaneously present as illustrated by Fig. 4.3.

## SUMMARY

The present thesis deals with very-low frequency spectra of the electrical noise in carbon film resistors and in bipolar planar transistors.

The basic knowledge required to approach the study of noise is introduced in chapter I by considering the properties of random phenomena. The fluctuations of electrons give rise to electrical noise, the power spectrum of which is considered especially at very low frequencies. In this frequency range, the flicker noise and the burst noise are the main noise components, which are a function of the frequency ( $\omega$ ) to some power  $-\beta$ .

Flicker noise is ubiquitous and its anomalous behaviour is exposed by considering the deviations of the value of  $\beta$  from unity in the noise power density spectrum  $S(\omega)$ .

Burst noise appears to be more sporadic in nature and its waveform is seen to be of a more defined type as of an unsymmetrical random telegraph signal. The value of the exponent  $\beta$  is close to 2.

The theoretical basis for measuring noise power spectra is presented in chapter II. Through the considerations made on the autocorrelation function of a noisy signal and the introduction of a spectral window we arrive at a theoretical measuring system for power spectra.

The importance of a low Q frequency window and of the prewhitening action is emphasised, while attention has been given to the necessary measuring time for the desired statistical accuracy. The frequency band was selected by changing the capacitors thus keeping the same noise producing elements in the circuit. The difficulty of measuring very-low frequency voltages is solved by the hybrid approach of an analogue-to-digital converter.

The realisation of an actual measuring channel for power spectra is presented in detail in chapter III. The first six blocks have been designed and constructed. The main ones among them are the pre-amplifier, the wide-band prewhitening filter and the selective amplifier. The pre-amplifier is operated in a hushed-mode yielding a low drift, low noise and low distortion performance. The first two differential stages are based on an improved collector-source current which consists of a compound transistor pnp-npn with an input base current in the nanoampere range. The linearity of the prewhitening filter is excellent and allows an easy recolouring of the power spectra at the output of the channel. Owing to the wiring complexity of the Twin-T circuit necessary for the selective amplifier, the required frequency compensation is obtained by a practical procedure. In the first few blocks it was essential to avoid the presence of burst noise in all transistors and to find some very well matched transistor pairs. The construction of these blocks required first-class components and a careful lay-out.

The noise power measurements obtained from carbon film resistors and planar bipolar transistors within the range of  $10^{-2}$  to 20 Hz are shown in chapter IV. By repeating noise power measurements during the same length of time on the same carbon resistor we have found that the flicker noise of some carbon resistors is a quasi-stationary random process.

The cause of this quasi-stationarity is thought to be found in the observed random bursts that change the noise excitation state of the carbon resistor. One and the same sample gave a spread from 0.8 to 1.6 in the value of  $\beta$ , which agrees with the spread found by most experimenters (chapter IV, table I) on different samples and frequency ranges. This fact helps to understand the difficulty encountered when repeating low-frequency noise measurements.

With respect to burst noise we have derived two expressions. The first is the mathematical expression of the noise power density spectrum of an unsymmetrical random telegraph signal between two levels. Secondly, considering that the flicker noise voltage is superimposed on the burst noise voltage and is proportional to the d.c. level of

the burst signal, an expression has been obtained for the noise spectrum  $S(\omega)$  when flicker and burst noise are simultaneously present.

We have measured the noise spectrum of transistors that showed to have burst noise in the frequency range given above, and have found that the spectrum follows the calculated expression.



## REFERENCES

### Chapter I

- 1-1 Diogène Laërce. Vies des Plus Illustres Philosophes Grecs de l'Antiquité. Traduites du grec. Vol. I. 250 a.c.
- 1-2 Stoney, G.J. "On the cause of double lines and equidistant satellites in spectra gases". Scit.Trans.Roy. Dublin Soct. 1891. July.
- 1-3 Brown, R. "On the existence of active molecules in organic and inorganic bodies". Phil.Mag. 1828, Vol.4, Sept. pp. 161-173.
- 1-4 Bendat, J.S.;Piersol, A.G. Measurement and Analysis of Random Data. John Wiley. 1966, p.12.
- 1-5 Nyquist, H. "Thermal agitation of electric charge in conductors". Phys.Review. 1928. Vol. 32, p. 110-13.
- 1-6 Bull, C.S. Fluctuations of Stationary and Non-Stationary Electron Currents. Butterworths. 1966, p.66.
- 1-7 Van der Ziel, A. Noise. Prentice Hall. 1954, p.31.
- 1-8 Brophy, J. Basic Electronics for Scientists. McGraw-Hill. 1966, p.269.
- 1-9 Bloodworth, G.G.;Hawkins, R.J. "The physical basis of current noise" Radio and Electro.Eng. 1969. Vol. 38, July. p. 17.
- 1-10 Johnson, J.B. "The Schottky effect in low frequency circuits". Phys.Review. 1925. Vol. 26, p. 71-85.
- 1-11 Bernamont, J. "Fluctuations de résistance dans un conducteur métallique de faible volume". Compt.Rd. 1934. Vol. 198, pp. 2144-6.

- 1-12 Meyer, E.;Thiede, H. "Resistance fluctuations in thin carbon films".(In German) E.N.T. 1935. Vol. 12, pp. 237-42.
- 1-13 Christensen, C.J.;Pearson, G.L. "Spontaneous resistance fluctuations in carbon microphones and other granular resistances". Bell.Syt.Tech.J. 1936. Vol. 15, pp. 197-223.
- 1-14 Van Vliet, K.M.;Van Leeuwen, C.J.;Blok, J.;Ris, C. "Measurements on current noise in carbon resistors and in thermistors". Physica. 1954. Vol. XX, pp. 481-96.
- 1-15 Fonger, W.W. "A determination of 1/f noise sources in semiconductor diodes and triodes". Transistor I. 1956. pp. 239-295.
- 1-16 Van Vliet, K.M. "Noise in semiconductors and photoconductors". Proc. IRE. 1958, June. pp. 1004-1018.
- 1-17 Attkinson, W.R.;Frey, L.;Newman, J. "Spectrum analysis of extremely low frequency variations of quartz oscillators". Proc. IEEE. 1963. Vol. 51, p. 379.
- 1-18 Mansour, I.R.M.;Hawkins, R.J.;Bloodworth, G.G. "Measurements of current noise in mos transistors from  $5 \cdot 10^{-5}$  to 1 Hz". Radio and Electro. Eng. 1968. April. pp. 212-216.
- 1-19 Malakof, A.N. "The problem of the flicker noise spectrum".(In Russian) Radiotekhnika and Elektronika. 1959. Vol. 4, pp. 54-62.
- 1-20 Van der Ziel, A. "Low frequency noise in vacuum tubes", in Noise in Electron Devices. Edt.Smullin-Haus. John Wiley, 1959. p. 67.
- 1-21 Kleyner, E.Yu.;Amiryan, R.A.; Vorob'yev, M.D. "Anomalous flicker noise in tubes with oxide cathodes". Radio Eng. and Electro.Phy. 1969. Vol. 14, pp. 636-38.

- 1-22 Vasseur, J.P. Propriétés et Applications des Transistors. Soc. Fran. de Docum.Electro.Paris. 1958. p. 450.
- 1-23 Van der Ziel, A. do. 1-7, p. 206.
- 1-24 Bess, L.;Kisner, L.S. "Investigation of 1/f noise spectra". Jour.App.Phy. 1966. Vol. 37. Augt. pp.3458-62.
- 1-25 Fetina, V.N. "Anomalies in the low frequency noise fluctuations observed in narrow germanium p-n junctions". Radio Eng. and Electro.Phy. 1966. Vol. 11. Sept. pp. 1444-48.
- 1-26 Verster, T.C. "Anomalies in transistor low-frequency noise". Proc. IEEE. 1967. Vol. 55. July. pp. 1204-5.
- 1-27 Nakahara, M; Iwasawa, H; and Yasutake, K. "Anomalous low-frequency noise enchancement beyond pinch-off in silicon n-channel mos transistors". Proc. IEEE. 1969. Vol. 57. Dec. pp. 2177-78.
- 1-28 Campbell, R.H.; Chipman, R.A. "Noise from current-carrying resistors 20 to 500 Kc". Proc. IRE. Waves and Electrons Sect. 1949. Augt. pp. 938-42.
- 1-29 Oakes, F. "The measurement of noise in resistors". Electro. Eng. 1950. Nov. pp. 464-69.
- 1-30 Kirby, P.L. "Current noise in fixed carbon resistors", in Noise in Electronic Devices. Chapman and Hall. 1961. pp. 78-85.
- 1-31 Pay, R.G.; given by Bell, D.A. Electrical Noise. Van Nostrand. 1960. p. 262.
- 1-32 Minden, H.T. "Noise behaviour of avalanche silicon diodes". Proc. IEEE. 1966. Vol. 54. Augt. pp. 1124-25.
- 1-33 Card, W.H.;Chaudhari, P.K. "Characteristics of burst noise". Proc. IEEE. 1965. Vol. 53. June. pp. 652-53.
- 1-34 Wolf, D.; Holler, E. "Bistable current fluctuations in reverse-biased p-n junctions of germanium". Jour.App. Phy. 1967. Vol. 38. Jan. pp. 189-92.

- 1-35 Giralt, G.;Martin, J.C.;Mateu-Perez, F.X. "Sur un phénomène de bruit dans les transistors, caractérisé par des créneaux de courant d'amplitude constante". Comt. Rd. Acad. Sc. Paris. 1965. Group V. pp. 5350-5353.
- 1-36 Giralt, G.;Martin, J.C.;Mateu-Perez, F.X. "Le bruit en créneaux des transistors plans au silicium". Electronic Letters. 1966. June. Vol. 2. pp. 228-29.
- 1-37 Martin, J.C.;Mateu-Perez, F.X.;Serra-Martin, F. "Mesures du bruit de fond des transistors plans aux très basses fréquences". Electronic Letters. 1966. Sept. pp. 343-345.
- 1-38 Hsu, S.T.;Whittier, R.J. "Characterization of burst noise in silicon devices". Solid-St.Elect. 1969. Vol. 12. Nov. pp. 868-78.
- 1-39 Widlar, R. "What is popcorn noise". Electro.Design.1968. No. 11. p. 88.
- 1-40 Smith, L.;Sheingold, D.H. "Noise and operational amplifier circuits". Analogue Dialogue. 1969. March. p.9.
- 1-41 Leonard, P.L.;Jaskolski, S.V. "An investigation into the origin and nature of popcorn noise". Proc. IEEE. 1969. Vol. 57. Oct. pp. 1786-88.

## Chapter II

- 2-1 Lee, Y.W. Statistical Theory of Communication. John Wiley. 1960. p. 329.
- 2-2 Lee, Y.W. do. p. 332.
- 2-3 Blackman, R.B.;Tukey, J.W. The Measurement of Power Spectra. Dover 1959. p. 70.
- 2-4 Blackman, R.B.;Tukey, J.W. do. p. 100.
- 2-5 Bendat, J.S.;Piersol, A.G. Measurement and Analysis of Random Data. John Wiley 1966. p. 269.

- 2-6 Bendat, J.S.;Piersol, A.G. do. p. 199.
- 2-7 Bendat, J.S.;Piersol, A.G. do. p. 261.
- 2-8 Richards, P.I. "Computing reliable power spectra", Spectrum  
IEEE. 1967. Jan. pp. 83-90.
- 2-9 Bull, C.S. Fluctuations of Stationary and Non-Stationary Elec-  
tron Currents. Butterworth. 1966. p. 160.

Chapter III

- 3-1 Volkens, W.K.;Pederson, N.E. "The hushed transistor amplifier".  
Teletech. and Electronic Indust.:Part I, 1955.  
Dec. p. 82. Pt. II, 1956. Jan. p. 70. Pt. III,  
1956. Feb. p. 72.
- 3-2 Owens, A.R.;Perry, M.A. "Low current amplifier using silicon  
planar transistors". Proc. IEE. 1965. vol. 112,  
Nov. p. 2005.
- 3-3 Chappell, A.D. "Effect to collector voltage and collector cur-  
rent on junction temperature". Elect.Letters.  
1965, Nov. p. 259.
- 3-4 Müller, O. "Thermal feedback and 1/f noise in transistors".  
1965 Internat.Solid St.Cirt.Conf. p. 68-69.
- 3-5 Reid, F.A. "Dynamic thermal response and voltage feedback in  
junction transistors". IBM-Journal. 1966. Jan.  
p. 95-97.
- 3-6 Herbst, L.J. "D.C. differential amplifier with very high com-  
mon-mode rejection". Elect. Letters. 1965. March.  
p. 41.
- 3-7 Reynolds, J. "Nonlinear distortions and their cancelations in  
transistors". IEEE Trans. Electron Devices.  
Vol. ED-12. 1965. Nov. p. 595-99.
- 3-8 Baxandall, P.J.;Shallow, E.W. "Constant current source with  
unusually high internal resistance and good  
temperature stability". Electr. Letters. 1966.  
Sept. p. 351.

- 3-9 Bhole, S.K.;Murphy, R.H. "Low drift design of differential amplifiers". Electron.Eng. 1966. Oct. p. 659-61.
- 3-10 Pinto, J.J. "Transistor low drift d.c. amplifiers". Electron. Eng. 1964. May. p. 304-308.
- 3-11 Hoffait, A.H.;Thornton, R.P. "Limitations of transistor d.c. amplifier". Proc. IEEE. 1964. Feb. p. 179.
- 3-12 Thornton, R.P. et alii. "Multistage Transistor Circuits". J. Wiley. 1965 SEEC vol. 5. p. 220.
- 3-13 Widlar, R.J. "An exact expression for the thermal variations of the emitter-base voltage of bipolar transistors". Proc. IEEE. 1967. Jan. p. 97.
- 3-14 Owens, A.R.;Jones, J.M. "Low-current operation of silicon planar transistors". Electron. Letters. 1965. Oct. n<sup>o</sup> 8. p. 242-3.
- 3-15 Chaplin, G.B.B. "D.C. amplifiers". Handbook of Semiconductor Electronics. Hunter. McGraw Hill. 1962. p. 13-3.
- 3-16 Bartolomew, C.Y. "Analysis of transistor  $I_{CBO}$  excess currents by gamma irradiation". IEEE Trans.Elect.Dev. 1969. Jan. pp. 153-4.
- 3-17 Hsu, S.T.;Whitter, R.J. "Characteristics of burst noise in silicon devices". Solid State Elect. 1969. Vol. 12. Nov. p. 869.
- 3-18 Cowles, L.G. Analysis and Design of Transistor Circuits. Van Nostrand. 1966. p. 25.
- 3-19 Baxandall, P.J.;Shallow, E.W. "Constant-current source with unusually high internal resistance and good temperature stability". Electr. Letters. 1966. Sept. 1966. n<sup>o</sup> 9. p. 351-52.
- 3-20 Nielson, E.G. "Behaviour of noise figure in junction transistors" Procd. IRE. 1957. Vol. 45. p. 957-63.
- 3-21 Rheinfelder, W.A. "Design of Low-Noise Transistor Input Circuits". Hayden. 1964. p. 13.

- 3-22 Faulkner, E.A.;Grimbley, J.B. "Reduction of flicker noise in transistor amplifiers". Electr. Letters. 1968. Vol. 4. n<sup>o</sup> 5. p. 80-81.
- 3-23 Hurley, R.B. "Junction Transistor Electronics". Wiley, 1958. p. 110-112.
- 3-24 Lotsch, K.V. "Nonlinear distortions and their cancellation in transistors". IEEE Trans. E-D. 1966. June. pp. 532-33.
- 3-25 Reynolds, J.;Khy, T.L. "Elimination of intermodulation in transistors". Proceed. IEEE. 1966. May. pp.801.
- 3-26 Navarro Borrás, F.;Rios, S. Analisis Matemático. Edt.Stylos. Madrid. 1944. p. 474.
- 3-27 Moll, J.L. "The evolution of the theory for the voltage-current characteristic of p-n junctions". Proc. IRE. 1958. June. p. 1072-82.
- 3-28 Holmes, P.J. "Transistor abnormalities as revealed by current-voltage characteristics". Radio and Elect.Eng. 1969. vol. 38. n<sup>o</sup> 5. Nov. p. 257.
- 3-29 Zaalberg van Zelst, J.J. "Calculations of impedances the phase-angle of which lies between prescribed values in a certain frequency range". (In Dutch) Philips Nat. Lab, 1961. Report No. 63/61.
- 3-30 Horowitz, I.M. "Exact design of transistor RC band-pass filters with prescribed active parameter insensitivity". IRE Trans. Cirt Theory. 1960. Sept. p. 313-320.
- 3-31 Klein, G.;Zaalberg van Zelst, J.J. "Precision Electronics". Philips Tech.Lib. 1967. p. 258.
- 3-32 Cowles, L.G. "The parallel-T R-C network". Procd. IRE. vol. 40. 1952. Dec. p. 1712-17.
- 3-33 Valley, G.E.;Wallman, H. "Vacuum Tube Amplifiers". McGraw. 1948. p. 394.

- 3-24 Hurley, R.B. do. 3-23, p. 101.
- 3-35 Murari, B. "Thermal drift in ultra low drift amplifiers".  
Proc. IEEE. 1965. May. p. 556.
- 3-36 Handbook of Operational Amplifier. Active RC Networks. Burr-  
Brown 1966. p. 74.

#### Chapter IV

- 4-1 Bernamont, J. "Fluctuations de résistance dans un conducteur  
métallique de faible volume". Comt.Rd.Acad.Sci.  
1934, vol. 198, pp. 1755-58.
- 4-2 Otto, R. "Noise in carbon microphone" (In German). Hochfreq.U.  
Elekt.Akust. 1935, vol. 45, pp. 187-98.
- 4-3 Meyer, E;and Theide, H. "Resistance fluctuations in thin car-  
bon films" (In German). E.N.T. 1935, vol. 12,  
pp. 237-42.
- 4-4 Christensen, C.J.;and Pearson, G.L. "Spontaneous resistance  
fluctuations in carbon microphones and other  
granular resistances". Bell Syst.Tech.J. 1936,  
vol. 15, pp. 197-223.
- 4-5 Abson, E.J.;Harris, W.;and Roberts, W.L. "Semiconductor-noise  
at low frequencies". T.R.E. 1946. Report 2051.  
22nd-Nov.
- 4-5 Campbell, R.H.;and Chipman, R.A. "Noise from current carrying  
resistors 20 to 500 Kc". Proc.I.R.E. 1949, vol.  
37, pp. 938-42.
- 4-7 Templeton, I.M.;and MacDonald, D.K.C. "The electrical conduc-  
tivity and current noise of carbon resistors".  
Proc.Phys.Soc.B. 1953, vol. 66, p. 680.
- 4-8 Van Vliet, K.M.;Van Leeuwen, C.J.;Block, J. and Ris, C. "Meas-  
urements on current noise in carbon resistors  
and in thermistors". Physica. 1954, vol. 20,  
pp. 481-96.



- 4-9 Kirby, P.L. "Current noise in fixed carbon resistors", in  
Noise in Electronic Devices. Chapman and Hall.  
1961, pp. 78-85.
- 4-10 Brophy, J.J. Basic Electronics for Scientists. McGraw-Hill,  
1966, p. 271.
- 4-11 Williams, J.L.; and Burdett, R.K. "Current noise in cermet  
resistor films". Brit.J.Appl.Phys. 1966, vol.  
17, pp. 977-78.
- 4-12 Mandelbrot, B. "Some noises with  $1/f$  spectrum, a bridge between  
direct current and white noise". IEEE trans.  
1967, I-T-13, pp. 289-98.
- 4-13 López de la Fuente, J. "Quasi-stationary noise in resistors".  
Electronics Letters. 1969, vol. 5, n<sup>o</sup> 12, pp.  
63-5.
- 4-14 Malakof, A.N. "The problem of the flicker-noise spectrum" (In  
Russian). Radiotek. and Electro. 1959, vol. 4,  
Jan. p. 59.
- 4-15 Brophy, J.J. "Statistics of  $1/f$  noise". Phy.Review. 1968, vol.  
166, n<sup>o</sup> 3, pp. 827-31.
- 4-16 Brophy, J.J. "Variance fluctuations in flicker noise and cur-  
rent noise". Journ.Appl.Phys. 1969, vol. 40,  
n<sup>o</sup> 9, p. 3553.
- 4-17 Radeka, V. " $1/f$  noise in physical measurements". IEEE trans.  
1969, N-Sc. vol. 16. Oct. p. 29.
- 4-18 Kenrick, G.W. "The analysis of irregular motions with appli-  
cations to the energy-frequency spectrum of  
static and telegraph signals". Phil.Mag.Ser.7.  
1929, vol. 7, pp. 176-96.
- 4-19 Lee, Y.W. Statistical Theory of Communication. J. Wiley, 1960,  
p. 49.

## ACKNOWLEDGEMENTS

The content of this thesis has been realised in the Electronics Group of the Electrical Engineering Department of the Eindhoven University of Technology under the leadership of Professors H. Groendijk and J.J. Zaalberg van Zelst.

I am greatly indebted to the Rector of the University, Prof.Dr.Ir. A.A.Th.M. van Trier, for giving me the opportunity of carrying out the research work, and to Professors H. Groendijk and J.J. Zaalberg van Zelst for their helpful guidance and discussions.

I would also like to express my gratitude to Dr. M.M. Abu-Zeid for his scientific assistance, to the other members of the staff for their help and interest, and to Mrs. A.M. Bogaerts who kindly prepared the final manuscript.

## CURRICULUM VITAE

- 7th November, 1927 : Born at Neguri-Guecho, Vizcaya, Spain
- 1934 : Grammar studies at the preparatory school of St. Edmund's College, Ware, England
- 1938 : Grammar School studies at the Sacred Heart High School, Vitoria, Spain
- July, 1946 : University Baccalaureate (B.U.), University of Valladolid, Spain
- October, 1946 : Studies of mathematics Academia Luz, Madrid, Spain
- October, 1951 : Joined the Society of Jesus (S.J.)
- July, 1957 : Licentiate in Philosophy (Ph.L.), Catholic University of Quito, Ecuador
- June, 1961 : Master of Science (Research) in Electrical Engineering (M.Sc.), St. Louis University, St. Louis, Mo. U.S.A.
- August, 1964 : Priesthood, Brussels, Belgium
- July, 1965 : Licentiate in Theology (Th.L.) Collège St. Albert, Louvain, Belgium
- October, 1965 : Started research work in the Electronics Group of the Electrical Engineering Department of the Eindhoven University of Technology, Netherlands.

## STELLINGEN - PROPOSITIONS

The noise of some carbon resistors at very-low frequencies is generated by a quasi-stationary random process.

Thesis. Sect. 4.2, 4.3.

## II

Even at very-low frequencies the burst noise component of the noise in planar bipolar transistors can be larger than the flicker noise component yielding at least one bump in the spectrum curve.

Thesis. Sect. 4.4.2, 4.5.

## III

The expression of the power spectrum of a random telegraph wave is given in the literature <sup>1</sup> for the situation of a symmetrical wave. Measurements of burst noise <sup>2</sup> are compared with such an expression. In general, such a procedure is not correct since the wave is unsymmetrical and a new expression is needed.

Thesis. Sect. 4.4.1, 4.5.

1. Lee, Y.W. Statistical Theory of Communication. J. Wiley, 1960, p. 221.
2. Jeager, R.C.; Brodersen, A.J. "Low-frequency noise sources in bipolar junction transistors". IEEE.Trans.E.D.-17, 1970, p. 131.

## IV

Modern scientific researchers should acquire a sufficient understanding of numerical analysis since by means of numerical methods digital computers have become a significant and universal instrument for solving broad classes of problems.

## V

Man must be educated through arts and sciences as a whole being, so that he obtains a broad background education and a deep specialisation in some field. Thus a graduated scholar in liberal arts is not more fully educated than a professional graduated from a science department.

## VI

The christian believer and scientific researcher may reach a total development of his personality by discovering the intelligence of nature as established by God in favour of mankind.

"L'analyse de la Matière révèle à qui sait voir, la priorité, la primauté de l'Esprit".

Teilhard de Chardin. Science et Christ. Ed.Seiul,Paris. 1965, p.57.

## VII

The scientist and the engineer of to-day are anxious of learning and knowing about the ideas of others engaged in the same field in other countries. Hence, the learning of technical foreign languages is compulsory and may be very much aided by following technical courses taught in foreign languages.

## VIII

The freshman student of engineering should be given some motivation and feeling for the need of mathematics and physics by means of guided experiments in his own desired future field. This experimental procedure can help the student to decide at the end of his first scholar year whether or not he should continue with technical studies without the need of having to take an entrance examination.

## IX

Technical education at its medium level should be given in close coordination with the actual industrialisation of products and methods.

## X

The technical institutions of developed countries have a moral obligation to help their homologous institutions of underdeveloped countries to acquire a better technical knowledge.